

Algorithm for Atmospheric Corrections of Aircraft and Satellite Imagery

Robert S. Fraser, Richard A. Ferrare, Yoram J. Kaufman,
and Shana Mattoo

DECEMBER 1989



(NASA-TM-100751) ALGORITHM FOR ATMOSPHERIC
CORRECTIONS OF AIRCRAFT AND SATELLITE
IMAGERY (NASA) 105 0 CSCL 09B

N90-13976

Unclas
G3/61 0251709

Algorithm for Atmospheric Corrections of Aircraft and Satellite Imagery

Robert S. Fraser
*Goddard Space Flight Center
Greenbelt, Maryland*

Richard A. Ferrare
*University Space Research Association
Greenbelt, Maryland*

Yoram J. Kaufman
*University of Maryland
College Park, Maryland*

Shana Mattoo
*Applied Research Corporation
Landover, Maryland*



National Aeronautics and
Space Administration

Goddard Space Flight Center
Greenbelt, MD

Abstract

This report describes a simple and fast atmospheric correction algorithm used to correct radiances of scattered sunlight measured by aircraft and/or satellite above a uniform surface. The atmospheric effect, the basic equations, a description of the computational procedure, and a sensitivity study are discussed. The program is designed to take the measured radiances, view and illumination directions, and the aerosol and gaseous absorption optical thicknesses to compute the radiance just above the surface, the irradiance on the surface, and surface reflectance. Alternatively, the program will compute the upward radiance at a specific altitude for a given surface reflectance, view and illumination directions, and aerosol and gaseous absorption optical thicknesses. The algorithm can be applied for any view and illumination directions and any wavelength in the range $0.48\text{ }\mu\text{m}$ - $2.2\text{ }\mu\text{m}$. The relation between the measured radiance and surface reflectance, which is expressed as a function of atmospheric properties and measurement geometry, is computed using a radiative transfer routine. The results of the computations are tabulated in a look-up table which forms the basis of the correction algorithm. The algorithm can be used for atmospheric corrections in the presence of a rural aerosol. The sensitivity of the derived surface reflectance to uncertainties in the model and input data is discussed.

PRECEDING PAGE BLANK NOT FILMED

Table of Contents

	Page
Abstract	iii
List of Tables	vii
List of Figures	viii
1.0 Introduction	1
1.1 Background	1
1.2 Intervening Atmosphere	1
1.3 Atmospheric Corrections	3
1.4 Algorithm	5
2.0 Atmospheric Effect	6
2.1 General Discussion	6
2.2 Mathematical Description	8
3.0 Correction Algorithm	11
3.1 Model Wavelengths	12
3.2 Aerosol Properties	14
3.3 Gaseous Absorption	18
3.4 Altitude Profiles	20
3.5 Molecular and Aerosol Optical Thickness	22
3.6 Measurement Altitudes	23
4.0 Look-up Tables	24
5.0 Computational Procedure	24
5.1 General	24
5.2 Input	29

5.3	Output	33
5.4	Summary of Error Messages	38
6.0	Sensitivity Study	41
6.1	Model Errors	42
6.1.1	Aerosol Single Scattering Phase Function	42
6.1.2	Polarization	68
6.1.3	Water Vapor and Ozone Absorption	68
6.1.4	Aerosol Absorption	70
6.1.5	Vertical Distribution of Aerosols	70
6.1.6	Bidirectional Reflectance	71
6.2	Interpolation Errors	72
6.3	Input Errors	73
7.0	Conclusion	74
8.0	References	75
9.0	Listing of FORTRAN program	79

List of Tables

Table		Page
1	Spectral bands, aerosol indices of refraction, and optical thicknesses	13
2	Aerosol size distribution parameters	17
3	Variables in the FIFEWAV program and associated subroutines and their equivalent in the text	26
4	Examples of input data	30
5	Examples of output results for the examples in Table 4	34
6	An example of output for interpolated radiation parameters	39
7	Examples of error messages for various errors in the input data	40
8	Case numbers assigned to sensitivity tests for the atmospheric correction algorithm	43
9	Summary of sensitivity results	48
10	Sensitivity results	52

List of Figures

Figure		Page
1	Surface reflectance and corresponding radiance above the atmosphere for a typical vegetation	7
2	Angular coordinates	10
3	Surface reflectance at the FIFE site	15
4	Aerosol particle number density altitude profiles	21
5	Aerosol single scattering phase functions	67

1.0 Introduction

1.1 Background

The purpose of this report is to describe a fast and simple atmospheric correction algorithm to derive the surface reflectance, and other parameters, from radiances measured by satellite and/or aircraft in the visible and near IR parts of the spectrum. The original version of this algorithm was developed to correct the radiances measured during FIFE (First ISLSCP Field Experiment - Sellers et al., 1988) which is taking place at the Konza Prairie in Kansas. While the algorithm has been designed to correct radiances measured over a rural site for the wavelength range $0.48 \mu\text{m} \leq \lambda \leq 2.2 \mu\text{m}$, a sensitivity study has shown that the algorithm can be a practical tool for many applications of remote sensing, for which a uniform surface can be assumed, and for which the optical characteristics of the aerosol do not differ significantly from the rural aerosol (the algorithm should not be applied for correcting for the effect of desert dust or fog). As a result we would like to bring the algorithm to the attention of the scientific and engineering community.

1.2 The Intervening Atmosphere

Atmospheric aerosols, which are liquid or solid particles suspended in the air, have a significant importance in evaluating satellite imagery for remote sensing of the earth's surface. The atmospheric aerosol results from natural sources (e.g. desert dust, condensation and oxidation of gases released from the biosphere and oceans) and anthropogenic sources (e.g. biomass burning and the industrial emission of gases which participate in atmospheric chemical reactions and condense into liquid particles). In the Southern Hemisphere, near Australia, the aerosol concentration is usually very low (aerosol optical thickness in the visible is less than 0.10) due to the low population, large ocean areas, and low humidity. In desert areas, dust storms can increase the optical thickness (τ) to $\tau = 2.0$ and above (hiding the sun). In the Northern Hemisphere the concentration may be rather large during long period of times, (e.g. the aerosol optical thickness is around 0.6 in the Eastern part of the United States during July and August - Kaufman and Fraser, 1983; Peterson et al., 1981), due to industrial pollution. In the state of Rondonia, Brazil, biomass burning due to deforestation generates dense smoke (optical thickness 1.0-3.0) that covers the area during most of the dry season. For an aerosol optical thickness over land larger than 0.20, aerosols affect a significant share of the outgoing visible radiation for a cloudless sky.

Therefore, since aerosols affect satellite imagery of the earth's surface, attempts for its correction should be taken.

Satellite images of the Earth's surface in the solar spectrum are contaminated by sunlight scattered towards the sensor by atmospheric molecules, aerosols, and clouds (path radiance). In addition, solar energy that is reflected from the Earth's surface and serves as the remote sensing signal, is attenuated by the atmosphere. This combined atmospheric effect is wavelength dependent, varies in time and space, and depends on the surface reflectance and its spatial variation. Correction for this atmospheric effect can produce remote sensing signals that are more closely related to the surface characteristics. Molecular scattering and absorption in the atmosphere can be accounted for satisfactorily. Gaseous absorption is minimized by choosing sensor bands in atmospheric windows. Therefore, aerosol scattering and absorption, and the presence of subpixel clouds, are the main variables in the atmospheric effect on satellite imagery.

For a cloudless sky, aerosol scattering is the major variable component of the atmospheric effect for dark surfaces, while aerosol absorption is important for bright surfaces (Fraser and Kaufman, 1985). In order to perform atmospheric corrections of remotely sensed data, the optical characteristics of the atmosphere must be estimated. These characteristics may be given in varying levels of detail--from considerable detail (profile of the extinction coefficient, the single-scattering albedo and the scattering phase function), to less detail (the vertical optical thickness, the average aerosol scattering phase function and single-scattering albedo).

In order to demonstrate the effect of the atmosphere on remote sensing we shall discuss vegetation as an example. We may distinguish among the following ecological regions:

- Over remote land areas, with no substantial anthropogenic aerosol contribution, and no dust, the aerosol optical thickness may vary between 0.02-0.10. For this variation and for typical aerosol characteristics (single scattering albedo $\omega_0 = 0.96$), the reflectance of the atmosphere alone will increase about 0.01 (Fraser and Kaufman, 1985), and a vegetation index (ratio between the difference in reflectances between the near IR and the visible and the sum - NDVI) of NDVI=0.60, as measured by satellite, will change to 0.58 (Holben, 1986). These changes are relatively small and, therefore, atmospheric correction in this case is not important for most applications. (Remote sensing of ocean color is affected by even a small aerosol optical thickness (Gordon et al., 1983).)

- Over typical land areas, anthropogenic aerosols and/or dust may generate optical thicknesses in the range 0.05-0.25. The corresponding atmospheric effect would change a surface reflectance of $\rho = 0.02$ to 0.04, and vegetation index of NDVI = 0.60 to 0.55. These are significant errors which necessitate atmospheric correction.

- Over polluted areas, with anthropogenic aerosols from industrial sources (e.g all of Eastern U.S. and Europe during the summer) or areas affected by dust, fog or smoke (tropical regions, regions in the far east and Sahel), the aerosol optical thickness may vary in the range 0.1-1.0. In this range of variation the atmospheric effects are very large. The surface reflectance would vary from 0.02 to 0.08 and the vegetation index would decrease from 0.6 to 0.45.

1.3 Atmospheric Corrections

The correction procedure requires information about the atmospheric optical characteristics. Due to the difficulty in determining these characteristics, the only operational use of atmospheric corrections today is that of the ocean color (Gordon et al., 1983), where the corrections depend on the condition of the very low reflectance of the water in the red. Otherwise, information on the atmospheric optical characteristics can be obtained from three different sources:

Climatology: Documented information on the atmospheric characteristics and their variation can be used to estimate the expected atmospheric effect for a specific part of the world and a specific season. Such documentation can be obtained from the analysis of measurements taken from the ground, and partially from the analysis of satellite data (Fraser et al., 1984; Kaufman, 1987; Kaufman et al., 1988). This source of information will be used for optical characteristics that cannot be determined otherwise for the particular image being corrected.

Measurements from the ground: The aerosol optical thickness can be obtained from sun-photometer measurements (King et al., 1978; Kaufman and Fraser, 1983). The phase function can be determined from inversion of solar almucantar measurements, and the single-scattering albedo from the collection of particles on filters, preferably by aircraft sampling of the entire atmospheric boundary layer. The single-scattering albedo can also be determined by measurements of the diffuse and direct flux (Herman et al., 1975; King and Herman, 1979; King, 1979) and by lidar techniques (Spinhirne et al., 1980). The

application of such measurements for atmospheric corrections is useful for intense field measurements, or for establishing the climatology of a given area.

Determination from satellite imagery: For the purpose of atmospheric corrections, the path radiance and the corresponding aerosol optical thickness can be derived from radiances detected by the satellite over a dark surface. Examples include many land surfaces in the blue spectrum, dense dark vegetation in the visible channels (Kaufman and Sendra, 1988), and water in the red and near IR. The wavelength dependence of the derived aerosol optical thickness (when available) can be used to estimate the particle size and the scattering phase function. In the past satellite imagery has been used to determine the aerosol optical thickness and other aerosol characteristics. The aerosol optical thickness has been derived from satellite imagery of oceans (Griggs, 1975; Mekler et al., 1977; Carlson, 1979; Koepke and Quenzel, 1979; Takayama and Takashima, 1986), and recently, over dense dark vegetation (Kaufman and Sendra, 1988). By using the difference in the brightness between a clear and a hazy day, Fraser et al. (1984) demonstrated that the difference in the optical thickness can be derived where the surface reflectance is less than 0.1. Determination of the aerosol single-scattering albedo and particle size was suggested by Kaufman et al. (1988) and Kaufman (1987), and applied to trace the evolution of smoke from a large forest fire (Ferrare et al., 1988). This method is useful to determine the aerosol characteristics (from imagery that includes water-land interfaces) in areas that suffer from substantial aerosol outbreaks (e.g. desert dust storms, smoke from fires and concentrated anthropogenic aerosol).

Once the atmospheric characteristics are specified, an atmospheric correction can be performed with an equation relating measured radiance to the optical properties of the atmosphere and surface. The computation requires application of complex and time consuming radiative transfer programs (Dave, 1972 a,b,c,d; Ahmad and Fraser, 1982). This report presents an algorithm that simplifies the correction procedure by using an a priori prepared look-up table that is based on radiative transfer computations. In essence, the algorithm simplifies the atmospheric correction procedure to a desktop operation, by sacrificing the flexibility to select specific aerosol size distributions and refractive indexes, but not optical thickness.

1.4 The algorithm

The algorithm is designed to compute the upward radiance for a given surface reflectance or to compute the surface reflectance for a given measured radiance, for almost any wavelength in the visible and near-IR spectrum (with appropriately specified gaseous absorption), for a wide range of observation zenith angles, solar illumination angles and azimuth angles between the observer and the solar rays, as well as any height of the observer (aircraft or satellite). Any practical value of the aerosol optical thickness can be used, but the algorithm is restricted to a specific aerosol size distribution and refractive index.

The relation between the measured radiance and the surface reflectance is expressed as a function of the path radiance, downward flux at the ground, atmospheric transmission, and the atmospheric backscattering ratio. Using this relation, a look-up table is constructed which relates the measured upward radiance to surface reflectance for several aerosol optical thicknesses, solar zenith angles, measurement wavelengths, and a range of observation directions. This look-up table is based on the tabulation of the results of radiative transfer computations which are made using a Dave (1972 a,b,c,d) code. It is assumed that the atmosphere and surface are horizontally homogeneous, and the surface reflects light according to Lambert's law. The light scattered by the atmosphere and the surface is assumed to be unpolarized. The atmosphere is also assumed to be cloud-free.

Radiation properties of the cloudless atmosphere depend on both molecular and aerosol constituents. Molecular scattering and absorption, except for water vapor absorption, are easy to account for. Aerosol effects are more variable and are therefore more difficult to correct. The parameters used to describe these aerosol effects are: the optical thickness which determines the amount of extinction, the single scattering albedo which determines the fraction of light scattered from the total extinction, and the single scattering phase function which describes how the light is scattered as a function of direction. For the most part, aerosol extinction is the dominant parameter in the aerosol component of the atmospheric effect (Fraser and Kaufman, 1985). Thus, in this algorithm the aerosol optical thickness is the only variable aerosol parameter. The algorithm uses a constant aerosol single scattering phase function and scattering albedo chosen to represent a rural environment. Because these assumptions can introduce error in the derived surface reflectances, a sensitivity analysis is performed to estimate the uncertainty in in derived surface reflectances.

In the first part of this document, the atmospheric effect and its effects on the surface reflectance are discussed. Next, a description of the equations used in the algorithm and the construction of the look-up table is given. A sensitivity study is then performed to estimate the errors associated with the initial assumptions, interpolation algorithm, and uncertainties in the input data. Finally, the FORTRAN code for the algorithm is listed.

2.0 Atmospheric Effect

2.1 General Discussion

The atmospheric effect is caused by the scattering and absorption of solar radiation by molecules and aerosols. There are three components to this effect :

- 1) The downward solar radiation is absorbed and scattered by the atmosphere and it is diffused by forward scattering. Because this diffusion increases the angular distribution of the radiation, the downward radiation interacts with the surface in a wide range of directions. Thus the surface reflection coefficient for this radiation is different from the reflection coefficient for the direct solar beam (Lee and Kaufman, 1986).
- 2) Radiant energy reaching a remote sensor is reflected from the ground both within the instantaneous-field-of-view (ifov) and from the region outside of it. Part of the reflected energy within the ifov is transmitted directly to a sensor and can be considered signal; the remaining radiation is absorbed and scattered. Part of the radiation that is reflected from outside of the ifov passes through the column containing the ifov and is scattered there towards the sensor. This component is associated with the adjacency effect. It augments the measured radiance and is partially corrected for when deriving the surface reflectance.
- 3) Radiation is scattered by the atmosphere into the ifov without being reflected by the surface. This component is called the path radiance and increases the apparent reflection of the surface.

An example of the difference between the spectral surface reflectance for typical vegetation (assumed Lambertian) and the corresponding upward radiance above the atmosphere is shown in Figure 1. In this figure, the upward radiance is normalized by the incident solar flux to produce reflectance units. This normalized radiance is the apparent reflectance as seen from the sensor. The reflectance of the earth-atmosphere system can be greater than the surface reflectance, the same, or weaker. In the visible spectrum the

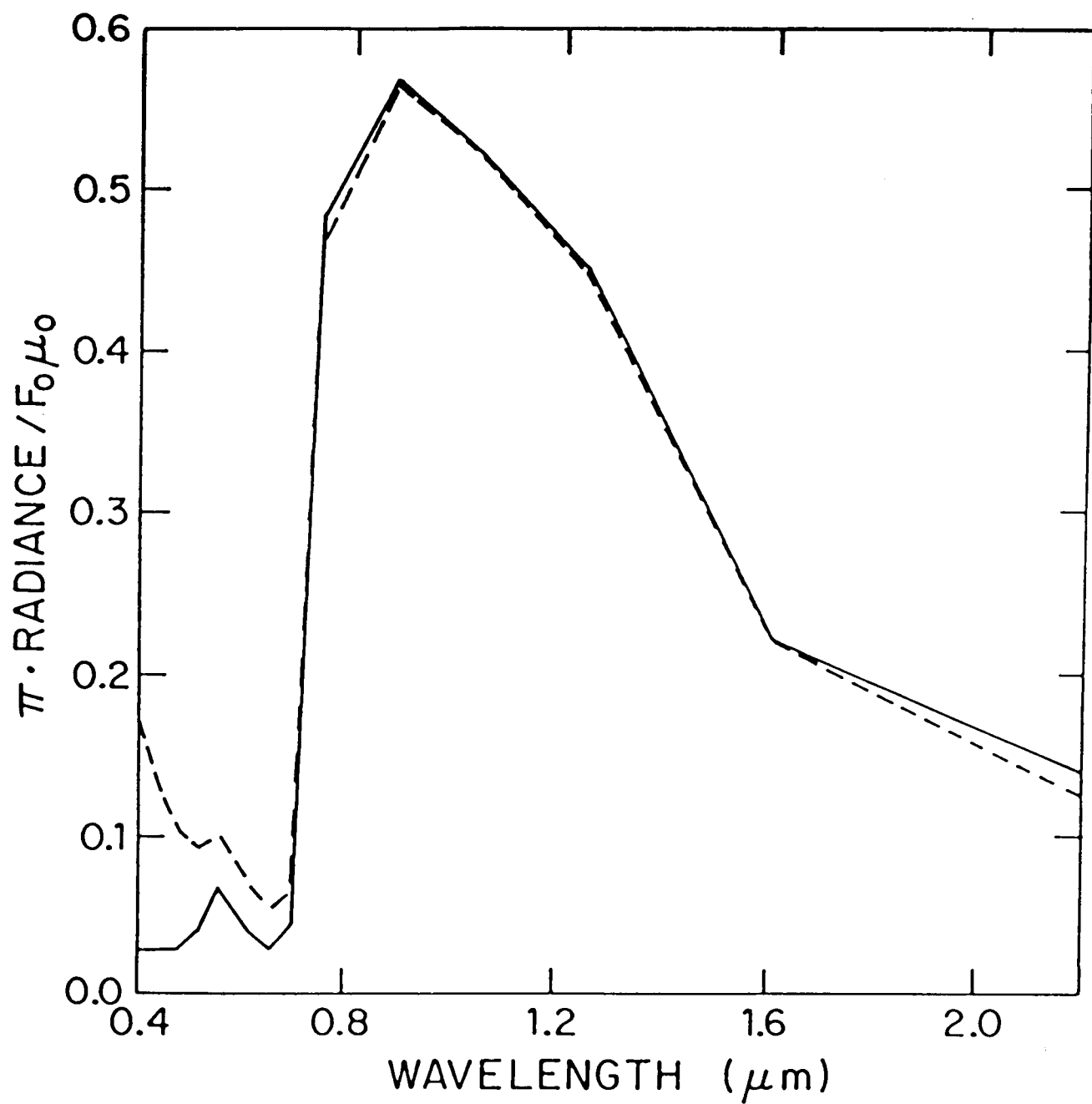


Figure 1. Surface reflectance (—) and the corresponding radiance (---) above the atmosphere for a typical vegetation. The radiance is normalized by F_0 , the incident solar flux, and by μ_0 , the cosine of the solar zenith angle (from Kaufman, 1987).

surface reflectance is weak, the path radiance is relatively strong, and the reflectance above the atmosphere exceeds that at the ground. In the near infrared ($0.7 < \lambda < 1.6 \mu\text{m}$) the surface reflectance is strong, and the reflectances at the surface and above the atmosphere are nearly the same. The loss of radiation from the surface by extinction is augmented at the same rate by atmospheric scattering. For wavelengths longer than $1.6 \mu\text{m}$, atmospheric scattering does not compensate for the attenuation loss.

2.2 Mathematical Description

In order to correct for the atmospheric effects discussed in the previous section, a relation is developed between the upward spectral radiance L^m measured from satellite or aircraft and the surface reflectance ρ : $L^m = f(\rho)$. The radiance is equivalent to the specific intensity as defined by Chandrasekhar (1960, p.1), except that the radiance, as used here, is the radiant energy within a unit wavelength interval instead of the energy per unit frequency. The function f depends on the atmospheric and surface optical properties, observation and sun directions, and wavelength. The radiance L^m can be expressed explicitly as a function of the path radiance L_o (upward radiance for zero surface reflectance), the downward flux through a horizontal surface at the ground F_d (for zero surface reflectance), the total (direct + diffuse) transmission from the surface to the observer T , and the atmospheric backscattering ratio s . It is assumed that the atmosphere and the surface are horizontally homogeneous, but the atmospheric optical properties vary in the vertical direction. The surface is assumed to reflect light according to Lambert's law. The light scattered by the cloud-free atmosphere and surface is assumed to be unpolarized. The relation between L^m and ρ is (Chandrasekhar, 1960)

$$L^m = L_o + \frac{(\rho F_d T)}{\pi (1 - s \rho)} \quad (1)$$

Here L^m is the spectral radiance measured from aircraft or satellite and is a function of λ , θ_o , τ_a , τ_{gs} , ω_o , τ_g , θ , Z , and ϕ , where

λ is the wavelength of the radiation,

θ_o is the solar zenith angle,

τ_a is the aerosol optical thickness (used with base e),

- τ_{gs} is the molecular scattering optical thickness,
- ω_0 is the ratio of the aerosol scattering and extinction optical thicknesses,
- τ_g is the gaseous absorption optical thickness,
- Z is the observation height,
- θ is the propagation direction zenith angle of the radiant energy at the ground,
- φ is the azimuth angle (azimuthal angles are measured with respect to the principal plane through the sun; 0° lies in the plane containing the direction of propagation of the direct sunlight).

Figure 2 shows the angular coordinates used in the algorithm. The functions L_o , T , F_d and s have the following functional dependences:

$$L_o = L_o(\lambda, \theta_o, \tau_a, \tau_{gs}, \tau_g, \omega_o, Z, \theta, \varphi) \quad F_d = F_d(\lambda, \theta_o, \tau_a, \tau_{gs}, \tau_g, \omega_o)$$

$$T = T(\lambda, \tau_a, \tau_{gs}, \tau_g, \omega_o, Z, \theta) \quad s = s(\lambda, \tau_a, \tau_{gs}, \tau_g, \omega_o)$$

The correction algorithm is based on the inverse of eq. (1), where the surface reflectance ρ can be expressed in terms of the measured radiance L^m :

$$\rho = \frac{f}{(1 + s f)} \quad (2)$$

where

$$f = \frac{\pi (L^m - L_o)}{(F_d T)} \quad (3)$$

The algorithm will compute L^m using (1) if ρ is given or will compute ρ using (2) and (3) if L^m is given. Other quantities computed are: the total irradiant flux F_g on a horizontal surface at the ground,

$$F_g = \frac{F_d}{(1 - s \rho)} \quad (4)$$

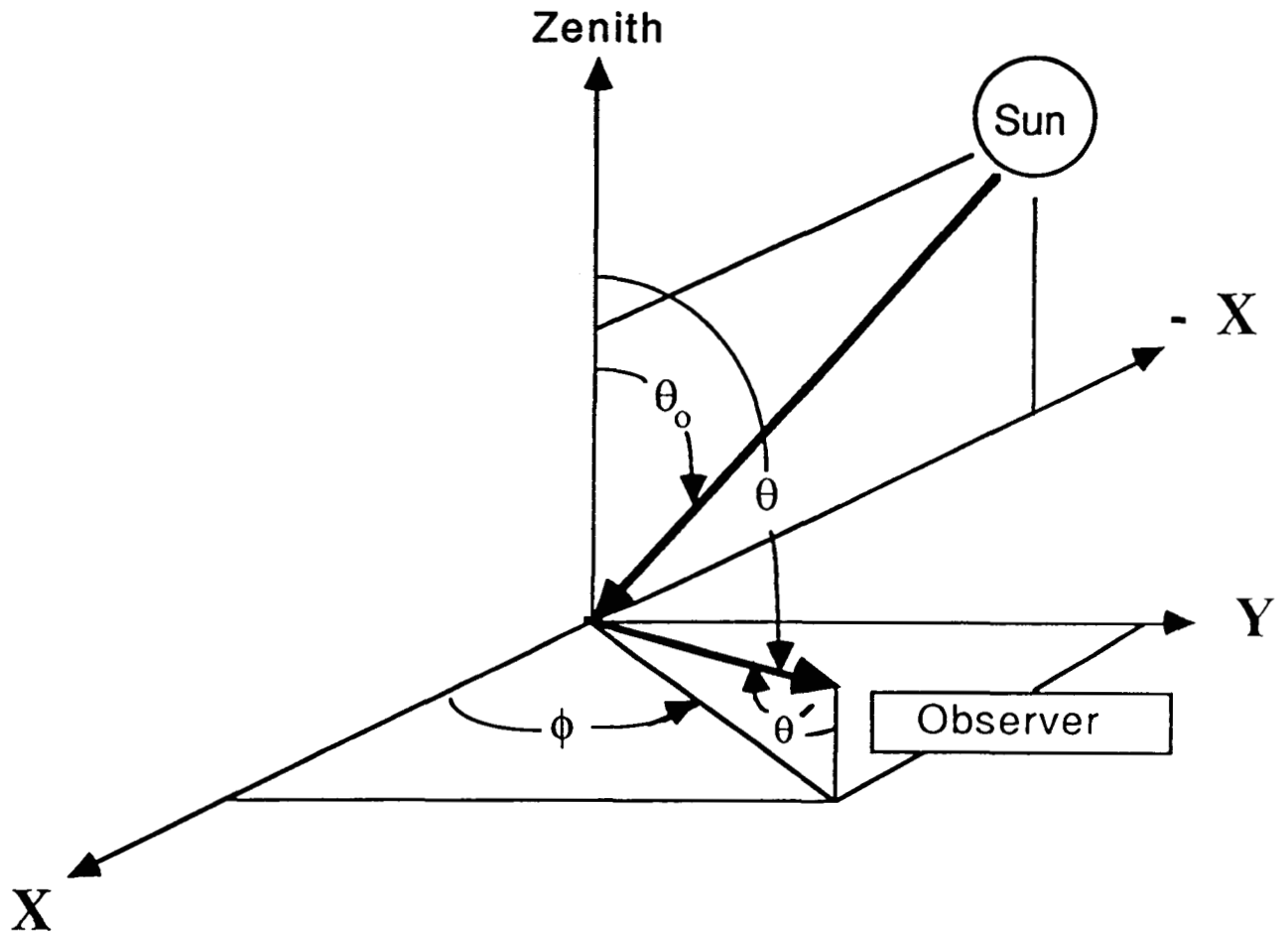


Figure 2. Angular coordinates used in the algorithm. The X-Y plane is a horizontal plane tangent to the earth's surface at the observation point. The solar zenith angle θ_o , observation zenith angle θ , observation scan angle θ' , and observation azimuth angle ϕ are shown. In this particular representation of planar geometry $\theta = \theta'$; the general relationship is given by eq. (9).

and the upward radiance L_g at the ground in the direction of observation.

$$L_g = \frac{\rho F_d}{\pi (1 - s \rho)} \quad (5)$$

3.0 Correction Algorithm

The correction program is based on the tabulation of the results of radiative transfer computations of L_o , F_d , s , and T/π (note that the transmission T is not tabulated). The primed parameters are normalized flux and radiance rather than their absolute values. The normalized values are related to their corresponding absolute values by the following equations:

$$F'_d(\theta_o, \tau_a) = \frac{F_d}{F_o \cos \theta_o} \quad L'_o(\theta_o, \theta, \phi, \tau_a, Z) = \frac{\pi L_o}{F_o \cos \theta_o} \quad (6)$$

The value of F_o represents the solar spectral flux passing through a surface orthogonal to its propagation at the top of the atmosphere. In order to use the table for atmospheric correction, the measured absolute radiance L^m is converted to $L^{m'}$ using

$$L^{m'} = \frac{\pi L^m}{F_o' \cos \theta_o} \quad (7)$$

where

$$F_o' = \frac{F_o}{R^2} \quad R = \frac{d}{d'} \quad (8)$$

and d is earth-sun distance for the day of the year when measurements are made, d' is the mean earth-sun distance, and F_o is the solar flux now computed for each of the spectral bands using the solar spectral flux data from Neckel and Labs (1984). Since the look-up table tabulates observation zenith angle θ of the line-of-sight from the ground to the observing platform, the scan angle θ' measured by aircraft or satellite is converted to observation zenith angle θ using

$$\theta = \sin^{-1} \left[\left(1 + \frac{Z}{r_s} \right) \sin \theta' \right] \quad (9)$$

where Z is the height of the sensor above the ground, and r_s is the radius of the earth.

The computations are performed by a Dave code (1972a, b, c, d) with a series of radiative transfer programs. These programs compute the flux and radiance of the scattered radiation emerging at any level of a plane-parallel atmosphere. Henceforth, primed fluxes and radiances indicate that they have been normalized as in eq. 6. Variables with the superscript m are measured.

3.1 Model Wavelengths

The look-up table is computed for the following wavelengths: 0.639, 0.845, 0.486, 0.587, 0.663, 0.837, 1.663, and 2.189 μm which correspond to the following sensors: NOAA-9 AVHRR band 1 (0.58 - 0.68 μm), band 2 (0.725 - 1.10 μm); Landsat-5 TM and NS-001 TMS band 1 (0.45 - 0.52 μm), band 2 (0.52 - 0.60 μm), band 3 (0.63 - 0.69 μm), band 4 (0.76 - 0.90 μm), band 5 (1.55 - 1.80 μm), and band 7 (2.10 - 2.35 μm). These wavelengths are listed in Table 1. The wavelength chosen to represent a particular band is computed by first calculating λ^*

$$\lambda^* = \frac{\int \lambda L^{m'} F_o \Psi d\lambda}{\int L^{m'} F_o \Psi d\lambda} \quad (10)$$

where

$L^{m'}$ = normalized radiance at the top of the atmosphere

F_o = extraterrestrial solar spectral flux

Ψ = response function of the sensor

The values for F_o are obtained from Neckel and Labs (1984) while the values for Ψ correspond to the specific sensor. For the NOAA-9 AVHRR and Landsat TM sensors, these values are obtained from Kidwell (1985) and Markham and Barker (1985), respectively. The effective wavelength λ^* in eq. 10 is a function of the normalized radiance, which is a function of the surface reflectance, aerosol optical thickness, and

Table 1. Spectral bands, aerosol refractive indices, and optical thicknesses.

	AVHRR				TM			
	1	2	1	2	3	4	5	7
<u>Sensor Wavelengths</u>								
50% minimum response (nm)	569.8	714.3	452.4	528.0	626.4	776.4	1567.5	2097.2
50% maximum response (nm)	699.3	982.2	517.8	609.3	693.2	904.5	1784.1	2349.0
peak response (nm)	680.0	760.0	503.0	594.0	677.0	800.0	1710.0	2200.0
model (equation 7) (nm)	639.0	844.6	486.2	586.9	662.7	837.3	1662.7	2188.6
<u>Indices of Refraction</u>								
n' (accumulation mode)	1.43	1.43	1.43	1.43	1.43	1.43	1.40	1.40
k (accumulation mode)	10 ⁻⁸	10 ⁻⁸	10 ⁻⁸	10 ⁻⁸	10 ⁻⁸	10 ⁻⁸	10 ⁻⁴	10 ⁻⁴
n' (coarse particle mode)	1.53	1.53	1.53	1.53	1.53	1.53	1.40	1.35
k (coarse particle mode)	10 ⁻⁷	10 ⁻⁷	10 ⁻⁷	10 ⁻⁷	10 ⁻⁷	10 ⁻⁷	10 ⁻⁴	0.00814
<u>Optical Thicknesses</u>								
<u>Molecular Scattering</u> τ_{gs}	0.0540	0.0180	0.159	0.0841	0.0449	0.0176	0.0012	0.0004
<u>Gaseous Absorption</u>								
Ozone $\tau_g^{O_3}$	0.0240	0.00064	0.00663	0.0317	0.0174	0.0000	0.0000	0.0000
Water Vapor $\tau_g^{H_2O}$	0.00605	0.0933	0.00000	0.0002	0.0068	0.0410	0.0957	0.0741
Carbon Dioxide $\tau_g^{CO_2}$	0.00071	0.0146	0.0000	0.0000	0.0000	0.0021	0.0077	0.0091
<u>Aerosol Absorption</u> ($\tau_a = 0.25$)								
τ_a^a	0.0148	0.0223	0.0130	0.0142	0.0150	0.0218	0.0423	0.0189
<u>Composite (section 3.3)</u>								
τ_g^H	0.0247	0.0152	0.0066	0.0317	0.0174	0.00206	0.00771	0.00908
τ_g^L	0.0208	0.1156	0.0130	0.0142	0.0218	0.0628	0.138	0.0930
τ_g	0.0455	0.131	0.0196	0.0459	0.0392	0.0648	0.146	0.102

geometry. The normalized radiance is computed for different models of the earth-atmosphere system representative of surface and atmospheric conditions expected for the FIFE Konza Prairie site. Figure 3 shows the surface reflectance profiles used to model this site. A similar approach can be used to determine the wavelengths which correspond to other sensors.

The algorithm is generalized to accept any wavelength in the range 0.48-2.2 μm . For wavelengths for which there are no entries in the look-up table (see Table 1), the algorithm will interpolate the atmospheric functions (L_0 , T , F_d , s) for the desired wavelength. The interpolation is performed assuming that aerosol parameters are proportional to the wavelength raised to a power:

$$\ln \tau_{gs} \sim -\ln \lambda, \quad \ln \tau_a \sim -\ln \lambda, \quad \ln P \sim \ln \lambda,$$

where P is the scattering phase function. As a result, the radiances in the look-up table can be interpolated linearly between the wavelengths on a log - log scale. The only nonlinear relation is between the gaseous absorptions in the different wavelengths. Correction for the gaseous absorption is discussed in section 3.3.

3.2 Aerosol Properties

Because the absorption and scattering of light by atmospheric aerosols is highly variable, some assumptions regarding the size, shape, and composition of the aerosol must be made. In this model, the aerosols are assumed to be spheres so that Mie theory can be used to calculate the scattering by aerosols. Although in general the aerosol particles are not spherical, it is assumed that the sizes assigned to the aerosol particles are the sizes of spheres that have similar scattering properties to the measured aerosol distribution (Shettle and Fenn, 1979). This assumption has further basis because it has been found that the aerosol particles become more spherical as the relative humidity increases (Nilsson, 1979).

The algorithm uses a bimodal aerosol size distribution which combines the optically effective fraction of the accumulation mode ($0.1 \mu\text{m} \leq d \leq 1.0 \mu\text{m}$) and the coarse particle mode ($d > 0.5 \mu\text{m}$). For the accumulation mode, the dry particles are assumed to be composed of 80% water soluble sulfates and 20% water insoluble, dust-like material (Nilsson, 1979). At 70% relative humidity, water composes half of the volume of these aerosols. The coarse particle mode aerosols are assumed to be made of mostly water insoluble, dust-like particles. The size distribution of the aerosols is represented as the sum of two log-normal distributions; the two distributions represent the accumulation and coarse

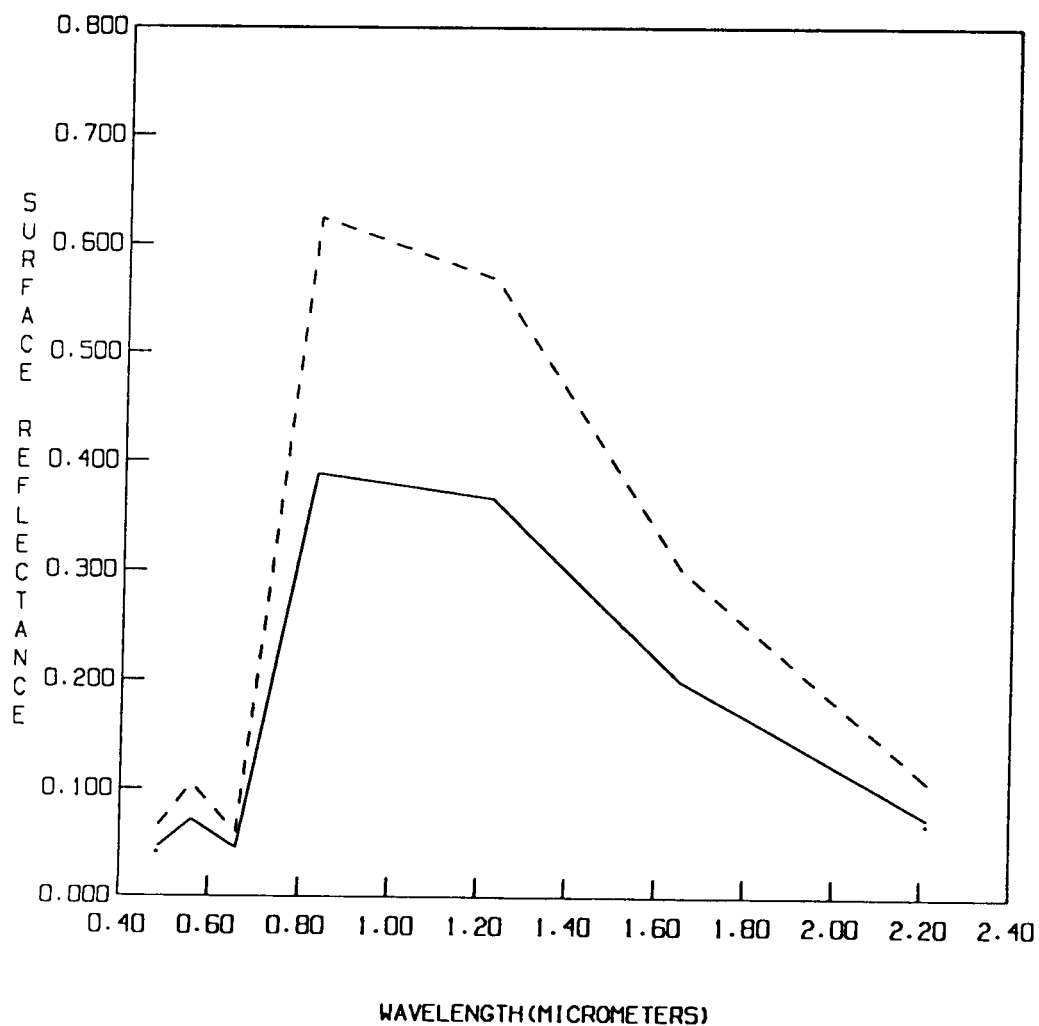


Figure 3. Surface reflectance for senescent grass from a burned surface on the Konza Prairie at the FIFE site. The first profile (—) is for nadir view, measured at 14:38 CDT on 15 July 1986 while the second profile (- - -) is for an observation zenith angle of 45° measured at 15:13 CDT on 15 July 1986 (Asrar, 1986, private communication).

particle modes. The number density function of particles of radius r per cubic centimeter of air per micrometer of radius is (Shettle and Fenn, 1979)

$$n(r) = \frac{dN(r)}{dr} = \sum_{i=1}^2 \left[\frac{N_i}{\ln(10) r \sigma_i \sqrt{2\pi}} \right] \exp \left[\frac{-(\log r - \log r_n^i)^2}{2\sigma_i^2} \right] \quad (11)$$

where

$N(r)$ = cumulative number density of particles of radius r

σ_i = standard deviation of the logarithm of the radius

r_n^i = geometric mean radius

N_i = total number density in i^{th} mode

The values of N_i , r_n^i , and σ_i used in the model correspond to the 70% relative humidity, rural aerosol model of Shettle and Fenn (1979); these values are shown in Table 2. The values of N_i shown in Table 2 are normalized such that $N_1 + N_2 = 1$ particle/cm³. This bimodal aerosol size distribution is assumed constant with height.

The composition of the aerosols is expressed in terms of the complex refractive index $n = n' - i k$. The refractive index for both the accumulation and coarse particle modes is assumed to depend on the wavelength. Five different real refractive indices are chosen (Nilsson, 1979) and are listed in Table 1. The imaginary index of refraction is modeled assuming that most of the aerosol consists of weakly absorbing particles with $k < 10^{-4}$, mixed with a small number of highly absorbing particles with $k \sim 1.0$. Although Shettle and Fenn (1979) choose to represent mixtures of this type with a composite imaginary refractive index in the range $0.001 < k < 0.01$, which is close to the values obtained by various remote sensing and in-situ techniques (Patterson and Grams, 1984; Reagan et al., 1980), this procedure is not adopted here because as Bohren and Huffman (1983) point out, no common substances exist which have an imaginary index in this range. In the correction algorithm, the imaginary refractive index corresponding to the weakly absorbing particles is used. The imaginary refractive indices for the accumulation mode, which are listed in Table 1, correspond to water while the values for the coarse particle mode correspond to crystalline quartz, which is a constituent of atmospheric dust (Nilsson, 1979). The aerosol refractive index is assumed to be constant with height.

Table 2. Aerosol size distribution parameters.

	<u>Accumulation mode</u>	<u>Coarse particle mode</u>
Geometric mean radius r_n^i	0.0285	0.457
Standard deviation of the logarithm (base 10) of the radius σ_i	0.81	0.81
Number density N_i	0.999875	0.000125

The aerosol absorption needed to match the experimentally measured value is modeled by adding the necessary absorption to the gaseous absorption values. Thus, it is assumed that the absorbing particles are small compared to the wavelength and that they occur separately from the other particles (external mode); in this case their scattering effects are small relative to their absorptive effects (Fraser and Kaufman, 1985). The required additional aerosol absorption amount is determined by the aerosol single scattering albedo ω_0 which is the ratio of scattering to extinction. Aerosol absorption is then given by $1 - \omega_0$. The values of ω_0 used in the algorithm are derived from the 70% relative humidity, rural aerosol model of Shettle and Fenn (1979). The single scattering albedos, shown in Table 1, range from 0.95 at 0.486 μm to 0.86 at 2.550 μm . These values for the visible spectrum agree with those reported by Waggoner et al. (1981) which lie in the range $0.89 \leq \omega_0 \leq 1.0$ for rural areas. The amount of additional aerosol absorption which is added to the gaseous absorption is

$$\tau_a^a = \tau_a (\omega_o' - \omega_o) \quad (12)$$

where

τ_a = aerosol optical thickness

ω_o' = single scattering albedo for chosen refractive index

ω_o = desired single scattering albedo

Since in general $k \ll 1$, then $\omega_o' \approx 1$, and

$$\tau_a^a \approx \tau_a (1 - \omega_o) \quad (13)$$

Should the algorithm be applied for an urban aerosol or smoke, where the single scattering albedo ω_o used in the formation of the look-up tables (see Table 1) may be smaller or larger than the new value ω_o^* , the difference in absorption can be corrected by adding (or subtracting) the excess absorption to the gaseous absorption:

$$\Delta\tau_a^a = \tau_a (\omega_o - \omega_o^*) \quad (14)$$

3.3 Gaseous Absorption

For the most part, the Landsat TM and NOAA AVHRR visible and near IR bands have been selected to minimize gaseous absorption. However, in some cases, the sensor

channel is either relatively broad (as in the case of AVHRR band 2) or lies within a broad gaseous absorption band (as in the case of TM bands 2 and 3 which lie within the ozone continuum) so that the absorption by atmospheric gases can be both significant and variable. In the atmospheric correction algorithm, gaseous absorption was computed using the LOWTRAN 6 code (Kneizys et. al., 1983) which computes atmospheric absorption from 0.250 μm to 28.5 μm due to water vapor, carbon dioxide (and other uniformly mixed gases), ozone, nitrogen continuum, oxygen, and HNO_3 . In the case of the AVHRR and TM bands, the absorbing gases are water vapor, carbon dioxide, and ozone. The gaseous absorption optical thickness in the vertical direction due to gaseous species x for each band is computed using

$$\tau_g^x = -\frac{1}{m} \ln \left[\frac{\int T_x L^{m'} F_o \Psi d\lambda}{\int L^{m'} F_o \Psi d\lambda} \right] \quad (15)$$

where

m = air mass along inclined path

T_x = transmittance due to gaseous species x

Since the gaseous absorption is quite variable, the algorithm uses a weighted average of the absorption values computed using the tropical, mid-latitude summer, and mid-latitude winter atmospheres given in the LOWTRAN 6 code. The weighted average of the gaseous absorption τ_g^{x*} used in the algorithm is given by

$$\tau_g^{x*} = 0.25 \tau_{g1}^x + 0.5 \tau_{g2}^x + 0.25 \tau_{g3}^x \quad (16)$$

where τ_{g1}^x , τ_{g2}^x , and τ_{g3}^x are the gaseous absorption values computed using the mid-latitude winter, mid-latitude summer, and tropical values respectively. The absorption optical thicknesses due to water vapor, carbon dioxide, and ozone for each band are shown in Table 1.

The algorithm can be applied to any specified gaseous optical thickness τ_g . An approximate correction is applied to the radiances in the look-up table to account for the excess (or deficit) in the absorption ($\Delta\tau_g$). The user may compute the required value of τ_g based on the sensor spectral response using the LOWTRAN program (Kneizys et al., 1983). For the correction of the look-up table we may distinguish between $\Delta\tau_{gL}$ - excess

or deficit in the gaseous absorption in the lower part of the atmosphere (e.g. water vapor), assumed to be mixed uniformly with the aerosol; and $\Delta\tau_{gH}$ excess or deficit in the gaseous absorption in the upper part of the atmosphere, above the aerosol layer (e.g. O₂, O₃, CO₂). The correction is performed by the following transformations in the look-up table:

$$L_o \rightarrow L_o \exp \left[- \left(\frac{\Delta\tau_{gL}}{2} + \Delta\tau_{gH} \right) \left(\frac{1}{\mu} + \frac{1}{\mu_o} \right) \right] \quad (17a)$$

$$F_d \rightarrow F_d \exp \left[\frac{ - (\Delta\tau_{gL} + \Delta\tau_{gH}) }{\mu_o} \right] \quad (17b)$$

$$T \rightarrow T \exp \left[\frac{ - (\Delta\tau_{gL} + \Delta\tau_{gH}) }{\mu} \right] \quad (17c)$$

$$s \rightarrow s \exp \left[- 2 \Delta\tau_{gL} \right] \quad (17d)$$

Here $\mu = \cos \theta$ and $\mu_o = \cos \theta_o$. In these equations the effect of multiple scattering on the path length through the atmosphere is neglected. It is also assumed that the path radiance L_o is generated above the middle of the boundary layer. As result, the additional gaseous attenuation is made by half of the boundary layer, but all of the atmosphere above. The parameter s is the reflectance of the atmosphere for radiation entering its base. The effective direction for reflection is 60°. Hence, the effective absorption optical thickness is twice the vertical value. Theses assumptions are based on our physical understanding of radiative transfer and are tested in Section 6.

3.4 Altitude Profiles

The radiative transfer computations require as input the altitude distributions of both the absorbing gases and aerosols. These two distributions have separate profiles. The altitude distribution of aerosols used in the algorithm is based on the 'average' distribution of Braslau and Dave (1973) which is shown in Figure 4. The aerosol altitude distribution is first scaled to obtain the desired aerosol optical thickness.

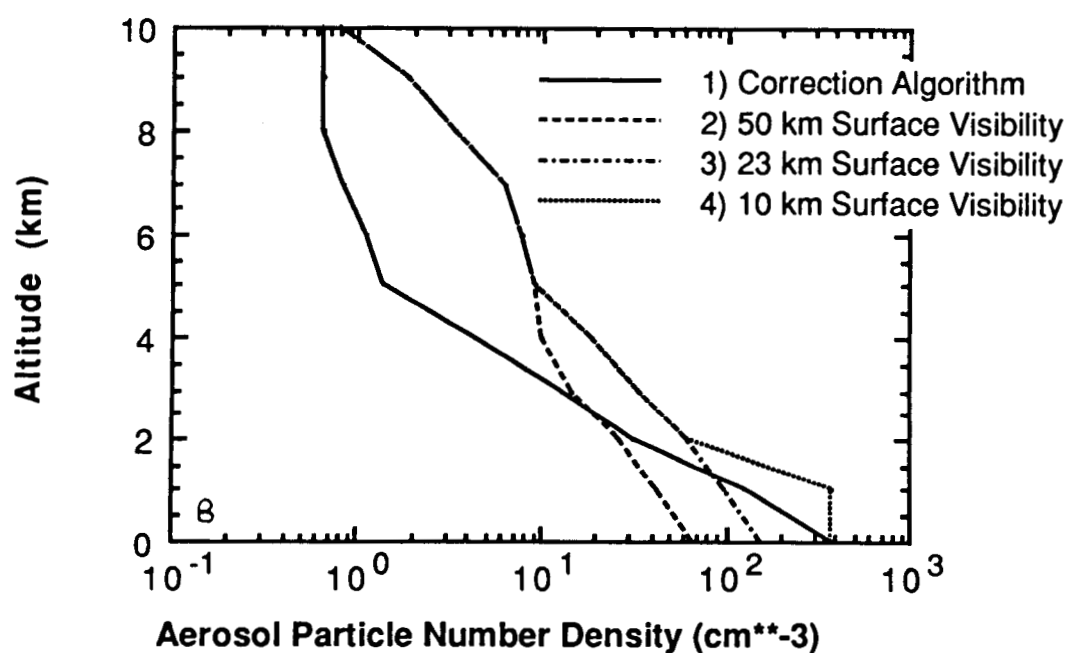
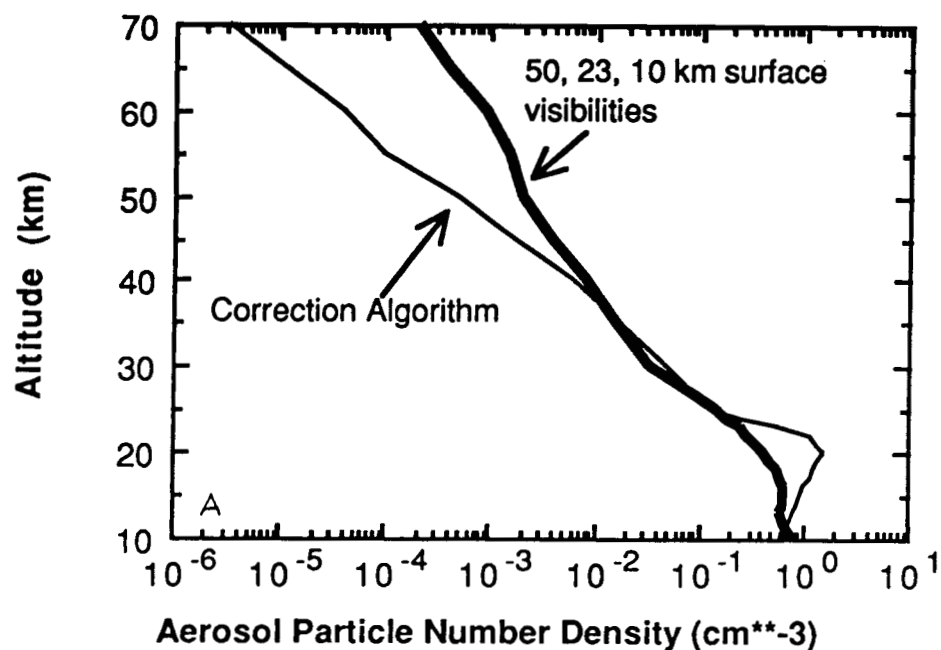


Figure 4. Aerosol particle number density profiles for: 1) 'average' distribution of Braslau and Dave (1973) used in the correction algorithm; 2) 50 km surface visibility, 3) 23 km surface visibility, and 4) 10 km surface visibility models from Shettle and Fenn (1979). Figure 4a is for altitudes between 10 and 70 km while figure 4b is for altitudes between 0 and 10 km. These profiles have been normalized for an aerosol optical thickness $\tau_a = 0.25$ at 0.55 μm .

Because the various gaseous absorbers described in the previous section have different altitude distributions, a composite altitude distribution is computed which accounts for all the absorbing gases including the aerosol absorption described in section 2.2. In this method, the total gaseous absorption is divided into "low" and "high" components. The "low" component is composed of water vapor and aerosol absorption while the "high" component is composed of ozone and CO₂ absorption. The "low" component uses an altitude distribution based on the 'average' aerosol profile of Braslau and Dave (1973), while the "high" component uses an altitude distribution based on the mid-latitude ozone profile of McClatchey et al. (1971). The altitude distributions of the "low" and "high" components are normalized and combined to produce an altitude profile that retains the maximum aerosol and water vapor absorption near the surface and the maximum ozone absorption in the lower stratosphere. Because the aerosol absorption is a function of the aerosol optical thickness (see eq. 13), the gaseous absorption profile is a function of aerosol optical thickness as well as wavelength. The atmospheric pressure profile used in the algorithm is adapted from the mid-latitude summer profile of McClatchey et al. (1971).

3.5 Molecular and Aerosol Optical Thickness

The molecular scattering (or Rayleigh) optical thickness τ_{gs} is computed for sea level from (Hansen and Travis, 1974)

$$\tau_{gs} = 0.008569 \lambda^{-4} (1 + 0.0113 \lambda^{-2} + 0.00013 \lambda^{-4}) \quad (18)$$

where the wavelength is in micrometers. This expression assumes the surface sea-level pressure is 1013 mb. In the case the surface is not at sea level. The value of the molecular scattering optical thickness τ_{gs} is assumed to vary according to:

$$\tau_{gs}(Z_0) = \tau_{gs}(0) \exp\left(\frac{-Z_0}{9}\right) \quad (19)$$

where Z_0 is the height of the surface above sea level in kilometers. In order to avoid a need for a new radiative transfer computation for each height of a surface, the computations are performed for $Z_0 = 0.4$ km, and the look-up table is adjusted each time the user specifies a different height. The algorithm adjusts the look-up table to account for the different molecular optical thickness by adjusting the wavelength of the radiation. Substitution of the relationship between λ and τ_{gs} (eq. 18) yields

$$\lambda(Z_0) = \lambda(0.4) \exp \left[\frac{(Z_0 - 0.4)}{36} \right] \quad (20)$$

For example, for $Z_0 = 0$ km, λ will increase by 1.1%, whereas for $Z_0 = 2$ km, λ will increase by 4.3%. The error introduced by this method is in the effective scattering phase function, but this change is negligible relative to the general uncertainty in the scattering phase function due to the uncertainty in the aerosol size distribution.

The relation between upward radiance and surface reflectance for each spectral band is computed for four aerosol optical thicknesses, $\tau_a = 0.0, 0.25, 0.50$, and 1.00 , except for TM bands 5 and 7 where only the first two values are used. These values are selected to cover the range of aerosol optical thicknesses which could be expected for most remote sensing applications.

3.6 Measurement Altitudes

The radiative transfer computations are tabulated at three measurement altitudes above the ground: 0.45 km, 4.5 km, and 80 km. The algorithm will use these altitudes to interpolate to the input measurement altitude. Since 80.0 kilometers is above the atmosphere, corrections to satellite measurements are made with the 80 km tables.

For altitudes less than 0.45 km, it is assumed that the aerosols and the absorbing gases are well mixed and it is possible to linearly interpolate between the atmospheric optical properties (L_0 and T) at $Z = 0$ km and at $Z = 0.45$ km above the ground:

$$L_0(Z) = L_0(Z = 0.45) \left(\frac{Z}{0.45} \right) \quad (21a)$$

$$T(Z) = (T(0.45) Z + (0.45 - Z)) / 0.45 \quad (21b)$$

For altitudes above 4.5 km, interpolations are performed between values of L_0 and T at 4.5 km and 80 km. Although the atmospheric model contains aerosols between these altitudes, the interpolations are based on the assumption that L_0 and T depend essentially on molecular scattering between 4.5 and 80 km. The interpolations are performed linearly as a function of the molecular scattering coefficient $\sigma_{gs}(Z)$:

$$\sigma_{gs}(Z) = \sigma_{gs}(0) \exp \left(\frac{-Z}{9} \right) \quad (22)$$

Hence the transmission and L_0 become

$$T(Z) = (T(80.0) - T(4.5)) * \frac{\exp(-4.5/9) - \exp(-Z/9)}{\exp(-4.5/9) - \exp(80/9)} \quad (23)$$

$$L_o(Z) = (L_o(80.0) - L_o(4.5)) * \frac{\exp(-4.5/9) - \exp(-Z/9)}{\exp(-4.5/9) - \exp(80/9)} \quad (24)$$

Between 0.45 km and 4.5 km the interpolation is uncertain due to the inhomogeneity of the aerosol layer. Since the linear interpolation used below 0.45 km is usually suitable to extrapolate for heights below 1 km, and the aerosol concentration decreases rapidly above 3 km so that the interpolation used above 4.5 km is appropriate for extrapolation to heights between 3 and 4.5 km, the algorithm extrapolates from these two regions to the desired height h ($0.45 \text{ km} < Z < 4.5 \text{ km}$), and chooses the result that shows a minimal atmospheric effect. Thus, the lower values of L_o and higher values of T are chosen for the solution.

4.0 Look-up Tables

The look-up tables used by the correction algorithm contain the normalized radiances and fluxes computed by the radiative transfer routines. The values generated are stored to be used by the main program. Eight look-up tables are produced, one table for each of the 2 AVHRR bands of 0.639 and 0.845 μm and one for each of the 6 TM bands of 0.486, 0.587, 0.663, 0.837, 1.663 and 2.189 μm . Each table is arranged for 3 heights of 0.45, 4.5 and 80.0 kilometers. Each table contains values for 9 solar zenith angles θ_o (10, 20, 30, 40, 50, 60, 66, 72, and 78°), 13 observation zenith angles θ (0° to 78°, every 6°), 19 observation azimuth angles (0° to 180°, every 10°, plus 5° and 175°), and 4 aerosol optical thicknesses τ_a (0.0, 0.25, 0.50 and 1.0) for all wavelengths, except for 1.663 and 2.189 μm where only first two optical thicknesses of 0.0 and 0.25 are used.

5.0 Computational Procedure

5.1 General

Input data to the correction program consists of the date, time, measurement wavelength, aerosol and gaseous absorption optical thicknesses at the measurement wavelength λ , solar zenith angle θ_o , observation scan angle θ' , observation azimuth angle ϕ , height of the surface above sea level Z_o , measurement height Z^m , and the measured spectral radiance in absolute L^m or reflectance $L^{m'}$ units (option 1), or surface reflectance ρ (option 2). The wavelength, solar and observation angles, and aerosol optical thickness

data must be in the ranges discussed above as no extrapolation is performed. If the selected wavelength or altitude does not match the values used to construct the look-up table, the algorithm interpolates on wavelength and altitude as described above.

If option 1 is selected, the program computes the surface reflectance ρ , total spectral irradiance on the surface F_g , and total spectral radiance of the ground L_g in the direction of observation using eq. 2, 3, 4 and 5. The total spectral irradiance F_g is computed in Watts/m²/μm and total upward spectral radiance L_g is computed in Watts/m²/μm/sr. If option 2 is selected, the program computes the absolute and normalized radiances L^m and $L^{m'}$, total spectral irradiance on surface F_g and the total upward spectral radiance L_g in Watts/m²/μm/sr.

The program for making atmospheric corrections consists of a main program called **FIFEWAV**. The computations are performed in single precision and seven subroutines are called at different stages by the main program. The listings of the main program and subroutines are given in section 9. The statement numbers for the program and subroutines are given in parentheses. Table 3 lists the variables appearing in the main program and associated subroutines and their equivalent in the text. The asterisk superscript indicates interpolated values. The subroutines called by the main program **FIFEWAV** are listed below:

Subroutine **READIN** (6350 - 6580): This subroutine reads the input data from unit number 5 and writes it on unit number 6. The purpose of this subroutine is to perform a check on the input data set.

Subroutine **FINDW** (6620 - 6860) : This subroutine checks to see if λ^m falls in the range of wavelengths for which look-up tables are available and picks two wavelengths between which λ^m falls. The subroutine prints an error message and returns the control to the main program if λ^m does not fall in the range of wavelengths look-up table provides. The main program processes a new data point.

Subroutine **INTSFX** (6900 - 7100): This subroutine computes values of the sun-earth distance R for 365 days of the year. These values are returned to the main program, which chooses the value of R for the day the measurements were made.

Subroutine **INTHGH** (7140 - 8530): This subroutine computes interpolated values of L_0 and T/π for the measured height $MHGH$ (eq. 21a , 21b, 23 and 24). The transmission T is divided by π to account for the π appearing in eq. (1).

Table 3. Variables appearing in FIFEWAV program and associated subroutines, and their equivalent in the text.

VARIABLES IN PROGRAM	VARIABLES IN TEXT	
ABSRAD	L_g	(section 5)
AIRR	F_g^*	(section 5)
AMU0	$\text{Cosine}(\theta_0^m)$	(eq. 1, 22)
ANGLE, PHI	ϕ	(eq. 1)
ARAD	L_g^*	(section 5)
FDOWN	F_d	(section 5)
FFLUX	F_o'	(eq. 22, 23)
FINT	L_o^*	(section 5)
FOIRR	F_o	(eq. 6)
FT	T^*/π	(section 5)
INT	L_o'	(section 5)
IRRID	F_g	(section 5)
MHGHT	Z^m	(eq. 1)
MINT	L^m, L'^m	(eq. 1, 22)
MPHI	ϕ^m	(eq. 1)
MTAU	τ_a^m	(eq. 1)
MTHET	θ^m	(eq. 1)
MTHETO	θ_0^m	(eq. 1)
MWAV	λ^m	(eq. 1)
NFDOWN	$F_d'^*$	(section 5)
OPTH	τ_a	(eq. 1)
PIT	T/π	(section 5)
R, RR	R	(eq. 23)
RHO	ρ	(section 5)
RHOS	ρ^*	(section 5)
SBAR	s	(eq. 1)
THE	θ	(eq. 1)
THETO	θ_0	(eq. 1)
WAV	λ	(eq. 1)

Subroutine **INTERP** (8570 - 9020): The purpose of this subroutine is to return to the main program the interpolated values of L_o^* , F_d^* , T^*/π , and s^* . This is a general purpose interpolation routine and is called at different stages by the main program. This subroutine does not allow any extrapolation and an error message is printed when the values are out of bounds. The asterisk indicates in most cases values interpolated from the look-up table.

Subroutine **INTEXP** (9040 - 9840): This subroutine sends exponentially interpolated values of L_o^* , F_d^* , T^*/π and s^* for the measured optical thickness MTAU. It calls a systems subroutine ZXGSN residing in IMSL math package.

Subroutine **ZXGSN** (9520): This subroutine is called by subroutine **INTEXP**, it computes the minimum of function on certain interval which is used for exponential interpolation.

PROCEDURE:

Subroutine **READIN** is called (490) to read the input data from unit number 5 and write it on unit number 6 as well as to perform a check on the input data. The main program reads the first two data cards from unit number 5 and writes the labels for output on unit number 6 and 56 (690 - 840). The program reads from unit 20 the solar spectral irradiances, which are used to compute the solar flux for the measured wavelength MWAV (870 - 950). The program enters into a loop over the number (INUM) of data points to be processed (1020). The program reads the values of time, λ^m , τ_a^m , θ_o^m , θ^m , ϕ^m , Z^m , L^m or L^m , τ_{gL} , τ_{gH} , and Z_0 if NOPT is 1, and values of time, λ^m , τ_a^m , θ_o^m , θ^m , ϕ^m , Z^m , ρ^m , τ_{gL} , τ_{gH} and Z_0 if NOPT is 2 (1190 - 1230). If values of absorptions τ_{gL} and τ_{gH} are 0.0, default values are computed by interpolating linearly from the values of TAUGL(λ) and TAUGH(λ) (330 - 340) for the measured wavelength λ^m (1300 - 1600).

Subroutine **FINDW** is called to select the look-up table for the two wavelengths between which λ^m lies by assigning the proper file number NFILE1 and NFILE2 (1700 - 1740). A new data point is read if subroutine **FINDW** does not find the input wavelength lying in the range of wavelengths for which look-up table is provided (0.486 - 2.2 μm).

The ratio of earth-sun distance (R, eq. 8) is computed for 365 days of the year by subroutine **INTSFX**. The program (1870 - 2020) changes the month and day to the

Julian day if MOPT is 1. The corrected values of incident solar flux F'_0 are computed by using eq. 8 (2150).

The observation scan angle of satellite or aircraft is changed to observation zenith angle at the ground by using eq. 9 (2250).

Statements (2610 - 3040) read the look-up table chosen for the two wavelengths on each side of the measured wave length λ^m . The parameters θ , ϕ , λ , τ_a , θ_0 , s , F'_d , L'_0 , and T/π are read for four optical thicknesses, except for wavelengths of 1.663 μm and 2.189 μm , for which look-up tables are available for only two optical thicknesses of 0.0 and 0.25. The subroutine INTHGH (3120) is called to compute the interpolated values of L'_0 and T/π for the measured height MHGHT (eq. 21a, 21b, 23 and 24). The statements (3170 - 3180) adjust the look-up table for the surface height SHGHT and then interpolate values of s , F'_d , L'_0 and T/π (3230 - 3410) for the measured wavelength λ^m (see documentation sec. 3.1). The excess or deficit gaseous absorption in the upper and lower atmosphere is computed (3450 - 3500) using τ_{gL} and τ_{gH} whose values are supplied as input parameters; or if values read are zero, default values computed earlier in program (1300 - 1600) are used. New values of s , L'_0 , F'_d , and T/π are computed (3540 - 3780) after adjusting for the excess and deficit of gaseous absorption (eq. 17a, 17b, 17c, and 17d).

The next step is to compute the interpolated values of L'_0 , F'_d , and T/π for the measured height and geometry (θ_0^m , θ^m , and ϕ^m). The mesh of the tables is small enough to allow accurate linear interpolations. The interpolations are made for each of the four aerosol optical thicknesses: 0.00, 0.25, 0.50, and 1.00. L'^*_0 is interpolated from the data set L'_0 for θ_0^m , ϕ^m , and θ^m ; F'^*_d is interpolated from the data set F'_d for θ_0^m ; and T^*/π is interpolated from the data set T/π for θ_m . To make these interpolations, subroutine INTERP (4050 - 4140) is called to compute the interpolated values of both L'_0 and F'_d for θ_0^m . The part of program between 4270 to 4430 calls subroutine INTERP to compute the interpolated values of L'_0 for ϕ_m . Subroutine INTERP is called again to compute the interpolated value of L'_0 and T/π for θ_m (4680 - 4770). If the measured θ_0^m , ϕ^m , or θ^m are out of the range of data tabulated for θ_0 , ϕ , and θ , subroutine INTERP returns control to the main program after printing an appropriate message. It does not allow any extrapolation. The program will then process a new data point if the error message is printed.

Subroutine INTEXP (4910) is called to perform exponential interpolations on four radiation parameters L_o^* , F_d^* , s , and T^*/π for measured optical thickness MTAU(4960 - 5190). Subroutine INTEXP checks the four parameters one by one for linearity and sends the control back to the main program if any of the functions are linear. The main program then calls the subroutine INTERP to perform linear interpolation.

Statement 5270 sends control to statement 5550 to compute the spectral radiance, if NOPT is 2. Statements 5280 to 5380 use the interpolated values L_o^* , F_d^* , and T^*/π to compute the surface reflectance ρ , total spectral irradiance F_g , and total spectral radiance of the ground L_g in the direction of observation (eq. 2, 3, and 4). The total spectral irradiance F_g is computed in Watts/m²/μm, and the total upward spectral radiance L_g is computed in Watts/m²/μm/sr. Statements 5440 - 5450 write the output on FORTRAN logical units 6 and 56.

Statements 5540 - 5790 use the interpolated values L_o^* , F_d^* , and T^*/π to compute the spectral radiance L^m , total spectral irradiance F_g , and total spectral radiance of the ground L_g in the direction of observation (eq. 2, 3, and 4) if MOPT is 2. The total spectral irradiance F_g is computed in Watts/m²/μm, and the total upward spectral radiance L_g is computed in Watts/m²/μm/sr. The output is written on FORTRAN logical units 6 and 56.

5.2 Input

Input data to this program consists of two input files. The first file (FORTRAN logical unit number 5) describes input to a particular case, while the second file (FORTRAN logical unit number 20) reads solar spectral irradiances (Neckel and Labs, 1984) as function of wavelength. The program uses 8 look-up tables which are not to be changed by the user (FORTRAN logical unit numbers 7 - 14). In order to demonstrate the input data, four cases representative of different options are presented. The input cards for all four runs are listed in Table 4.

INPUT FROM UNIT NUMBER 5: (see Table 4)

1. The first card contains the labels to identify the input parameters in step 2 below.
2. The second card contains the options for determining the units for the measured reflectance or radiance, the format for the date of the measured data, and the option either to compute the surface reflectance or radiance.

TABLE 4. EXAMPLES OF INPUT DATA.

```

(RUN 1)
IOPT  MOPT NOPT
  1    1    1
INUM   MON DAY YEAR  TIME  ZONE
  6    7  28 1987  CDT
TIME  MWAV  MTAU  MTHETO  MTHET  MPHI  MHGHT  MINT    TAUL    TAUH    SHGHT
1010  0.486 0.250 26.00   0.00   0.00  80.00  00.11409 00.0001 00.0070 00.400
1011  0.486 0.250 26.00   0.00   0.00   4.50  00.08089 00.0001 00.0070 00.400
1012  0.486 0.250 26.00   0.00   0.00   0.45  00.05125 00.0001 00.0070 00.400
1013  0.486 0.250 26.00  18.00 150.00  80.00  00.12345 00.0001 00.0070 00.400
1014  0.486 0.250 26.00  18.00 150.00   4.50  00.08649 00.0001 00.0070 00.400
1015  0.486 0.250 26.00  18.00 150.00   0.45  00.05263 00.0001 00.0070 00.400

(RUN 2)
IOPT  MOPT NOPT
  1    2    1
INUM   DAY YEAR TIME  ZONE
  6  209 1987  CDT
TIME  MWAV  MTAU  MTHETO  MTHET  MPHI  MHGHT  MINT    TAUL    TAUH    SHGHT
1010  0.486 0.250 26.00   0.00   0.00  80.00  00.11409 00.0001 00.0070 00.400
1011  0.486 0.250 26.00   0.00   0.00   4.50  00.08089 00.0001 00.0070 00.400
1012  0.486 0.250 26.00   0.00   0.00   0.45  00.05125 00.0001 00.0070 00.400
1013  0.486 0.250 26.00  18.00 150.00  80.00  00.12345 00.0001 00.0070 00.400
1014  0.486 0.250 26.00  18.00 150.00   4.50  00.08649 00.0001 00.0070 00.400
1015  0.486 0.250 26.00  18.00 150.00   0.45  00.05263 00.0001 00.0070 00.400

(RUN 3)
IOPT  MOPT NOPT
  2    1    1
INUM   MON DAY YEAR  TIME  ZONE
  6    7  28 1987  CDT
TIME  MWAV  MTAU  MTHETO  MTHET  MPHI  MHGHT  MINT    TAUL    TAUH    SHGHT
1010  0.486 0.250 26.00   0.00   0.00  80.00  63.12500 00.0001 00.0070 00.400
1011  0.486 0.250 26.00   0.00   0.00   4.50  44.75500 00.0001 00.0070 00.400
1012  0.486 0.250 26.00   0.00   0.00   0.45  28.35600 00.0001 00.0070 00.400
1013  0.486 0.250 26.00  18.00 150.00  80.00  68.30400 00.0001 00.0070 00.400
1014  0.486 0.250 26.00  18.00 150.00   4.50  47.85900 00.0001 00.0070 00.400
1015  0.486 0.250 26.00  18.00 150.00   0.45  29.12000 00.0001 00.0070 00.400

(RUN 4)
IOPT  MOPT NOPT
  1    1    2
INUM   MON DAY YEAR  TIME  ZONE
  6    7  28 1987  CDT
TIME  MWAV  MTAU  MTHETO  MTHET  MPHI  MHGHT  MRHO    TAUL    TAUH    SHGHT
1010  0.486 0.250 26.00   0.00   0.00  80.00  00.05000 00.0001 00.0070 00.400
1011  0.486 0.250 26.00   0.00   0.00   4.50  00.05000 00.0001 00.0070 00.400
1012  0.486 0.250 26.00   0.00   0.00   0.45  00.05000 00.0001 00.0070 00.400
1013  0.486 0.250 26.00  18.00 150.00  80.00  00.05000 00.0001 00.0070 00.400
1014  0.486 0.250 26.00  18.00 150.00   4.50  00.05000 00.0001 00.0070 00.400
1015  0.486 0.250 26.00  18.00 150.00   0.45  00.05000 00.0001 00.0070 00.400

```

IOPT , MOPT , NOPT (FORMAT: 3I5)

- For **IOPT = 1** measured radiance should be in reflectance units - L^m .
- For **IOPT = 2** measured radiance should be in absolute radiance units of $Watts/m^2/sr/\mu m$.
- For **MOPT = 1** the day, month and year should be provided.
- For **MOPT = 2** the day of year (Julian date) and year should be given.
- For **NOPT = 1** surface reflectance (RHOS) is computed.
- For **NOPT = 2** radiance (MINT) is computed for the input geometry and height; the measured surface reflectance (MRHO) is input. The variable name MINT is used for programming convenience. MINT is a computed and not measured when **NOPT = 2**.

Run 1 and run 2 choose the **IOPT = 1** option for selecting reflectance units of measured radiance and **NOPT = 1** option to compute surface reflectance. **MOPT** (the option to select the day of year) is set to 1 and 2, respectively. Run 3 chooses **IOPT = 2** and **MOPT = NOPT = 1**. Run 4 selects **NOPT** to be 2 and **IOPT** and **MOPT** to be 1.

3. The third card contains the labels to identify the input parameters in step 4 below.

4. The fourth card contains the information about the number of data points **INUM** to be processed, the date, and information about the time zone (e.g Central, Pacific, or Mountain and Daylight or Standard Time). The information about the time zone is not used for any computations. There are two options for this input card depending on the value of **MOPT** (FORMAT 4I5, 30A1):

For **MOPT = 1:** **INUM, IMONTH, IDAY, IYEAR, TIME_ZONE**

e.g.: (1, 12, 25, 1987, CDT) for 1 data point to be processed for December 25, 1987, and the time zone is CDT or Central Daylight Time.

For **MOPT = 2:** **INUM, IDAY, IYEAR, TIME_ZONE**

e.g.: (1, 359, 1987, CDT)

The fourth row of run 1 reads number of data points, month, day, and year. The fourth row of run 2 reads number of data points, the Julian day and year for which the measurements are made. The radiance is read in reflectance units for both runs 1 and 2.

5. The fifth card contains the labels to identify the input parameters in step 6 below.

6. The sixth card can be repeated for the number of data points INUM. The data points should be for the same date. The following names in parentheses are the variable names used by the program. The sixth card contains values of time in hours and minutes (without punctuation; this input parameter is not used in any computations but is merely for the record) (MTIME), measured wavelength λ^m (MWAV) in micrometers, measured aerosol optical thickness τ_a^m (MTAU) for the measured wavelength λ^m , solar zenith angle θ_o^m (MTHET0) in degrees, observation scan angle $\theta^{m'}$ (MTHET) in degrees, observation azimuth angle ϕ^m (MPHI) in degrees, observation height Z^m (MHGHT) in kilometers, and spectral radiance $L^{m'}$ or L^m (MINT) from satellite or aircraft in reflectance or absolute units depending on option (IOPT) read in the first card, τ_{gL} (TAUGL), τ_{gH} (TAUGH), and Z_0 (SHGHT) in the following format:

MTIME, MWAV, MTAU, MTHET0, MTHET, MPHI, MHGHT, MINT,
TAUGH, TAUGL, SHGHT

FORMAT (I5,1x, F 6.3, F 6.3, 4F7.2,F10.5,3F8.4)

Card 6 for run 3 reads the measured radiance in absolute units. Card 6 for run 4 when NOPT is 2 reads the surface reflectance value MRHO in the following format:

MTIME, MWAV, MTAU, MTHET0, MTHET, MPHI, MHGHT, MRHO,
TAUGH, TAUGL, SHGHT

FORMAT (I5,1x, F 6.3, F 6.3, 4F7.2,F10.5,3F8.4)

INPUT FROM LOOK-UP TABLE (UNIT NUMBERS 7 - 14):

The input from the look-up table is read after the execution of the statements given in parentheses. Subroutine FINDW (1610) searches the data base and then reads only the

required table for the two wavelengths between which measured wavelength λ^m (MWAV) lies. The following are obtained:

1. values of observation zenith angle θ in degrees (2610, 2650)
2. values of observation azimuth angle ϕ in degrees (2610, 2660)
3. values of wavelength λ in micrometers, aerosol optical thickness τ_a , reflectance of atmosphere s , flux incident on surface F'_d (2830 - 2840)
4. a blank line
5. values of atmospheric radiance L'_o in reflectance units (2920 - 2950)
6. values of transmission from surface T/π (3000).

5.3 Output

A successful execution of this FORTRAN program will result in the output described below, which is written to FORTRAN logical unit numbers 6 and 56. Four cases representative of the different options discussed in section 5.2 are shown in Table 5.

OUTPUT TO UNIT NUMBER 6: (see Table 5.)

The input data set is written as it is read from unit number 5. The message 'END OF INPUT DATA SET AS READ FROM UNIT NUMBER 5' marks the end of input data set. The next line of this output contains the information about the date for which measurements are made:

For MOPT = 1, month, day, year, and time zone will be written (Table 5, run 1).

For MOPT = 2, Julian day, year, and time zone will be written (Table 5, run 2).

Each subsequent line gives the measured and derived output for each data point processed. The first seven entries on a line provide information about the following input parameters as read from logical unit number 5: time (Central, Pacific, or Mountain and Daylight or Standard) in hours and minutes, measured wavelength (λ^m) in micrometers, measured aerosol optical thickness (τ_a^m), solar zenith angle (θ_o^m) in degrees at the time of observation, measured observation zenith angle (θ^m) in degrees, measured observation azimuth angle (ϕ^m) in degrees, and measured observation height (Z^m) in kilometers. The

TABLE 5. CONTINUED

(RUN2)

START OF INPUT DATA AS READ FROM UNIT NUMBER 5

IOPT MOPT NOPT

1 2 1

INUM DAY YEAR TIME ZONE

6 209 1987 CDT

TIME	MWAV	MTAU	MTHETO	MTHET	MPHI	MHGT	MINT	TAUL	TAUH	SHGHT
1010	0.486	0.250	26.00	0.00	0.00	80.00	00.11409	00.0001	00.0070	00.400
1011	0.486	0.250	26.00	0.00	0.00	4.50	00.08089	00.0001	00.0070	00.400
1012	0.486	0.250	26.00	0.00	0.00	0.45	00.05125	00.0001	00.0070	00.400
1013	0.486	0.250	26.00	18.00	150.00	80.00	00.12345	00.0001	00.0070	00.400
1014	0.486	0.250	26.00	18.00	150.00	4.50	00.08649	00.0001	00.0070	00.400
1015	0.486	0.250	26.00	18.00	150.00	0.45	00.05263	00.0001	00.0070	00.400

END OF INPUT DATA SET AS READ FROM UNIT NUMBER 5

JULIAN DATE 209/ 1987 TIME ZONE CDT

TIME	WAVELENGTH MICROMETERS	OPTICAL THICKNESS	SOLAR			OBSERVATION			OBSERVATION			FLIGHT LEVEL			GROUND LEVEL		
			ZENITH ANGLE DEG	ZENITH ANGLE DEG	ZENITH ANGLE DEG	AZIMUTH ANGLE DEG	HEIGHT KM	RADIANCE W/M**2/UM/SR	RELATIVE RADIANCE RADIANCE*PI/F0/U0	DOWNWARD IRRADIANCE W/M**2/UM	UPWARD RADIANCE W/M**2/UM/SR	REFLECTANCE					
1010	0.486	0.25	26.00	0.00	0.00	0.00	80.00	63.18	0.1141	1702.	28.41	0.052					
1011	0.486	0.25	26.00	0.00	0.00	0.00	4.50	44.79	0.0809	1701.	27.73	0.051					
1012	0.486	0.25	26.00	0.00	0.00	0.00	0.45	28.38	0.0512	1701.	27.21	0.050					
1013	0.486	0.25	26.00	18.23	150.00	150.00	80.00	68.36	0.1234	1702.	28.40	0.052					
1014	0.486	0.25	26.00	18.01	150.00	150.00	4.50	47.90	0.0865	1701.	27.80	0.051					
1015	0.486	0.25	26.00	18.00	150.00	150.00	0.45	29.15	0.0526	1701.	27.22	0.050					

TABLE 5. CONTINUED

(RUN3)
START OF INPUT DATA AS READ FROM UNIT NUMBER 5

IOPT	MON	DAY	YEAR	TIME	ZONE	TAU	TAUH	SHGHT
1	28	1987	CDT					
2	7	28	1987	CDT				
3	6	28	1987	CDT				
4	6	28	1987	CDT				
5	6	28	1987	CDT				
6	6	28	1987	CDT				
7	6	28	1987	CDT				
8	6	28	1987	CDT				
9	6	28	1987	CDT				
10	6	28	1987	CDT				
11	6	28	1987	CDT				
12	6	28	1987	CDT				
13	6	28	1987	CDT				
14	6	28	1987	CDT				
15	6	28	1987	CDT				

END OF INPUT DATA SET AS READ FROM UNIT NUMBER 5

DATE	TIME	WAVELENGTH	MICROMETERS	OPTICAL THICKNESS	SOLAR ZENITH ANGLE	OBSERVATION ZENITH ANGLE	OBSERVATION AZIMUTH	OBSERVATION HEIGHT	RELATIVE RADIANCE	GROUND LEVEL		
										DOWNWARD IRRADIANCE	UPWARD RADIANCE	REFLECTANCE
7/ 28/ 1987	1010	0.486	0.25	26.00	0.00	0.00	0.00	80.00	0.1140	1701.	28.34	0.052
	1011	0.486	0.25	26.00	0.00	0.00	0.00	4.50	0.0808	1701.	27.68	0.051
	1012	0.486	0.25	26.00	0.00	0.00	0.00	0.45	0.0512	1701.	27.18	0.050
	1013	0.486	0.25	26.00	18.23	150.00	150.00	80.00	0.1233	1701.	28.33	0.052
	1014	0.486	0.25	26.00	18.01	150.00	150.00	4.50	0.0864	1701.	27.75	0.051
	1015	0.486	0.25	26.00	18.00	150.00	150.00	0.45	0.0526	1701.	27.19	0.050

TABLE 5. CONTINUED

(RUN4)

START OF INPUT DATA AS READ FROM UNIT NUMBER 5

IOPT	MOPT	NOPT	INUM	MON	DAY	YEAR	TIME	ZONE	CDT	TIME	MWAV	MTAU	MTHETO	MTHET	MPHI	MHGT	SURREF	TAUL	TAUH	SHGHT
1	1	2	6	7	28	1987	CDT													
1010	0.486	0.250	26.00	0.00	0.00	80.00	00.05000	00.0001	00.0070	00.400										
1011	0.486	0.250	26.00	0.00	0.00	4.50	00.05000	00.0001	00.0070	00.400										
1012	0.486	0.250	26.00	0.00	0.00	0.45	00.05000	00.0001	00.0070	00.400										
1013	0.486	0.250	26.00	18.00	150.00	80.00	00.05000	00.0001	00.0070	00.400										
1014	0.486	0.250	26.00	18.00	150.00	4.50	00.05000	00.0001	00.0070	00.400										
1015	0.486	0.250	26.00	18.00	150.00	0.45	00.05000	00.0001	00.0070	00.400										

END OF INPUT DATA SET AS READ FROM UNIT NUMBER 5

DATE	7/	28/	1987	TIME	ZONE	CDT	FLIGHT LEVEL				GROUND LEVEL					
							OBSERVATION	AZIMUTH	OBSERVATION	HEIGHT	RELATIVE	RADIANCE	DOWNWARD	UPWARD		
TIME	WAVELENGTH	OPTICAL	THICKNESS	SOLAR	ZENITH	ANGLE	OBSERVATION <td>ZENITH</td> <td>ANGLE</td> <td>OBSERVATION <td>HEIGHT <td>RADIANCE <td>RADIANCE <td>IRRADIANCE <td>RADIANCE <td>REFLECTANCE </td></td></td></td></td></td></td>	ZENITH	ANGLE	OBSERVATION <td>HEIGHT <td>RADIANCE <td>RADIANCE <td>IRRADIANCE <td>RADIANCE <td>REFLECTANCE </td></td></td></td></td></td>	HEIGHT <td>RADIANCE <td>RADIANCE <td>IRRADIANCE <td>RADIANCE <td>REFLECTANCE </td></td></td></td></td>	RADIANCE <td>RADIANCE <td>IRRADIANCE <td>RADIANCE <td>REFLECTANCE </td></td></td></td>	RADIANCE <td>IRRADIANCE <td>RADIANCE <td>REFLECTANCE </td></td></td>	IRRADIANCE <td>RADIANCE <td>REFLECTANCE </td></td>	RADIANCE <td>REFLECTANCE </td>	REFLECTANCE
	MICROMETERS			ANGLE	DEG	DEG	ANGLE	DEG	DEG	ANGLE	KM	W/M**2/UM/SR	W/M**2/UM/SR	W/M**2/UM/SR	W/M**2/UM/SR	
1010	0.486	0.25		26.00	0.00	0.00	80.00	62.11	0.1122	1701.	27.07	0.050				
1011	0.486	0.25		26.00	0.00	0.00	4.50	44.24	0.0799	1701.	27.07	0.050				
1012	0.486	0.25		26.00	0.00	0.00	0.45	28.26	0.0510	1701.	27.07	0.050				
1013	0.486	0.25		26.00	18.23	150.00	80.00	67.31	0.1215	1701.	27.07	0.050				
1014	0.486	0.25		26.00	18.01	150.00	4.50	47.28	0.0854	1701.	27.07	0.050				
1015	0.486	0.25		26.00	18.00	150.00	0.45	29.02	0.0524	1701.	27.07	0.050				

eighth and ninth entries depend on **IOPT**. For **IOPT** = 1, the measured radiance L^m is given in reflectance units and labeled under **RELATIVE RADIANCE**; the corresponding radiance in absolute units is computed by the the program and is labeled under **RADIANCE**. For **IOPT** = 2, the measured radiance L^m is given in absolute units and is labeled under **RADIANCE**; the corresponding radiance in reflectance units is computed by the the program and is labeled under **RELATIVE RADIANCE**. Next three surface quantities are computed and given as values for total spectral irradiance F_g , total spectral radiance L_g , and surface reflectance ρ (eq.2,3 and 4). The output in Table 5 for run 4 computes the eighth and ninth columns, since **NOPT** = 2 and the surface reflectance is input (column 12).

OUTPUT TO UNIT NUMBER 56: (see Table 6)

The label for this output shown in table 6 reads **INTERPOLATED RADIATION PARAMETERS**. The second line gives information about the date and time zone of the input data set. Each subsequent line gives the measured and derived output for each data point processed. The first seven entries on a line provide information about the following input parameters as read from logical unit number 5: time (Central, Pacific, or Mountain and Daylight or Standard) in hours and minutes, measured wavelength (λ^m) in micrometers, measured aerosol optical thickness (τ_a^m), solar zenith angle (θ_o^m) in degrees at the time of observation, measured observation zenith angle (θ^m) in degrees, measured observation azimuth angle (ϕ^m) in degrees, and measured observation height (Z^m) in kilometers. The eighth and ninth entries depend on **IOPT** and **NOPT**. For **IOPT** = 1 and **NOPT** = 1, the measured radiance L^m is given in reflectance units and labeled under **RELATIVE RADIANCE**; the corresponding radiance in absolute units is computed by the the program and is labeled under **RADIANCE**. For **IOPT** = 2 and **NOPT** = 1, the measured radiance L^m is given in absolute units and is labeled under **RADIANCE**; the corresponding radiance in reflectance units is computed by the the program and is labeled under **RELATIVE RADIANCE**. IF **NOPT** = 2 the values of radiance in absolute and reflectance units are computed by the program. Next three quantities are computed and given as values for L_o' , F_d' , s , and transmission T (eq. 6).

5.4 Summary of Error Messages

A summary of error messages is given in Table 7. First, examples of input data are given followed by the different error messages that would result. For the sixth row and second column of the upper table, where the input measured wavelength $\lambda^m = 0.345$, it

TABLE 6. EXAMPLE OF OUTPUT FOR INTERPOLATED RADIATION PARAMETERS.

INTERPOLATED RADIATION PARAMETERS													

DATE	7/	28/	1987	TIME	ZONE	CDT							
TIME	WAVELENGTH	OPTICAL	SOLAR	OBSERVATION	OBSERVATION	HEIGHT	RADIANCE	RELATIVE	LSUBO	FSUBD	T	S	
		THICKNESS	ZENITH	ANGLE	ANGLE			RADIANCE*PI/F0/U0	SUPERPRIME	SUPERPRIME			
			ANGLE	DEG	DEG	KM	W/M* *2/UM/SR						
	MICROMETERS												
1010	0.486	0.25	26.00	0.00	0.00	80.00	63.1804	0.1141	0.0732	0.8714	0.8871	0.1654	
1011	0.486	0.25	26.00	0.00	0.00	4.50	44.7950	0.0809	0.0386	0.8714	0.9400	0.1654	
1012	0.486	0.25	26.00	0.00	0.00	0.45	28.3811	0.0512	0.0077	0.8714	0.9863	0.1654	
1013	0.486	0.25	26.00	18.00	150.00	80.00	68.3637	0.1234	0.0828	0.8714	0.8798	0.1654	
1014	0.486	0.25	26.00	18.00	150.00	4.50	47.8961	0.0865	0.0443	0.8714	0.9351	0.1654	
1015	0.486	0.25	26.00	18.00	150.00	0.45	29.1453	0.0526	0.0091	0.8714	0.9849	0.1654	

does not lie between the range (0.486 - 2.2 μm), for which the look-up table is available (section 4.0). The subroutine FINDW prints an error message '*Measured wavelength 0.345 is out of range. The data point #1 is not processed; Actual range (0.486 - 2.2 μm)*'. For the following rows (2, 3, 4, and 5) of input data, the measured aerosol optical thickness τ_a^m , solar zenith angle θ_o^m , observation zenith angle θ^m , and observation azimuth angle ϕ^m are out of the ranges of values provided by the look up table (section 4.0). The subroutine INTERP prints error messages stating the variables which are out of range.

6.0 Sensitivity Study

A careful error analysis would be extensive, because so many measurement and surface parameters are involved. Instead an attempt is made to estimate the maximum errors that might occur during FIFE in estimating the surface reflectance (ρ). The errors given here are not root-mean-square errors. The surface radiance L_g error can be calculated with the reflectance error and eq. 5. The irradiance at the ground (F_g (eq.4) and also F_d (eq. 4 and 5)) is not affected appreciably by the perturbations. The main source of error usually is caused in estimation of the path radiance (L_o). The absolute surface reflectance error is insensitive to strength of the reflectance.

The perturbations are placed in three categories: model errors, interpolation errors, and uncertainties in the input data (input errors). The model parameters studied are:

- 1) uncertainty in the aerosol single scattering phase function
- 2) uncertainty due to the neglect of polarization in the radiative transfer computations
- 3) uncertainty in water vapor and ozone absorption
- 4) uncertainty in aerosol absorption
- 5) uncertainty in the height distribution of aerosols

Since the algorithm must interpolate parameters on aerosol optical thickness τ_a , solar zenith angle θ_o , observation zenith angle θ , azimuth angle ϕ , wavelength λ , and height Z , the errors introduced by these interpolations are studied. Finally, because the input data will have some uncertainty associated with them, the effects of errors in the input radiance, input aerosol optical thickness, and input geometry are studied. The studies described above are mostly performed for a wavelength $\lambda = 0.486 \mu\text{m}$, since the atmospheric effects generally are the greatest at the shortest wavelength. Unless stated otherwise, the

unperturbed simulation model has an aerosol optical thickness $\tau_a = 0.25$, three observation altitudes (0.45 km, 4.5 km, 80 km), and two view geometries (Model 1: $\theta_0 = 30^\circ$, $\theta = 0^\circ$, $\phi = 0^\circ$; Model 2: $\theta_0 = 30^\circ$, $\theta = 18^\circ$, $\phi = 150^\circ$). In order to estimate the largest errors, the wavelength, geometry, and aerosol optical thickness are varied in a few cases where the errors are larger.

In the discussion which follows, a description of each type of sensitivity test is given in Table 8, followed by a discussion of the results. The first part gives results of model errors, the second part of interpolation errors, and the third part of input errors. A summary of the sensitivity results is shown in Table 9, which shows the errors in the derived surface reflectance for two observation geometries in the case of the model errors. For interpolation and input errors, the resulting errors in the derived surface reflectance are shown for only one geometry. Table 10 gives additional details concerning the errors and radiation parameters.

6.1 Model Errors

The atmospheric correction algorithm causes errors because the model does not represent exactly the state of the atmosphere at the time of an observation. The simulated measured remote radiance or surface reflectance is first computed with a radiative transfer model that contains the perturbation. These computations produce a given perturbed radiance $L^m + \Delta L^m$ at the sensor altitude, as well as the other radiation parameters. The perturbed radiance $L^m + \Delta L^m$ serves as an input in the correction algorithm, resulting in a derived perturbed surface reflectance $\rho + \Delta\rho$.

6.1.1 Aerosol Single Scattering Phase Function

The scattering effects of aerosols increase with increasing aerosol optical thickness, which usually is largest at the shortest wavelengths; but compared with molecular scattering, the relative contribution by the aerosols to backward scattering decreases with decreasing wavelength. Therefore, an intermediate wavelength of $0.639 \mu\text{m}$ (AVHRR band 1) is used for the phase function sensitivity study.

The phase function sensitivity test is performed using two phase functions which differ appreciably from the one used in the model. As discussed previously, the aerosol single scattering phase function used in the algorithm is computed for two log-normal aerosol size distributions combined, which are chosen to represent accumulation and coarse particle modes. The first phase function used in this sensitivity analysis is chosen from a

Table 8. Case numbers assigned to Sensitivity Tests for the Atmospheric Correction Algorithm

KEY	
θ_o	= Solar zenith angle ($^{\circ}$)
θ	= Observation zenith angle ($^{\circ}$)
λ	= Wavelength (μm)
p	= Surface reflectance for no error
p_d	= Derived surface reflectance for the given error
$\%p$	= Percentage error in derived surface reflectance
τ_a	= Aerosol optical thickness
ϕ	= Azimuth angle ($^{\circ}$)
F_g	= Irradiance ($\text{Watts}/\text{m}^2\text{-}\mu\text{m}$) on a horizontal surface at the ground for no error
F_{gd}	= Derived irradiance ($\text{Watts}/\text{m}^2\text{-}\mu\text{m}$) on a horizontal surface at the ground for the given error
$\%F_g$	= Percentage error in the derived irradiance
L_d	= Input radiance (reflectance units) for the given error
L_g	= Upward radiance ($\text{Watts}/\text{m}^2/\mu\text{m}/\text{sr}$) at the ground for no error
$\%L_g$	= Percentage error in the derived radiance at the ground
L_{gd}	= Derived radiance ($\text{Watts}/\text{m}^2/\mu\text{m}/\text{sr}$) at the ground for the given error

Table 8 continued

L^m = Input radiance (reflectance units) at sensor height for no error

$\%L$ = Percentage error in input radiance at sensor height

Z = Altitude (km)

A) Model Errors

Case Description

Aerosol Single Scattering Phase Function:

- 1 Single mode, log-normal aerosol size distribution (refractive index $n = 1.349 - 0.008i$) geometric mean mass radius $r_m = 0.60 \mu m$, $\sigma = 0.6$
- 2 Power law aerosol size distribution ($\nu = 4$), refractive index $n = 1.53 - 10^{-8}i$

Polarization:

- 3 Wavelength = $0.486 \mu m$ (TM band 1)
- 4 Wavelength = $0.639 \mu m$ (AVHRR band 1)
- 5 Wavelength = $0.845 \mu m$ (AVHRR band 2)

Water vapor absorption:

- 6 Water vapor absorption optical thickness $\tau_g = 0.0486$ (AVHRR band 2)

Table 8 continued

7 Water vapor absorption optical thickness $\tau_g = 0.1235$ (AVHRR band 2)

Ozone absorption:

8 Ozone absorption optical thickness $\tau_g = 0.039$ (TM band 2)

9 Ozone absorption optical thickness $\tau_g = 0.024$ (TM band 2)

Aerosol single scattering albedo:

10 Aerosol single scattering albedo $\omega_o = 0.84$

10a Aerosol single scattering albedo $\omega_o = 0.77$

Aerosol height distribution:

11 Model 1. 50 km visibility, rural in boundary layer; 50 km visibility spring/summer in upper troposphere

12 Model 2. 23 km visibility, rural in boundary layer; 23 km visibility spring/summer in upper troposphere

13 Model 3. 10 km visibility, rural in boundary layer; 10 km visibility spring/summer in upper troposphere

Table 8 continued

B) Interpolation Errors.

Case Description

- 14 For input $\tau_a = 0.375$, algorithm interpolates between $\tau_a = 0.25$ and $\tau_a = 0.50$
- 15 For input $\theta_o = 26^\circ$, algorithm interpolates between $\theta_o = 20^\circ$ and $\theta_o = 30^\circ$
- 16 For input $\theta = 20^\circ$, algorithm interpolates between $\theta = 18^\circ$ and $\theta = 24^\circ$
- 17 For input $\phi = 145^\circ$, algorithm interpolates between $\phi = 140^\circ$ and $\phi = 150^\circ$

18-32 Descriptions are given in Table 9.

C) Input Errors.

Case Description

- 33 Input error in radiance of 5%
- 34 Input error in radiance of 10%
- 35 Input error in aerosol optical thickness of $\Delta\tau_a = 0.10$ for true $\tau_a = 0.25$
- 36 Input error in aerosol optical thickness of $\Delta\tau_a = 0.05$ for true $\tau_a = 0.25$
- 37 Input error in aerosol optical thickness of $\Delta\tau_a = 0.20$ for true $\tau_a = 1.00$

Table 8 continued

38	Input error in aerosol optical thickness of $\Delta\tau_a = 0.10$ for true $\tau_a = 1.00$
39	Input error in solar zenith angle of $\Delta\theta_0 = 4^\circ$ for true $\theta_0 = 30^\circ$
40	Input error in solar zenith angle of $\Delta\theta_0 = 2^\circ$ for true $\theta_0 = 30^\circ$
41	Input error in observation zenith angle of $\Delta\theta = 2^\circ$ for true $\theta = 0^\circ$
42	Input error in observation zenith angle of $\Delta\theta = 4^\circ$ for true $\theta = 0^\circ$
43	Input error in azimuth angle of $\Delta\phi = 2^\circ$ for true $\phi = 0^\circ$
44	Input error in azimuth angle of $\Delta\phi = 4^\circ$ for true $\phi = 150^\circ$

Table 9. Summary of sensitivity results.

KEY

ρ	=	Surface reflectance for no error
$\% \rho$	=	Percentage error in derived surface reflectance
L_g	=	Upward radiance ($\text{Watts/m}^2/\text{sr}/\mu\text{m}$) at the ground for no error
$\% L$	=	Percentage error in input radiance at $Z = 80 \text{ km}$

A1. Model errors.

Geometry 1: $\theta_o = 30^\circ$, $\theta = 0^\circ$, $\phi = 0^\circ$, $\tau_a = 0.25$, $Z = 80 \text{ km}$
 Geometry 2: $\theta_o = 30^\circ$, $\theta = 18^\circ$, $\phi = 150^\circ$, $\tau_a = 0.25$, $Z = 80 \text{ km}$

Case	Geometry 1					Geometry 2					Description of perturbation
	$\lambda(\mu\text{m})$	L_g	$\%L$	ρ	$\% \rho$	L_g	$\%L$	ρ	$\% \rho$		
1	0.639	0.0741	-9.7	0.05	-18.0	0.0803	11.8	0.05	-24.0	single mode, log-normal aerosol size distribution (refractive index $n = 1.349 - 0.008i$) geometric mean mass radius $r_m = 0.60 \mu\text{m}$, $\sigma = 0.6$	
2	0.639	0.0741	15.4	0.05	28.0	0.0803	13.1	0.05	26.0	power law aerosol size distribution ($V = 4$), (refractive index $n = 1.53 - 10^{-8} i$)	
3	0.486	0.1122	2.3	0.05	5.9	0.1230	3.1	0.05	10.2	polarization: $\lambda=0.486 \mu\text{m}$ (TM band 1)	
4	0.639	0.0746	1.0	0.05	2.0	0.0783	1.3	0.05	2.1	polarization: $\lambda = 0.639 \mu\text{m}$ (AVHRR band 1)	

Table 9 continued

Case	Geometry 1				Geometry 2				Description of perturbation
	λ	L_g	$\%L$	ρ	$\% \rho$	L_g	$\%L$	ρ	
5	0.845	0.1635	0.2	0.20	0.0	0.1594	0.3	0.20	0.5 polarization: $\lambda = 0.845 \mu\text{m}$ (AVHRR band 2)
6	0.845	0.1635	9.9	0.20	11.5	0.1594	9.9	0.20	11.0 water vapor absorption optical thickness $\tau_{g2}^{\text{H}_2\text{O}} = 0.0486$, model $\tau_{g2}^{\text{H}_2\text{O}} = 0.0933$
7	0.845	0.1635	-6.1	0.20	-7.0	0.1594	-6.1	0.20	-7.0 water vapor absorption optical thickness $\tau_{g2}^{\text{H}_2\text{O}} = 0.1235$, model $\tau_{g2}^{\text{H}_2\text{O}} = 0.0933$
8	0.587	0.0830	1.9	0.05	4.0	0.0902	2.0	0.05	4.0 ozone absorption optical thickness $\tau_{g3}^{\text{O}} = 0.039$, model $\tau_{g3}^{\text{O}} = 0.032$
9	0.587	0.0830	-1.3	0.05	-2.0	0.0902	-1.3	0.05	-4.0 ozone absorption optical thickness $\tau_{g3}^{\text{O}} = 0.024$, model $\tau_{g3}^{\text{O}} = 0.032$
10	0.486	0.1122	-0.3	0.05	0.0	0.1230	-3.4	0.05	-10.0 aerosol single scattering albedo $\omega_0 = 0.84$, model $\omega_0 = 0.96$
Geometry: $\theta_0 = 64^\circ$, $\theta = 56^\circ$, $\phi = 15^\circ$, $\tau_a = 0.35$, $\omega_0 = 0.91$, $Z = 80 \text{ km}$, $\rho = 0.6$, $\lambda = 0.845 \mu\text{m}$									
10a	0.845	0.342	-10.5	0.60	-10.7				reduced aerosol ω_0 to 0.77
11	0.486	0.1122	0.0	0.05	0.0	0.1230	0.0	0.05	0.0 aerosol height distribution (50 km visibility)
12	0.486	0.1122	-0.1	0.05	0.0	0.1230	-0.1	0.0	-0.0 aerosol height distribution (23 km visibility)
13	0.486	0.1122	-0.2	0.05	0.0	0.1230	-0.3	0.05	0.0 aerosol height distribution (10 km visibility)

Table 9 continued

B) Interpolation errors.

Geometry: $\theta_0 = 30^\circ$, $\theta = 18^\circ$, $\phi = 150^\circ$, $\tau_a = 0.25$, $Z = 80$ km, $\rho = 0.05$, $\lambda = 0.486$ μm , $Lg = 0.1230$

Case	% ρ	Description of perturbation
14	0.0	For input $\tau_a = 0.375$, algorithm interpolates between $\tau_a = 0.25$ and $\tau_a = 0.50$
15	6.0	For input $\theta_0 = 26^\circ$, algorithm interpolates between $\theta_0 = 20^\circ$ and $\theta_0 = 30^\circ$
16	0.0	For input $\theta = 20^\circ$, algorithm interpolates between $\theta = 18^\circ$ and $\theta = 24^\circ$
17	0.0	For input $\phi = 145^\circ$, algorithm interpolates between $\phi = 140^\circ$ and $\phi = 150^\circ$
18	6.0	For input $\lambda = 0.500$ μm , algorithm interpolates between $\lambda = 0.486$ μm and $\lambda = 0.586$ μm
19	5.0	For input $\lambda = 0.600$ μm , algorithm interpolates between $\lambda = 0.587$ μm and $\lambda = 0.639$ μm
20	5.0	For input $\lambda = 0.752$ μm , algorithm interpolates between $\lambda = 0.663$ μm and $\lambda = 0.837$ μm
21	-2.0	For input $\lambda = 0.840$ μm , algorithm interpolates on τ_g , $\rho = 0.05$
22	-2.0	For input $\lambda = 0.840$ μm , algorithm interpolates on τ_g , $\rho = 0.10$
23	-1.0	For input $\lambda = 0.840$ μm , algorithm interpolates on τ_g , $\rho = 0.20$
24	2.0	For input surface height of 0.0 km above sea level, algorithm interpolates on τ_{gs}
25	-8.0	For input surface height of 1.0 km above sea level, algorithm interpolates on τ_{gs}
26	8.0	For input $Z = 6.50$ km, algorithm interpolates between $Z = 4.5$ km and $Z = 80$ km
27	2.0	For input $Z = 2.96$ km, algorithm interpolates between $Z = 0.45$ km and $Z = 4.5$ km
28	2.0	For input $Z = 0.23$ km, algorithm interpolates between $Z = 0.0$ km and $Z = 0.45$ km

Table 9 continued

Case	%p	Description of perturbation
Errors for large solar and nadir angles. Interpolations are made on τ_a , θ_o , θ , and ϕ .		
29	22.0	For $Z = 80$ km, $\lambda = 0.639$ μm , $\tau_a = 0.35$, $\theta_o = 74^\circ$, $\theta = 56^\circ$, $\phi = 15^\circ$, $\rho = 0.05$
30	8.0	For $Z = 80$ km, $\lambda = 0.639$ μm , $\tau_a = 0.35$, $\theta_o = 74^\circ$, $\theta = 56^\circ$, $\phi = 165^\circ$, $\rho = 0.05$
31	-32.0	For $Z = 80$ km, $\lambda = 0.639$ μm , $\tau_a = 0.10$, $\theta_o = 74^\circ$, $\theta = 56^\circ$, $\phi = 15^\circ$, $\rho = 0.05$
32	-6.0	For $Z = 80$ km, $\lambda = 0.639$ μm , $\tau_a = 0.10$, $\theta_o = 74^\circ$, $\theta = 56^\circ$, $\phi = 165^\circ$, $\rho = 0.05$
C) Input errors.		
Geometry: $\theta_o = 30^\circ$, $\theta = 0^\circ$, $\phi = 0^\circ$, $\tau_a = 0.25$, $Z = 80$ km, $\rho = 0.05$, $\lambda = 0.486$, $L_g = 0.1122$		
Case	%p	Description of perturbation
33	14.0	Input error in radiance of 5%
36	6.0	Input error in aerosol optical thickness of $\Delta\tau_a = 0.05$ for true $\tau_a = 0.25$
38	28.0	Input error in aerosol optical thickness of $\Delta\tau_a = 0.10$ for true $\tau_a = 1.0$
40	0.0	Input error in solar zenith angle of $\Delta\theta_o = 2^\circ$ for true $\theta_o = 30^\circ$
41	2.0	Input error in observation zenith angle of $\Delta\theta = 2^\circ$ for true $\theta = 0^\circ$
44	0.0	Input error in azimuth angle of $\Delta\phi = 2^\circ$ for true $\phi = 150^\circ$

Table 10. Sensitivity Results

A) Model errors.

CASE	λ	θ_0	θ	ϕ	τ_a	Z	L^m	L_d	$\%L$	ρ	ρ_d	$\%p$	F_g	F_{gd}	$\%F_g$	L_g	L_{gd}	$\%L_g$	
1	0.639	30.0	0.0	0.0	0.25	80.00	0.0741	0.0669	-9.7	0.050	0.041	-18.0	1449.7	1440.0	-0.67	23.1	18.8	-18.6	
							4.50	0.0637	0.0572	-10.2	0.050	0.042	-16.0	1449.7	1440.1	-0.66	23.1	19.3	-16.4
							0.45	0.0501	0.0476	-4.9	0.050	0.047	-6.0	1449.7	1440.7	-0.62	23.1	21.6	-6.5
							80.00	0.0803	0.0709	11.8	0.050	0.038	-24.0	1449.7	1439.6	-0.69	23.1	17.4	-24.7
							4.50	0.0684	0.0597	12.7	0.050	0.040	-20.0	1449.7	1439.9	-0.68	23.1	18.3	-20.8
	0.45	0.0517	0.0484	6.4	0.050	0.046	-8.0	1449.7	1440.6	-0.63	23.1	21.1	-8.7						
2	0.639	30.0	0.0	0.0	0.25	80.00	0.0741	0.0855	15.4	0.050	0.064	28.0	1449.7	1451.9	0.1	23.1	29.5	28.1	
							4.50	0.0637	0.0742	16.4	0.050	0.062	24.0	1449.7	1451.6	0.1	23.1	28.8	24.7
							0.45	0.0501	0.0537	7.2	0.050	0.054	8.0	1449.7	1450.3	0.0	23.1	25.0	8.2
							80.00	0.0803	0.0909	13.1	0.050	0.063	26.0	1449.7	1451.7	0.1	23.1	29.1	26.1
							4.50	0.0684	0.0785	14.8	0.050	0.062	24.0	1449.7	1451.5	0.1	23.1	28.6	24.0
	0.45	0.0517	0.0552	6.8	0.050	0.054	8.0	1449.7	1450.3	0.0	23.1	24.9	8.0						

CASE	λ	θ_0	θ	ϕ	τ_a	Z	L^m	L_d	$\%L$	ρ	ρ_d	$\%p$	Fg	Fgd	$\%Fg$	Lg	Lgd	$\%Lg$	
3	0.486	30.0	0.0	0.0	0.25	80.00	0.1129	0.1155	2.3	0.051	0.054	5.9	1690.8	1690.7	-0.01	27.4	29.1	6.6	
							4.50	0.0799	0.0812	1.5	0.050	0.052	4.0	1690.6	1690.1	-0.03	27.2	28.0	2.9
							0.45	0.0516	0.0516	0.0	0.051	0.050	-2.0	1690.8	1689.6	-0.07	27.5	26.9	2.2
							18.0	150.0											
							80.00	0.1221	0.1259	3.1	0.049	0.054	10.2	1690.2	1690.7	-0.03	26.3	29.1	10.6
4	0.639	30.0	0.0	0.0	0.25	80.00	0.0847	0.0847	0.0	0.048	0.048	0.0	1690.1	1689.0	-0.06	26.1	25.8	-1.2	
							4.50	0.0526	0.0518	-1.6	0.500	0.490	-2.0	1690.6	1689.3	-0.08	27.1	26.3	-2.9
							0.45	0.0746	0.0754	1.0	0.051	0.052	2.0	1449.8	1449.7	-0.01	23.4	24.0	2.6
							18.0	150.0											
							80.00	0.0646	0.0651	0.7	0.051	0.052	2.0	1449.9	1449.7	-0.01	23.6	24.0	1.7
							0.45	0.0505	0.0507	0.2	0.050	0.051	2.0	1449.8	1449.5	-0.02	23.4	23.5	0.4
							80.00	0.0783	0.0794	1.3	0.048	0.049	2.1	1449.3	1449.2	-0.01	21.9	22.6	3.2
							4.50	0.0669	0.0675	1.0	0.048	0.049	2.1	1449.4	1449.2	-0.01	22.2	22.6	1.8
							18.0	150.0											
							80.00	0.0511	0.0515	0.7	0.049	0.050	2.0	1449.6	1449.3	-0.02	22.8	23.1	1.3

Table 10 continued

CASE	λ	θ_0	θ	ϕ	τ_a	Z	L^m	Ld	$\%L$	ρ	ρ_d	$\%p$	Fg	Fgd	$\%Fg$	Lg	Lgd	$\%Lg$
5	0.845	30.0	0.0	0.0	0.25	80.00	0.1592	0.1595	0.2	0.200	0.200	0.0	863.2	862.3	0.10	54.9	54.9	0.0
						4.50	0.1589	0.1592	0.2	0.200	0.200	0.0	863.2	862.3	0.10	54.9	54.9	0.0
						0.45	0.1617	0.1618	0.0	0.199	0.199	0.0	863.2	862.3	0.10	54.8	54.6	-0.4
			18.0	150.0		80.00	0.1601	0.1606	0.3	0.195	0.196	0.5	862.9	862.1	-0.09	53.6	53.8	0.4
						4.50	0.1595	0.1598	0.2	0.196	0.196	0.0	863.0	862.1	-0.10	53.8	53.8	0.0
						0.45	0.1618	0.1620	0.1	0.198	0.198	0.0	863.1	862.2	-0.10	54.3	54.3	0.0
6	0.845	30.0	0.0	0.0	0.25	80.00	0.1635	0.1798	9.9	0.200	0.223	11.5	863.2	913.6	5.8	55.0	64.6	17.4
						4.50	0.1625	0.1785	9.8	0.200	0.222	11.0	863.2	913.5	5.8	55.0	64.3	16.9
						0.45	0.1636	0.1758	7.5	0.200	0.215	7.5	863.2	913.1	5.8	55.0	62.5	22.7
			18.0	150.0		80.00	0.1594	0.1752	9.9	0.200	0.222	11.0	863.2	913.7	5.9	55.0	64.9	18.0
						4.50	0.1590	0.1746	9.8	0.200	0.221	10.5	863.2	913.6	5.8	55.0	64.6	17.5
						0.45	0.1623	0.1745	7.5	0.200	0.215	7.5	864.1	913.1	5.8	55.0	62.5	13.6

Table 10 continued

CASE	λ	θ_0	θ	ϕ	τ_a	Z	L^m	L_d	$\%L$	ρ	ρ_d	$\%p$	Fg	Fgd	$\%Fg$	Lg	Lgd	$\%Lg$	
7	0.845	30.0	0.0	0.0	0.25	80.00	0.1635	0.1536	-6.1	0.200	0.186	-7.0	863.2	831.5	-3.7	55.0	49.2-10.5		
							4.50	0.1625	0.1527	-6.0	0.200	0.187	-6.5	863.2	831.6	-3.6	55.0	46.8-14.9	
							0.45	0.1636	0.1554	-5.0	0.200	0.190	-5.0	863.2	831.7	-3.6	55.0	50.3 -8.5	
							80.00	0.1594	0.1497	-6.1	0.200	0.186	-7.0	863.2	831.5	-3.7	55.0	49.2-10.5	
							4.50	0.1590	0.1420-10.7	0.200	0.177-11.5		863.2	831.5	-3.7	55.0	49.5-10.0		
8	0.587	30.0	0.0	0.0	0.25	80.00	0.1623	0.1541	-5.0	0.200	0.190	-5.0	864.1	831.7	-3.6	55.0	50.3 -8.5		
							4.50	0.0683	0.0652	-4.5	0.050	0.046	-8.0	1599.5	1612.4	0.8	25.5	23.6 -7.4	
							0.45	0.0499	0.0497	-0.5	0.050	0.050	0.0	1599.5	1613.3	0.9	25.4	25.7 1.2	
							80.00	0.0902	0.0920	2.0	0.050	0.052	4.0	1599.5	1613.7	0.9	25.5	26.7 4.7	
							4.50	0.0734	0.0698	-4.8	0.050	0.046	-8.0	1599.5	1612.4	0.8	25.5	23.6 -7.5	
9	0.587	30.0	0.0	0.0	0.25	80.00	0.1623	0.1541	-5.0	0.200	0.190	-5.0	864.1	831.7	-3.6	55.0	50.3 -8.5		
							4.50	0.0683	0.0652	-4.5	0.050	0.046	-8.0	1599.5	1612.4	0.8	25.5	23.6 -7.4	
							0.45	0.0499	0.0497	-0.5	0.050	0.050	0.0	1599.5	1613.3	0.9	25.4	25.7 1.2	
							80.00	0.0902	0.0920	2.0	0.050	0.052	4.0	1599.5	1613.7	0.9	25.5	26.7 4.7	
							4.50	0.0734	0.0698	-4.8	0.050	0.046	-8.0	1599.5	1612.4	0.8	25.5	23.6 -7.5	
10	0.587	30.0	0.0	0.0	0.25	80.00	0.1623	0.1541	-5.0	0.200	0.190	-5.0	864.1	831.7	-3.6	55.0	50.3 -8.5		
							4.50	0.0683	0.0652	-4.5	0.050	0.046	-8.0	1599.5	1612.4	0.8	25.5	23.6 -7.4	
							0.45	0.0499	0.0497	-0.5	0.050	0.050	0.0	1599.5	1613.3	0.9	25.4	25.7 1.2	
							80.00	0.0902	0.0920	2.0	0.050	0.052	4.0	1599.5	1613.7	0.9	25.5	26.7 4.7	
							4.50	0.0734	0.0698	-4.8	0.050	0.046	-8.0	1599.5	1612.4	0.8	25.5	23.6 -7.5	

Table 10 continued

CASE	λ	θ_0	θ	ϕ	τ_a	Z	L^m	L_d	$\%L$	ρ	ρ_d	$\%p$	Fg	Fgd	$\%Fg$	Lg	Lgd	$\%Lg$
9	0.587	30.0	0.0	0.0	0.25	80.00	0.0830	0.0819	-1.3	0.050	0.049	-2.0	1599.5	1584.8	-0.9	25.5	24.7	-3.2
						4.50	0.0683	0.0670	-1.8	0.050	0.049	-2.0	1599.5	1584.8	-0.9	25.5	24.7	-3.2
						0.45	0.0499	0.0495	-0.9	0.050	0.049	-2.0	1599.5	1584.8	-0.9	25.4	24.7	-3.1
						80.00	0.0902	0.0890	-1.3	0.050	0.048	-4.0	1599.5	1584.6	-0.9	25.5	24.2	-5.1
						4.50	0.0734	0.0720	-1.9	0.050	0.048	-4.0	1599.5	1584.8	-0.9	25.5	24.2	-5.1
10	0.486	30.0	0.0	0.0	0.25	80.00	0.1122	0.1118	-0.3	0.050	0.050	0.0	1690.5	1642.5	-2.8	26.9	26.1	-2.9
						4.50	0.0795	0.0776	-2.4	0.050	0.048	-4.0	1690.5	1642.0	-2.8	26.9	25.1	-6.6
						0.45	0.0507	0.0496	-2.0	0.050	0.049	-2.0	1690.5	1642.2	-2.8	26.9	25.6	-4.9
						80.00	0.1230	0.1188	-3.4	0.050	0.045	-10.0	1690.5	1641.3	-2.9	26.9	23.5	-12.6
						4.50	0.0860	0.0816	-5.2	0.050	0.045	-10.0	1690.5	1641.3	-2.9	26.9	23.5	-12.6
11	0.486	30.0	0.0	0.0	0.25	80.00	0.1122	0.1118	-0.3	0.050	0.050	0.0	1690.5	1642.5	-2.8	26.9	26.1	-2.9
						4.50	0.0795	0.0776	-2.4	0.050	0.048	-4.0	1690.5	1642.0	-2.8	26.9	25.1	-6.6
						0.45	0.0507	0.0496	-2.0	0.050	0.049	-2.0	1690.5	1642.2	-2.8	26.9	25.6	-4.9
						80.00	0.1230	0.1188	-3.4	0.050	0.045	-10.0	1690.5	1641.3	-2.9	26.9	23.5	-12.6
						4.50	0.0860	0.0816	-5.2	0.050	0.045	-10.0	1690.5	1641.3	-2.9	26.9	23.5	-12.6

Table 10 continued

CASE	λ	θ_0	θ	ϕ	τ_a	Z	L^m	L_d	$\%L$	ρ	ρ_d	$\%p$	F_g	F_{gd}	$\%F_g$	L_g	L_{gd}	$\%L_g$
11	0.486	30.0	0.0	0.0	0.25	80.00	0.1122	0.1122	0.0	0.050	0.050	0.0	1690.5	1691.1	0.03	26.9	26.9	0.0
						4.50	0.0795	0.0780	-2.0	0.050	0.048	-4.0	1690.5	1690.5	0.0	26.9	25.8	-4.0
						0.45	0.0507	0.0485	-4.3	0.050	0.047	-6.0	1690.5	1690.2	-0.01	26.9	25.3	-5.9
						80.00	0.1230	0.1230	0.0	0.050	0.050	0.0	1690.5	1691.1	0.03	26.9	26.9	0.0
						4.50	0.0860	0.0840	-2.4	0.050	0.048	-4.0	1690.5	1690.5	0.0	26.9	25.8	-4.1
			18.0	150.0														
						0.45	0.0523	0.0495	-5.4	0.050	0.047	-6.0	1690.3	1690.2	-0.02	26.9	25.3	-5.9
12	0.486	30.0	0.0	0.0	0.25	80.00	0.1122	0.1120	-0.1	0.050	0.050	0.0	1690.5	1690.9	0.02	26.9	26.9	0.0
						4.50	0.0795	0.0780	-1.9	0.050	0.048	-4.0	1690.5	1690.4	-0.01	26.9	25.8	-4.1
						0.45	0.0507	0.0491	-3.0	0.050	0.048	-4.0	1690.5	1690.4	-0.01	26.9	25.8	-4.1
						80.00	0.1230	0.1229	-0.1	0.050	0.050	-0.0	1690.5	1690.9	0.02	26.9	26.9	0.0
						4.50	0.0860	0.0842	-2.1	0.050	0.048	-4.0	1690.5	1689.4	-0.01	26.9	25.8	-4.1
			18.0	150.0														
						0.45	0.0523	0.0502	-3.9	0.050	0.048	-4.0	1690.3	1689.4	-0.01	26.9	25.8	-4.1

Table 10 continued

CASE	λ	θ_0	θ	ϕ	τ_a	z	L^m	L_d	$\%L$	ρ	ρ_d	$\%p$	F_g	F_{gd}	$\%F_g$	L_g	L_{gd}	$\%L_g$
13	0.486	30.0	0.0	0.0	0.25	80.00	0.1122	0.1119	-0.2	0.050	0.050	0.0	1690.5	1690.8	0.0	26.9	26.9	0.0
						4.50	0.0795	0.0801	0.7	0.050	0.051	2.0	1690.5	1691.1	0.0	26.9	27.5	2.2
						0.45	0.0507	0.0495	-2.3	0.050	0.049	-2.0	1690.5	1690.6	0.0	26.9	26.4	-1.9
			18.0	150.0		80.00	0.1230	0.1227	-0.3	0.050	0.050	0.0	1690.5	1690.8	0.0	26.9	26.9	0.0
						4.50	0.0860	0.0866	0.7	0.050	0.051	2.0	1690.5	1691.1	0.0	26.9	27.5	2.2
						0.45	0.0523	0.0518	-1.0	0.050	0.048	-4.0	1690.3	1690.3	0.0	26.9	25.8	-4.1

B) Interpolation errors.

CASE	λ	θ_0	θ	ϕ	τ_a	Z	L^m	L_d	$\%L$	ρ	ρ_d	$\%p$	F_g	F_{gd}	$\%F_g$	L_g	L_{gd}	$\%L_g$
14	0.486	30.0	0.0	0.0	0.375	80.00	0.1180	0.1180	0.0	0.050	0.050	0.0	1651.1	1650.8	-0.02	26.3	26.1	-0.8
						4.50	0.0845	0.0845	0.0	0.050	0.050	0.0	1651.1	1650.9	-0.02	26.3	26.3	0.0
						0.45	0.0527	0.0527	0.0	0.050	0.051	2.0	1651.1	1651.2	0.0	26.3	26.6	1.1
			18.0	150.0		80.00	0.1299	0.1299	0.0	0.050	0.050	0.0	1651.1	1650.7	-0.02	26.3	26.2	-0.4
						4.50	0.0920	0.0920	0.0	0.050	0.050	0.0	1651.1	1650.9	-0.01	26.3	26.4	0.4
						0.45	0.0550	0.0550	0.0	0.050	0.051	2.0	1651.1	1651.3	0.01	26.3	26.7	1.5
15	0.486	26.0	0.0	0.0	0.25	80.00	0.1141	0.1141	0.0	0.050	0.052	4.0	1702.2	1700.0	-0.12	27.1	28.4	4.7
						4.50	0.0809	0.0809	0.0	0.050	0.051	2.0	1702.2	1699.7	-0.15	27.1	27.7	2.2
						0.45	0.0512	0.0512	0.0	0.050	0.050	0.0	1702.2	1699.4	-0.16	27.1	27.2	0.4
			18.0	150.0		80.00	0.1235	0.1235	0.0	0.050	0.053	6.0	1702.2	1700.1	-0.12	27.1	28.5	5.2
						4.50	0.0865	0.0865	0.0	0.050	0.051	2.0	1702.2	1699.7	-0.15	27.1	27.8	2.6
						0.45	0.0526	0.0526	0.0	0.050	0.050	0.0	1702.2	1699.4	-0.16	27.1	27.2	0.4

Table 10 continued

CASE	λ	θ_0	θ	ϕ	τ_a	Z	L^m	L_d	$\%L$	ρ	ρ_d	$\%p$	F_g	F_{gd}	$\%F_g$	L_g	L_{gd}	$\%L_g$
16	0.486	30.0	20.0	150.0	0.25	80.00	0.1242	0.1242	0.0	0.050	0.050	0.0	1690.5	1690.5	0.0	26.9	26.8	-0.2
						4.50	0.0864	0.0864	0.0	0.050	0.050	0.0	1690.5	1690.5	0.0	26.9	26.9	0.0
						0.45	0.0524	0.0524	0.0	0.050	0.050	0.0	1690.3	1690.5	0.0	26.9	26.9	0.0
17	0.486	30.0	18.0	145.0	0.25	80.00	0.1122	0.1122	0.0	0.050	0.050	0.0	1690.5	1690.5	0.0	26.9	26.9	0.0
						4.50	0.0793	0.0793	0.0	0.050	0.050	0.0	1690.5	1690.5	0.0	26.9	26.7	-0.6
						0.45	0.0507	0.0507	0.0	0.050	0.050	0.0	1690.3	1690.5	0.0	26.9	26.4	-1.9

Table 10 continued

C) Input errors.

CASE	λ	θ_0	θ	ϕ	τ_a	z	L^m	L_d	$\%L$	ρ	ρ_d	$\%p$	F_g	F_{gd}	$\%F_g$	L_g	L_{gd}	$\%L_g$
33	0.486	30.0	0.0	0.0	0.25	80.00	0.1122	0.1178	5.0	0.050	0.057	14.0	1690.5	1692.5	0.1	26.9	31.0	15.1
						4.50	0.0795	0.0835	5.0	0.050	0.055	10.0	1690.5	1691.9	0.1	26.9	29.5	9.7
						0.45	0.0507	0.0532	5.0	0.050	0.053	6.0	1690.5	1691.3	0.0	26.9	28.5	5.9
						80.00	0.1234	0.1295	5.0	0.050	0.058	16.0	1690.5	1692.8	0.1	26.9	31.3	16.2
			30.0	120.0			0.0860	0.0903	5.0	0.050	0.055	10.0	1690.5	1692.0	0.1	26.9	29.8	10.6
						0.45	0.0521	0.0547	5.0	0.050	0.053	6.0	1690.5	1691.4	0.1	26.9	28.5	6.1
34	0.486	30.0	0.0	0.0	0.25	80.00	0.1122	0.1234	10.0	0.050	0.064	28.0	1690.5	1694.6	0.2	26.9	34.7	28.9
						4.50	0.0795	0.0875	10.0	0.050	0.060	20.0	1690.5	1693.2	0.2	26.9	32.1	19.4
						0.45	0.0507	0.0557	10.0	0.050	0.056	12.0	1690.5	1695.1	0.3	26.9	30.1	11.8
						80.00	0.1234	0.1357	10.0	0.050	0.066	32.0	1690.5	1695.1	0.3	26.9	35.7	32.5
			30.0	120.0		4.50	0.0860	0.0946	10.0	0.050	0.060	20.0	1690.5	1693.5	0.2	26.9	32.6	21.2
						0.45	0.0521	0.0573	10.0	0.050	0.056	12.0	1690.5	1692.3	0.1	26.9	30.3	12.7

Table 10 continued

CASE	λ	θ_0	θ	ϕ	τ_a	Z	L^m	L_d	$\%L$	ρ	ρ_d	$\%p$	Fg	Fgd	$\%Fg$	Lg	Lgd	$\%Lg$
35	0.486	30.0	0.0	0.0	0.25	80.00	0.1122	0.1122	0.0	0.050	0.055	10.0	1690.5	1722.6	1.9	26.9	30.3	12.5
						4.50	0.0795	0.0795	0.0	0.050	0.054	8.0	1690.5	1722.3	1.9	26.9	29.5	9.7
						0.45	0.0507	0.0507	0.0	0.050	0.051	2.0	1690.5	1721.6	1.8	26.9	27.7	3.1
			30.0	120.0		80.00	0.1234	0.1234	0.0	0.050	0.056	12.0	1690.5	1722.9	1.9	26.9	30.9	15.0
						4.50	0.0860	0.0860	0.0	0.050	0.055	10.0	1690.5	1722.6	1.9	26.9	30.1	11.8
						0.45	0.0521	0.0521	0.0	0.050	0.051	2.0	1690.5	1721.7	1.8	26.9	27.9	3.8
36	0.486	30.0	0.0	0.0	0.25	80.00	0.1122	0.1122	0.0	0.050	0.053	6.0	1651.1	1706.6	0.9	26.9	28.6	6.3
						4.50	0.0795	0.0795	0.0	0.050	0.052	4.0	1651.1	1706.4	0.9	26.9	28.2	4.9
						0.45	0.0507	0.0507	0.0	0.050	0.050	0.0	1651.1	1706.1	0.9	26.9	27.3	1.6
			30.0	120.0		80.00	0.1234	0.1234	0.0	0.050	0.053	6.0	1651.1	1706.7	1.0	26.9	28.6	6.2
						4.50	0.0860	0.0860	0.0	0.050	0.052	4.0	1651.1	1706.5	0.9	26.9	28.5	5.9
						0.45	0.0521	0.0521	0.0	0.050	0.050	0.0	1651.1	1706.1	0.9	26.9	27.3	1.5

Table 10 continued

CASE	λ	θ_0	θ	ϕ	τ_a	Z	L^m	L_d	$\%L$	ρ	ρ_d	$\%p$	F_g	F_{gd}	$\%F_g$	L_g	L_{gd}	$\%L_g$		
37	0.486	30.0	0.0	0.0	1.00	80.00	0.1545	0.1545	0.0	0.050	0.071	42.0	1457.7	1524.7	4.6	26.4	34.9	32.0		
								4.50	0.1210	0.1210	0.0	0.050	0.071	42.0	1457.7	1524.6	4.6	26.4	34.8	31.5
								0.45	0.0712	0.0712	0.0	0.050	0.060	20.0	1457.7	1521.1	4.3	26.4	29.1	10.0
								80.00	0.1716	0.1716	0.0	0.050	0.071	42.0	1456.7	1524.7	4.7	26.4	34.9	32.0
								4.50	0.1343	0.1343	0.0	0.050	0.074	48.0	1456.7	1525.5	4.7	26.4	36.3	37.2
38	0.486	30.0	0.0	0.0	1.00	80.00	0.1545	0.0703	0.0	0.050	0.061	22.0	1456.7	1521.5	4.4	26.4	29.7	12.4		
								4.50	0.1210	0.1210	0.0	0.050	0.064	28.0	1457.7	1491.1	2.3	26.4	30.6	15.7
								0.45	0.0712	0.0712	0.0	0.050	0.059	18.0	1457.7	1489.7	2.2	26.4	28.3	7.0
								80.00	0.1716	0.1716	0.0	0.050	0.064	28.0	1456.7	1491.2	2.4	26.4	30.7	16.0
								4.50	0.1343	0.1343	0.0	0.050	0.064	28.0	1456.7	1491.1	2.4	26.4	30.6	15.7
39	0.486	30.0	0.0	0.0	1.00	80.00	0.1545	0.0703	0.0	0.050	0.059	18.0	1456.7	1489.6	2.3	26.4	28.1	6.2		
								4.50	0.1210	0.1210	0.0	0.050	0.064	28.0	1457.7	1491.1	2.3	26.4	30.6	15.7
								0.45	0.0712	0.0712	0.0	0.050	0.059	18.0	1457.7	1489.7	2.2	26.4	28.3	7.0
								80.00	0.1716	0.1716	0.0	0.050	0.064	28.0	1456.7	1491.2	2.4	26.4	30.7	16.0
								4.50	0.1343	0.1343	0.0	0.050	0.064	28.0	1456.7	1491.1	2.4	26.4	30.6	15.7

Table 10 continued

CASE	λ	θ_0	θ	ϕ	τ_a	Z	L^m	L_d	$\%L$	ρ	ρ_d	$\%p$	F_g	F_{gd}	$\%F_g$	L_g	L_{gd}	$\%L_g$	
39	0.486	30.0	0.0	0.0	0.25	80.00	0.1122	0.1122	0.0	0.050	0.050	0.0	1690.5	1699.3	0.5	26.9	27.1	0.5	
								4.50	0.0795	0.0	0.050	0.050	0.0	1690.5	1699.2	0.5	26.9	26.8	0.3
								0.45	0.0507	0.0	0.050	0.050	0.0	1690.5	1699.2	0.5	26.9	26.8	0.3
								80.00	0.1234	0.0	0.050	0.052	4.0	1690.5	1700.0	0.6	26.9	28.3	5.1
								4.50	0.0860	0.0	0.050	0.051	2.0	1690.5	1699.6	0.5	26.9	27.5	2.3
40	0.486	30.0	0.0	0.0	0.25	80.00	0.1122	0.1122	0.0	0.050	0.050	0.0	1690.5	1694.9	0.3	26.9	27.0	0.3	
						4.50	0.0795	0.0795	0.0	0.050	0.050	0.0	1690.5	1694.9	0.3	26.9	26.9	0.2	
						0.45	0.0507	0.0507	0.0	0.050	0.050	0.0	1690.5	1694.9	0.3	26.9	26.9	0.1	
						80.00	0.1234	0.1234	0.0	0.050	0.051	2.0	1690.5	1695.2	0.3	26.9	27.6	2.5	
						4.50	0.0860	0.0860	0.0	0.050	0.050	0.0	1690.5	1695.0	0.3	26.9	27.2	1.1	
						0.45	0.0521	0.0521	0.0	0.050	0.050	0.0	1690.5	1699.3	0.5	26.9	27.0	0.3	

Table 10 continued

CASE	λ	θ_0	θ	ϕ	τ_a	Z	L^m	L_d	$\%L$	P	p_d	$\%p$	Fg	Fgd	$\%Fg$	Lg	Lgd	$\%Lg$
41	0.486	30.0	0.0	0.0	0.25	80.00	0.1122	0.1122	0.0	0.050	0.051	2.0	1690.5	1676.9	0.8	26.9	27.6	2.7
							4.50	0.0795	0.0795	0.0	0.050	0.0	1690.5	1690.4	0.0	26.9	26.7	0.8
							0.45	0.0507	0.0507	0.0	0.050	0.0	1690.5	1690.6	0.0	26.9	27.0	0.3
42	0.486	30.0	0.0	0.0	0.25	80.00	0.1122	0.1122	0.0	0.050	0.053	6.0	1690.5	1691.2	0.0	26.9	28.3	5.3
							4.50	0.0795	0.0795	0.0	0.050	2.0	1690.5	1690.9	0.0	26.9	27.6	2.7
							0.45	0.0507	0.0507	0.0	0.050	0.0	1690.5	1690.6	0.0	26.9	27.1	0.6
43	0.486	30.0	0.0	0.0	0.25	80.00	0.1122	0.1122	0.0	0.050	0.050	0.0	1690.5	1690.5	0.0	26.9	26.9	0.0
							4.50	0.0795	0.0795	0.0	0.050	0.0	1690.5	1690.5	0.0	26.9	26.9	0.0
							0.45	0.0507	0.0507	0.0	0.050	0.0	1690.5	1690.5	0.0	26.9	26.9	0.0
44	0.486	30.0	30.0	150.0	0.25	80.00	0.1234	0.1234	0.0	0.050	0.050	0.0	1690.5	1690.5	0.0	26.9	26.9	0.0
							4.50	0.0860	0.0860	0.0	0.050	0.0	1690.5	1690.5	0.0	26.9	26.9	0.0
							0.45	0.0521	0.0521	0.0	0.050	0.0	1690.5	1690.5	0.0	26.9	26.9	0.0

library of phase functions that were computed for 19 models of the accumulation mode. The size distribution is a single log-normal aerosol size distribution with an index of refraction of $n = 1.349 - 0.008i$, geometric mean mass radius $r_m = 0.6 \mu\text{m}$, and standard deviation of the logarithm of the radius $\sigma = 0.61$. This phase function is compared with the phase function used in the algorithm in Figure 5 along. The second phase function used in the sensitivity analysis is chosen assuming a power law aerosol size distribution. The power chosen is $v = 4$ where

$$\frac{dn}{d\ln r} \sim r^{-v}$$

and the index of refraction is $n = 1.53 - 10^{-7}i$. This phase function is also shown in Figure 5. Chayanova and Shifrin (1966) found this power law most closely matched the model number 4 (the surface visibility is 20 km) aerosol phase function measured by Barteneva (1960). These two models are designated as cases 1 and 2 in Tables 8-10. Figure 5 shows that the bimodal log-normal phase function used in the algorithm lies between the two phase functions used in the sensitivity study for scattering angles greater than about 50° . Therefore, these two phase functions are chosen to represent extreme experimental conditions where the true aerosol scattering in the backward direction does not match the scattering assumed in the model.

Both of the phase functions used in the sensitivity analysis produced errors in the derived surface reflectance of approximately $\pm 20\text{-}30\%$. The phase function derived using the single mode log-normal aerosol size distribution produced surface reflectance values too small, while the phase function derived using the power size distribution produced surface reflectance values too large. It should be noted that the two phase functions were chosen to represent the possible extremes in the scattering phase function (for large scattering angles) so that the errors associated with uncertainties in the phase function should usually be smaller.

Large negative reflectance errors (case 1) indicate that the algorithm will return negative reflectances, if the actual reflectance is weak. The large negative percentage reflectance error corresponds to an error magnitude of $\Delta\rho = -0.012$. If the simulation surface reflectance was less than $+0.012$, the algorithm would return a negative reflectance.

The large errors associated with these uncertainties in the aerosol single scattering phase function indicate that the algorithm in its present form is limited to applications where the aerosol scattering phase function closely matches the function used in the algorithm.

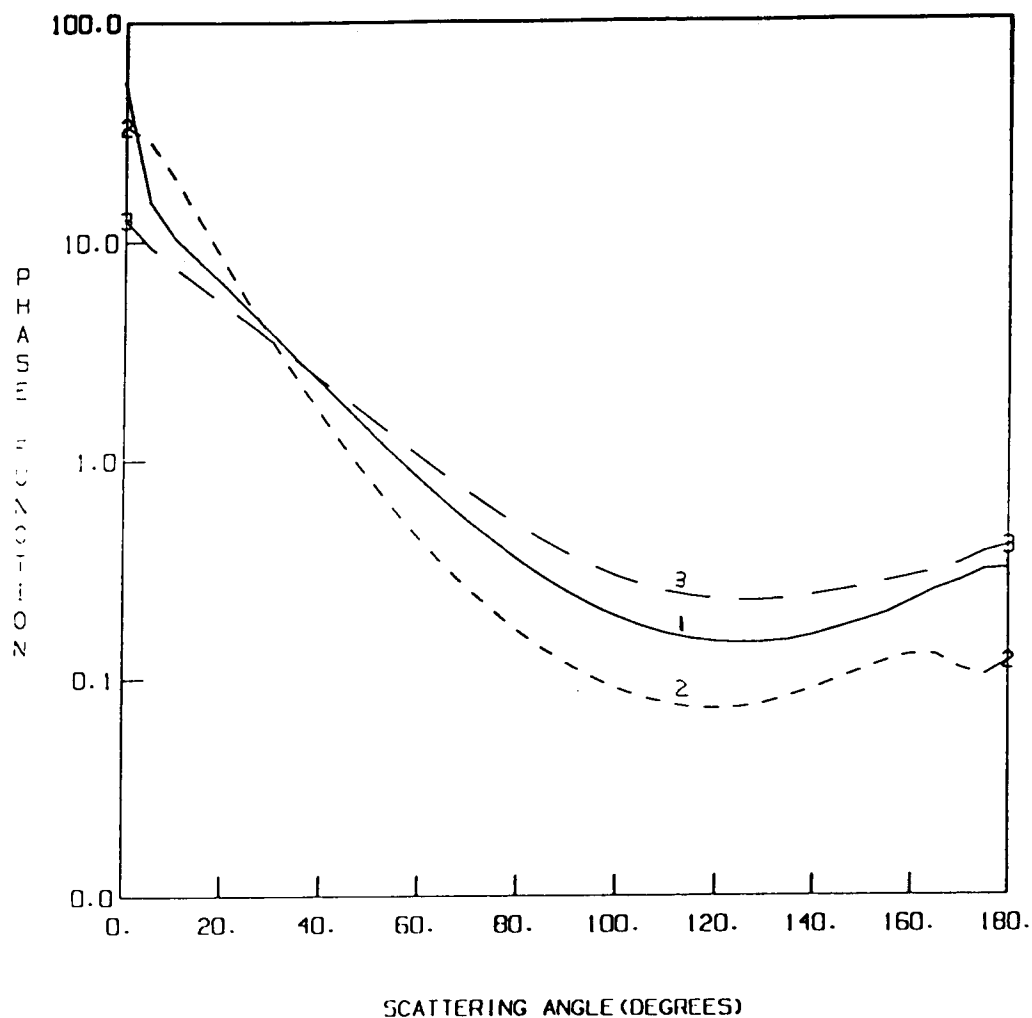


Figure 5. Aerosol single scattering phase functions derived from: 1) bimodal log-normal aerosol size distribution used in the unperturbed model (—), 2) single log-normal aerosol size distribution with an index of refraction $n = 1.349 - 0.008i$, geometric mean mass radius $r_m = 0.6 \mu\text{m}$, standard deviation of the logarithm of the radius $\sigma = 0.61$ (- -), and 3) power law aerosol size distribution with $\nu = 4$ and an index of refraction $n = 1.53 - 10^{-7}i$ (— · —).

However, the algorithm could be easily modified for use with other aerosol size distributions by replacing the look-up tables of path radiance, downward flux, transmission, and atmospheric backscattering ratio with values generated for a more appropriate aerosol size distribution. It is not necessary for these values to be generated by the same Dave (1972 a,b,c,d) radiative transfer code used to derive the values used here as long as the values tabulated are defined as in eq. (6-8).

6.1.2 Polarization

The algorithm which performs the atmospheric corrections uses tabulated radiances and fluxes computed with a Dave radiative transfer code. This code is based upon the scalar form of the radiative transfer equation, where the assumption is that the light scattered by the atmosphere and the earth's surface is unpolarized. If the atmospheric optical thickness is small this assumption is satisfactory, since the primary source of the light scattered by the atmosphere is the direct, unpolarized sunlight. The polarization errors are caused by second and higher order scattering of light that is polarized, and increase with optical thickness and decreasing wavelength. Light scattered by the surface, and especially by the atmosphere, is polarized.

Therefore, sensitivity tests are performed to estimate surface reflectance errors caused by neglect of polarization. In these tests, polarization is accounted for by another Dave code, similar in all other aspects to the scalar code. These sensitivity tests are performed for three wavelengths (cases 3,4,5): 0.486 μm (TM band 1), 0.639 μm (AVHRR band 1), and 0.845 μm (AVHRR band 2). Errors in derived surface reflectance associated with the assumption of unpolarized light are less than 3% for $\lambda \geq 0.639 \mu\text{m}$ (cases 4 and 5), but increase to approximately 10% for $\lambda = 0.486 \mu\text{m}$ (TM band 1). Although the results are not shown in the tables, the errors associated with the assumption of unpolarized light generally decrease with decreasing aerosol optical thickness because less multiple scattering occurs.

6.1.3 Water Vapor and Ozone Absorption

Another potential source of error which is examined is the effect of using an incorrect value of the gaseous absorption. Since most of the gaseous absorption in the Landsat TM and NOAA AVHRR visible and near IR bands is contributed by either water vapor or ozone, the sensitivity tests are run at those wavelengths where absorption by these

constituents is the largest. For water vapor this occurs for AVHRR band 2 while for ozone this occurs for TM band 2.

Since the amount of an absorbing gas is variable, the algorithm uses a weighted average of the gaseous absorption values computed for the tropical, mid-latitude summer, and mid-latitude winter models given in the LOWTRAN code. Most of the weight is given to the mid-latitude summer profile (see eq. 16). In the case of AVHRR band 2, the algorithm uses a water vapor gaseous absorption optical thickness of $\tau_g = 0.0933$. The gaseous absorption optical thicknesses computed using the mid-latitude winter and tropical profiles are used for the sensitivity studies. Therefore, two tests are made to estimate the uncertainty due to water vapor absorption; the first test uses the mid-latitude winter value of $\tau_g = 0.0486$ (case 6) while the second test uses the tropical value of $\tau_g = 0.1235$ (case 7).

A change in the total amount of water vapor between the algorithm and mid-latitude winter profiles (case 6) causes errors as large as 11% in the derived surface reflectance for AVHRR band 2. Since the difference in the total water vapor amounts between the algorithm and tropical profiles is smaller than the difference between the algorithm and mid-latitude winter profiles, the magnitude of the error that results from using the tropical profile is less--7% (case 7). These errors can be reduced significantly by applying the water vapor correction given in Section 3.3.

A second set of tests is conducted to determine the sensitivity of the model to changes in ozone absorption. Since TM band 2 has the largest ozone absorption, the ozone absorption sensitivity tests are run at this wavelength. As in the case of water vapor absorption discussed above, the algorithm uses a weighted average of the mid-latitude winter, mid-latitude summer, and tropical profiles computed using the LOWTRAN code to derive a value of ozone absorption optical thickness of $\tau_g = 0.032$ for TM band 2. The first of two sensitivity tests are run using the mid-latitude winter ozone absorption optical thickness $\tau_g = 0.039$ (case 8) while the second test is run using the tropical value of $\tau_g = 0.024$ (case 9). The magnitude of errors in the the derived surface reflectance in TM band 2 caused by variations in mid-latitude winter and tropical profiles to the algorithm ozone amounts is 2-4% (cases 8 and 9).

6.1.4 Aerosol Absorption

The sensitivity of the correction algorithm to aerosol absorption is tested by changing the aerosol single scattering albedo ω_0 , which is the ratio of aerosol scattering to extinction. The algorithm uses values of ω_0 derived for the 70%-relative-humidity, rural model of Shettle and Fenn (1979); in this model the aerosol single scattering albedo varies from 0.95 at $\lambda = 0.486 \mu\text{m}$ to 0.86 at $\lambda = 2.550 \mu\text{m}$. Values of the single scattering albedo for the visible spectrum, reported by Waggoner et al. (1981), range from $0.54 \leq \omega_0 \leq 0.61$ for urban industrial areas, $0.73 \leq \omega_0 \leq 0.87$ for urban residential areas, and $0.89 \leq \omega_0 \leq 1.00$ for rural areas. These values agree with the values used by Shettle and Fenn. In the sensitivity test (case 10), a value of $\omega_0 = 0.84$ at $0.486 \mu\text{m}$ is based upon the average measured values in residential urban areas of Michigan and Missouri (Waggoner et al., 1981). Since the algorithm is designed to correct radiances measured over rural sites, this should represent a rather extreme (but possible) departure from the usual case.

The derived surface reflectance is somewhat sensitive to changes in aerosol absorption (case 10). This sensitivity appears to depend strongly on geometry, as the resulting errors in the derived reflectance vary between -10 to 0% for the case when the single scattering albedo decreased from 0.95 to 0.84.

Another study of the effect of aerosol absorption error on the derived surface reflectance is given out of sequence (case 10a), because the unperturbed model is different. The emphasis is on a large solar zenith angle ($\theta_0 = 64^\circ$), long path through the atmosphere ($\theta = 56^\circ$), and rather large aerosol optical thickness ($\tau_a = 0.35$). Interpolations are made on all these variables plus the azimuth. Also, the simulated surface reflectance is high (0.6). The error (-0.11%) is significant. The error would be less with smaller optical thickness, however.

6.1.5 Vertical Distribution of Aerosols

The next sensitivity test deals with errors which result from uncertainty in the vertical distribution of aerosols. The altitude distribution of aerosols used in the algorithm is based on the 'average' distribution described by Braslau and Dave (1973) which is shown in Figure 4. The sensitivity of the results to this distribution is tested by using three different profiles which are constructed using the aerosol models described by Shettle and Fenn (1979). In these models, the atmosphere is divided into four regions: boundary layer (0 - 2 km), upper troposphere (2 - 9 km), stratosphere (9 - 30 km), and upper atmosphere

(30 - 100 km). All three of the models use the background aerosol models for the stratosphere and upper atmosphere regions; the perturbation models differ in the boundary layer and upper troposphere regions. The first model (case 11) uses the 50-km-visibility, rural model in the boundary layer and the 50-km-visibility, spring/summer model in the upper troposphere. The second model (case 12) uses the 23-km-visibility, rural model in the boundary layer and the 23-km-visibility, spring/summer model in the upper troposphere. The third model (case 13) uses the 10-km-visibility, rural model in the boundary layer and the 23-km-visibility, spring/summer model in the upper troposphere. The vertical distributions of aerosol corresponding to these three models are shown in Figure 4. These profiles are normalized to produce an optical thickness of $\tau_a = 0.25$ at $0.550 \mu\text{m}$. Since the average visibility in the midwestern U.S. is about 20 km (Husar and Holloway, 1984), a maximum visibility of 50 km and a minimum visibility of 10 km are chosen to represent the extremes used for the construction of the altitude distribution of aerosols.

Uncertainty in the height distribution of aerosols has a negligible effect on the surface reflectance when measured from the top of the atmosphere, since the aerosol distribution is normalized such that the total aerosol optical thickness below the sensor remains the same (cases 11, 12 and 13). However, if a sensor is within the atmosphere, there will be small differences in the optical thickness of aerosols above and below the sensor, depending upon which aerosol distribution is used. The magnitude of the derived reflectance errors is less than 7% at aircraft heights (Table 10).

6.1.6 Bidirectional Reflectance Errors

The final model error concerns the assumption that the surface is Lambertian. Surfaces do not reflect light according to Lambert's Law as is assumed for the current atmospheric correction algorithm. Lee and Kaufman (1986) calculated the error in the derived surface reflectance for a model which also assumed Lambert reflection. Their study utilized actual surface bidirectional reflectances for pasture as measured by Kriebel (1977). The absolute errors in estimates of surface reflectance are a few hundredths when the solar zenith angle is small because the surface is nearly Lambertian. The errors are also small where the surface reflectance is weak. The derived surface reflectance errors become large (about 0.1), however, for moderate haze, when the surface reflectance is both high and strongly anisotropic. Errors in the derived surface reflectance and radiance, but not the irradiance, will not be significant if the surface reflectance is weak; however, the errors can be important for strong bidirectional reflectance.

6.2 Interpolation Errors

The correction algorithm is based on a series of look-up tables relating surface reflectance to measured upward radiance for various aerosol optical thicknesses and geometries. As a result, the algorithm must interpolate to determine the reflectance corresponding to an arbitrary input radiance, aerosol optical thickness, gaseous absorption optical thickness, altitude, and geometry. (No extrapolation is permitted.) The simulations are chosen to show the largest interpolation errors. The interpolation errors are computed by comparing the reflectance errors derived from simulated radiances with those derived with the correction algorithm.

The first interpolation sensitivity test (case 14) is performed using the standard test input parameters described earlier ($\lambda = 0.486 \mu\text{m}$, $\theta_0 = 30^\circ$, $\theta = 0^\circ$, $\phi = 0^\circ$), except with an aerosol optical thickness of $\tau_a = 0.375$, which requires the algorithm to interpolate between $\tau_a = 0.25$ and $\tau_a = 0.50$. Note that the reflectance errors are deviations from the correct value of $\rho = 0.05$ for cases 14-21 and 24-32; the unperturbed reflectance changes only for cases 22 and 23. The next run (case 15) tests the interpolation on solar zenith angle. The solar zenith angle interpolation test is run using the standard test input parameters except with a solar zenith angle of 26° which requires the algorithm to interpolate between $\theta_0 = 20^\circ$ and $\theta_0 = 30^\circ$. Similar tests are run for the observation zenith angle (case 16) and the azimuth angle (case 17). The observation zenith angle interpolation test was run using $\theta = 20^\circ$, which requires the algorithm to interpolate between $\theta = 18^\circ$ and $\theta = 24^\circ$. The azimuth angle interpolation test was run using $\phi = 145^\circ$ so that the algorithm interpolated between $\phi = 140^\circ$ and $\phi = 150^\circ$. Separate interpolations on τ_a , θ , and ϕ result in errors less than 1% in the derived surface reflectance, while the interpolation on θ_0 can result in an error as large as 4%.

Errors associated with interpolation on wavelength are shown in cases 18 - 20. The input wavelengths are 0.5, 0.6 and $0.775 \mu\text{m}$. In these cases, the error in derived surface reflectance is at most 6%.

Since the algorithm may also interpolate on gaseous absorption, sensitivity tests are also made to determine the uncertainty involved with this interpolation. In cases 21-23 the algorithm uses the input gaseous absorption value τ_g computed using the LOWTRAN 6 code and the radiances associated with TM band 4 ($0.840 \mu\text{m}$) (which has a narrow bandwidth and relatively small gaseous absorption) to determine the surface reflectance

seen by the AVHRR band 2 (which has a wide bandwidth and relatively large gaseous absorption). These tests show the algorithm underestimates the surface reflectance by only about 1-2%.

Sensitivity tests are also made to determine the errors associated with adjustments to the look-up tables corresponding to different input surface heights. As discussed in section 3.5, the algorithm makes the adjustment by changing the wavelength slightly (eq. 20). Cases 24 and 25 show that this adjustment results in rather large errors in the derived surface reflectance of -8%.

Errors associated with interpolation on the measurement altitude Z are studied. The radiative transfer computations are tabulated at three altitudes: 0.45 km, 4.5 km, and 80 km. In cases 26 to 28 input observation altitudes of $Z = 0.23$ km, 2.96 km, and 6.5 km are used. The derived surface reflectance errors are as large as 8%.

Finally, errors associated with interpolation for large solar and viewing zenith angles are given. Interpolations are made with respect to τ_a , θ_o , θ , and ϕ ; the surface reflectance $\rho = 0.05$ (cases 29 -32). Case 29 shows that the error is appreciable for a rather large optical thickness. This large error depends on the nonlinear change in radiance as the azimuth increases from 10° to 20° . If the same test is made, except that the azimuth is 165° , the error reduces to 8% (case 30). When the optical thickness decreases to $\tau_a = 0.1$ (case 31), however, the error has a large negative value. The derived value is $\rho = 0.034$, compared with the simulation value of $\rho = 0.050$. Again, if the azimuth is changed from near-forward (case 31) to near-backward (case 32), the magnitude of the error decreases to 6%.

6.3 Input Errors

A third set of sensitivity tests is performed to estimate the errors in the derived surface reflectance resulting from errors or uncertainties in the input data. Each test is performed with the algorithm model, except that an incorrect value of one of the input parameters is used.

The first test introduces a 5% error into the input radiance (case 33). As would be expected, the algorithm is very sensitive to such an error. If the input radiance error increases to 10% (case 34 in Tables 8 and 10), the reflectance error doubles to 28%. The relative errors in the derived surface reflectance can be as large as two to three times the relative errors in the input radiance.

Errors in the input optical thickness occur because of measurement errors, and the optical thickness is not measured at the same time and place of the remote measurement. Tests are made with an error in the input aerosol optical thickness of $\Delta\tau_a = 0.05$ for the case where the correct input is $\tau_a = 0.25$ (case 36), and for $\Delta\tau_a = 0.1$ when $\tau_a = 1.0$ (case 38). The derived surface reflectance errors caused by optical thickness errors are largest when the surface reflectance is weak. Hence, the errors are computed for visible reflectance of visible light from vegetation ($\rho = 0.05$). The resulting surface reflectance error of 0.003 is insensitive to errors of 0.05 for moderate aerosol optical thickness (case 36). For $\tau_a = 1.0$ and larger aerosol optical thickness error of 0.1, the error in the derived surface reflectance increases to $\Delta\rho = 0.014$ (case 38).

The solar zenith angle test is run by introducing an error of $\Delta\theta_o = 2^\circ$ (case 40) when the correct input is $\theta_o = 30^\circ$. Similarly, the sensitivity of the results to errors in the input observation zenith angle is tested by introducing an error of $\Delta\theta = 2^\circ$ (case 41) when the correct input is $\theta = 0^\circ$. Finally, the sensitivity to errors in the input azimuth angle is tested by introducing an error of $\Delta\phi = 2^\circ$ for the case when the correct input is $\phi = 0^\circ$ (case 44). Errors in the input values of solar zenith, observation zenith, and azimuth angles generally result in negligible errors of less than 2% in the derived surface reflectance.

7.0 Conclusion

An algorithm is developed to account for atmospheric effects when deriving surface reflectance properties from visible and near-infrared radiances measured by aircraft or satellite over rural areas. The radiance that would be measured for a given surface reflectance can be derived, also. The algorithm uses a tabulated set of radiances computed for various wavelengths, solar and observation angles, and aerosol optical thicknesses. All aerosol parameters have been assumed, except for the aerosol optical thickness, which is an input value. Since the algorithm performs essentially interpolations, it is fast; therefore, it is well suited for reducing observations in many wavelengths. Otherwise, the effect of the atmosphere requires many radiative transfer computations.

Large errors in derived parameters, rather than rms errors are estimated. Among the largest model errors are those caused by uncertainties in the aerosol scattering phase function; in this case surface reflectance and radiance errors reach ± 20 -30%. Thus, in its current configuration, the algorithm is suitable for only a rural, bimodal log-normal aerosol size distribution. However, the algorithm could be easily modified for use with other

aerosol size distributions by replacing the radiance look-up tables with values generated for a more appropriate aerosol size distribution.

Errors in the derived surface reflectance can be large when either the slant path through the atmosphere of sunlight or light reflected from the ground is long. The uncertainty in the amount of water vapor causes an error of 5% in the reflectance for AVHRR band 2. This error can be reduced significantly by using measurements of the total amount of water vapor at the time of measurement. The mesh for the tabulated radiation parameters is fine enough so that linear interpolation results in small reflectance errors (<4%).

Of the errors in the input parameters required by the correction algorithm, errors in the measured radiance can result in large errors in the derived radiance and reflectance but not irradiance. Absolute measured radiance errors of 5-10% are expected. Therefore, the derived surface radiances and reflectances will deviate by at least 5-10% from the correct values even without any errors in the atmospheric correction algorithm. Large errors in the derived surface reflectance can also result from errors in the input values of aerosol optical thickness. Optical thickness errors should be less than 0.05 so that the corresponding surface reflectance errors are less than 10% for a dark surface ($\rho = 0.05$).

Acknowledgement: We appreciate Mr. Brian Markham's early efforts to use the tables, and thereby bring to our attention places to improve their accuracy.

8.0 References

- Ahmad, Z. and R.S. Fraser, 1982: An iterative radiative transfer code for ocean-atmosphere system, *J. Atmos. Sci.*, **39**, 656-665.
- Barteneva, C.D., 1960: Scattering functions of light in the atmospheric boundary layer., *Izv. Geophys. Ser.*, 1852-1865.
- Bohren, C.F. and D.R. Huffman, 1983: *Absorption and scattering of light by small particles.*, Wiley, New York.
- Braslau, N. and J.V. Dave, 1973: Effect of aerosols on the transfer of solar energy through realistic model atmospheres. Part I: Non-absorbing aerosols., *J. Appl. Meteor.*, **12**, 601-615.
- Carlson T.N., 1979: Atmospheric turbidities in Saharan dust outbreaks as determined by analysis of satellite brightness data, *Mon. Wea. Rev.*, **107**, 322-335.

- Chandrasekhar, S., 1960: *Radiative Transfer*, Dover, New York.
- Chayanova, E.A. and K.S. Shifrin, 1966: The scattering indicatrix of the atmospheric boundary layer., *Izv., Atm. and Oceanic Phys.*, **4**, No. 2, 233-235.
- Dave, J.V., 1972a: *Development of programs for computing characteristics of ultraviolet radiation - Technical Report - Scalar Case, Program I*, FSC-72-0009, IBM Federal Systems Division, Gaithersburg, Maryland.
- , 1972b: *Development of programs for computing characteristics of ultraviolet radiation - Technical Report - Scalar Case, Program II*, FSC-72-0011, IBM Federal Systems Division, Gaithersburg, Maryland.
- , 1972c: *Development of programs for computing characteristics of ultraviolet radiation - Technical Report - Scalar Case, Program III*, FSC-72-0012, IBM Federal Systems Division, Gaithersburg, Maryland.
- , 1972d: *Development of programs for computing characteristics of ultraviolet radiation - Technical Report - Scalar Case, Program IV*, FSC-72-0013, IBM Federal Systems Division, Gaithersburg, Maryland.
- Ferrare, R.A., R.S. Fraser and Y.J. Kaufman 1988: Satellite remote sensing of large scale air pollution - measurements of forest fires smoke, submitted to *J. Geoph. Res.*
- Fraser, R.S., Y.J. Kaufman, and R.L. Mahoney, 1984: Satellite measurements of aerosol mass and transport, *Atmos. Environ.*, **18**, 2577-2584.
- Fraser, R.S. and Y.J. Kaufman, 1985: The relative importance of aerosol scattering and absorption in remote sensing., *IEEE Trans. Geosc. Remote Sensing*, **GE-23**, No. 5, 625-633.
- Gordon, H.R., D.K. Clark, J.W. Brown, O.B. Brown, R.H. Evans, and W.W. Broenkow, 1983: Phytoplankton pigment concentration in the middle Atlantic bight: Comparison of ship determination and CZCS estimates, *Appl. Optics*, **22**, 20-36.
- Griggs, M., 1975: Measurements of atmospheric aerosol optical thickness over water using ERTS-1 data, *J. Air Pollut. Control Ass.*, **25**, 622-626.
- Hansen, J.E. and L.D. Travis, 1974: Light scattering in planetary atmospheres., *Space Sci. Rev.*, **16**, No. 4, 527-610.

- Herman, B.M., R.S. Browning, and J. DeLuise, 1975; Determination of the effective imaginary term of the complex index of refraction of atmospheric dust by remote sensing: The diffuse-direct radiation method., *J. Atmos. Sci.*, **32**, 918-925.
- Holben B.N., 1986: Characteristics of maximum value composite images for temporal AVHRR data, *Int. J. Rem. Sens.*, **7**, 1417-1437.
- Husar, R.B. and J.M. Holloway, 1984: Properties and climate of atmospheric haze., *Hygroscopic Aerosols*, (L.H. Ruhnke and A. Deepak, eds.), A. Deepak, Hampton, VA, 129-170.
- Kaufman, Y.J., 1987: Satellite sensing of aerosol absorption, *J. Geoph. Res.*, **92**, 4307-4317.
- Kaufman, Y.J. and R.S. Fraser, 1983: Light extinction by aerosols during summer air pollution, *J. Appl. Meteor.*, **22**, 1694-1706.
- Kaufman, Y.J., R.S. Fraser and R.A. Ferrare, 1988: Satellite remote sensing of large scale air pollution - method, submitted to *J. Geoph. Res.*
- Kaufman Y.J. and C. Sendra, 1988: Automatic atmospheric correction, accepted to *Int. J. Rem. Sens.*
- Kidwell, C.D, 1985: NOAA Polar Orbiter Data User's Guide, NOAA-NESDIS, Washington, D.C., 20233
- King, M. D. 1979: Determination of the ground albedo and the index of absorption of atmospheric particulates by remote sensing. Part II: application, *J. Atmos Sci.*, **36**, 1072-1083.
- King, M. D. and B. M. Herman, 1979: Determination of the ground albedo and the index of absorption of atmospheric particulates by remote sensing. Part I: theory, *J. Atmos Sci.*, **36**, 163-173.
- King M.D., D.M. Byrne, B.M. Herman and J.A. Reagan, 1978: Aerosol size distribution obtained by inversion of optical depth measurements, *J. Atmos. Sci.*, **35**, 2153-2167.
- Knieszys, F.X., E.P. Shettle, W.O. Gallery, J.H. Chetwynd, L.W. Abreu, J.E.A. Selby, S.A. Clough, R.W. Fenn, 1983: *Atmospheric transmittance/radiance: computer code LOWTRAN 6*, AFGL-TR-83-0187, Air Force Geophysics Lab, Hanscom AFB, MA.

- Koepke, P. and H. Quenzel, 1979: Turbidity of the atmosphere determined from satellite calculation of optimum viewing geometry, *J. Geoph. Res.*, **84**, 7847-7855.
- Kriebel, K.T., 1977: *Reflection properties of vegetated surfaces: tables of measured spectral biconical reflectance factors*, Muenchener Universitaets-Schriften, Meteorologisches Institut, Wissenschaftl. Mitteilung 29, 1977.
- Lee, T. and Y.J. Kaufman, 1986: The effect of surface nonlambertianity on remote sensing., *IEEE Trans. Geosc. Remote Sensing*, GE-24, No. 5, 699-708.
- Markham, B. and J.L. Barker, 1985: Spectral characterization of the Landsat TM sensors, *Landsat-4 Science Characterization - Early Results*, 2, NASA Conf. Pub. 2355, 235-276.
- McClatchey, R.A., R.W. Fenn, J.E.A. Selby, F.E. Volz, J.S. Garing, 1971: *Optical properties of the atmosphere.*, AFCRL-71-0279, Air Force Cambridge Research Lab, Hanscom AFB, MA.
- Mekler Yu., H. Quenzel, G. Ohring, and I. Marcus, 1977: Relative atmospheric aerosol content from ERTS observations, *J. Geoph. Res.*, **82**, 967-972.
- Neckel, H. and D. Labs, 1984: The solar radiation between 3300 and 12500 Å, *Solar Phys.*, **90**, 205-258.
- Nilsson, B., 1979: Meteorological influence on aerosol extinction in the 0.2 - 40 µm wavelength range, *Appl. Opt.*, **18**, 3457-3473.
- Patterson, E.M. and G.W. Grams, 1984: Determination of aerosol absorption and scattering in the free troposphere, *IRS '84: Current Problems in Atmospheric Radiation, Proceedings of the International Radiation Symposium*, Perugia, Italy, 21-28 Aug. 1984, Deepak, Hampton, VA.
- Peterson, J. T., E. C. Flowers, G. J. Berri, C. L. Reynolds, J. H. Rudisil, 1981: Atmospheric turbidity over central North Carolina, *J. Appl. Meteor.*, **20**, 229-241.
- Reagan, J.A., D.M. Byrne, M.D. King, J.D. Spinhirne, and B.M. Herman, 1980: Determination of the complex refractive index of atmospheric particulates from bistatic-monostatic lidar and solar radiometer measurements., *J. Geophys. Res.*, **85**, 1591-1599.

Sellers, P.J., F.G. Hall, G. Asrar, D.E. Strebel, and R.E. Murphy, 1988: The First ISLSCP Field Experiment (FIFE)., *Bull. Amer. Meteor. Soc.*, **69**, No. 1, 22-27.

Shettle, E.P. and R.W. Fenn, 1979: *Models for the aerosols of the lower atmosphere and the effects of humidity variations on their optical properties.*, AFGL-TR-79-0214, Air Force Geophysics Lab, Hanscom AFB, MA.

Spinhirne, J.D., J.A. Reagan, and B.M. Herman, 1980; Vertical distribution of aerosol extinction cross section and inference of aerosol imaginary index in the troposphere by lidar technique, *J. Appl. Meteor.*, **19**, 426-438.

Takayama, Y., and T. Takashima, 1986: Aerosol optical thickness of yellow sand over the yellow sea derived from NOAA satellite data, *Atmos. Environ.*, **20**, 631-638.

Waggoner, A.P., R.E. Weiss, N.C. Ahlquist, D.S. Covert, S. Will, and R.C. Charlson, 1981: Optical characteristics of aerosols., *Atmos. Environ.*, **15**, No. 11, 1891-1909.

9.0 FORTRAN Listing

The FORTRAN code for the atmospheric correction algorithm is given in the pages which follow. The line numbers are listed to the right of each line.

```

C THIS SOFTWARE WAS DEVELOPED BY                                FIF00010
C      SHANA MATTOO,ARC AND GSFC                                FIF00020
C      C109D,BLD22,TEL# 286-2120                                FIF00030
C *****                                                        FIF00040
C * THIS MAIN PROGRAM IS BASED ON THE ATMOSPHERIC CORRECTION OF UPWARD* FIF00050
C * RADIANCE MEASURED FROM AIRCRAFT OR SATELLITE.IT DERIVES DOWNWARD * FIF00060
C * IRRADIANCE, UPWARD RADIANCE, AND REFLECTANCE ALL FOR THE GROUND * FIF00070
C * LEVEL.THIS PROGRAM ALSO HAS A OPTION TO COMPUTE THE UPWARD * FIF00080
C * RADIANCE IF THE SURFACE REFLECTANCE IS PROVIDED. * FIF00090
C *****                                                        FIF00100
C SUBROUTINES USED:                                            FIF00110
C 1. READIN                                                    FIF00120
C 2. FINDW                                                    FIF00130
C 3. INTSFX                                                    FIF00140
C 4. INTHGH                                                    FIF00150
C 5. INTERP                                                    FIF00160
C 6. INTEXP                                                    FIF00170
C 7. SYSTEM SUBROUTINE IMSL(ZXGSN) (LOOK IN SUBROUTINE INTEXP) FIF00180
C (BE SURE TO LINKTO PROPER SYSTEMS LIBRARY CONTAING IMSL) FIF00190
C                                                                FIF00200
C                                                                FIF00210
C      REAL * 4 MWAV,MTAU,MINT,MTHET0,MTHET,MPHI,MHGHT,RHOS,MRHO,SBARN FIF00220
C      REAL *4 HGHT(3),THE(13),INT(9,4,13,19),WAV,OPTH(4),FDOWN(9,4) FIF00230
C      REAL *4 SBAR(4),PIT(13,4),THET0(9),NEW(30),YY(1),NEWN(30) FIF00240
C      REAL *4 SBARW(2,4),PITW(2,13,4,3),FDOWNW(2,9,4) FIF00250
C      REAL *4 INTW(2,9,4,3,13,19),INTWH(2,9,4,13,19),PITWH(2,13,4) FIF00260
C      REAL *4 NEWINT(4,13,19),NFDOWN(4),NEWNEW(4,13),FINT(4),FT(4) FIF00270
C      REAL *4 F,AIRR,ARAD,PHI(19) FIF00280
C      REAL *4 F0IRR(100),WAVE(100),R(365) FIF00290
C      REAL *4 LEAP(12)/30.,29.,31.,30.,31.,30.,31.,31.,30.,31.,30.,31./ FIF00300
C      REAL *4 NLEAP(12)/30.,28.,31.,30.,31.,30.,31.,31.,30.,31.,30.,31./ FIF00310
C      REAL *4 WAVEN(8)/.486,.587,.639,.663,.837,.845,1.663,2.189/ FIF00320
C      REAL *4 TAUGH(8)/.0070,.0320,.0247,.0174,.0021,.0152,.0077,.0091/ FIF00330
C      REAL *4 TAUGL(8)/.0130,.0142,.0208,.0218,.0628,.1156,.1380,.0930/ FIF00340
C      CHARACTER * 1 LINE(132) FIF00350
C      CHARACTER * 1 LINE2(80) FIF00360
C      CHARACTER * 1 LL(30) FIF00370
C      INTEGER ANGLE(19) FIF00380
C                                                                FIF00390
C      DEFINE PI FIF00400
C      PI=ARCOS(-1.00) FIF00410
C                                                                FIF00420
C ***** FIF00430
C * CALL SUBROUTINE READIN * FIF00440
C ***** FIF00450
C SUBROUTINE READIN READS THE INPUT DATA AND WRITES IT ON UNIT 6, TO FIF00460
C PERFORM A CHECK ON INPUT DATA. FIF00470
C                                                                FIF00480
C      CALL READIN FIF00490
C                                                                FIF00500
C      LINE2 READS THE TITLE FOR THE VALUES OF FOLLOWING INPUT QUANTITIES. FIF00510
C      READ THE IOPT, MOPT AND NOPT. IOPT IS OPTION FOR UNITS OF RADIANCE. FIF00520
C      IF OPTION IS 1, UNITS SHOULD BE IN REFLECTANCE UNITS;IF IOPT=2 FIF00530
C      THE UNITS OF REFLECTANCE SHOULD BE IN ABSOLUTE UNITS.IF MOPT IS 1 FIF00540
C      THE DAY, MONTH AND YEAR FOR WHICH DATA IS MEASURED SHOULD BE FIF00550
C      GIVEN; AND IF MOPT IS 2 THE DAY OF THE YEAR AND THE YEAR SHOULD BE FIF00560
C      GIVEN .NOPT IS OPTION FOR COMPUTING SURFACE REFLECTANCE OR RADIANCE. FIF00570
C      IF NOPT IS 1 SURFACE REFLECTANCE IS COMPUTED AND IF NOPT IS 2 RADIANCE FIF00580
C      IS COMPUTED. FIF00590
C                                                                FIF00600

```

READ (5,1003) LINE2	FIF00610
READ (5,9) IOPT,MOPT,NOPT	FIF00620
	FIF00630
C	FIF00640
C LINE2 READS THE TITLE FOR THE VALUES OF FOLLOWING INPUT QUANTITIES:	FIF00650
C INUM THE NUMBER OF DATA POINTS TO BE PROCESSED, MONTH,DAY, YEAR AND	FIF00660
C TIME ZONE FOR WHICH MEASURED DATA ARE PROVIDED.	FIF00670
C	FIF00680
READ (5,1003) LINE2	FIF00690
IF (MOPT .EQ.1) READ (5,10) INUM, IMONTH, IDAY, IYEAR, LL	FIF00700
IF (MOPT .EQ.2) READ (5,10) INUM, IDAY, IYEAR, LL	FIF00710
READ (5,1003) LINE2	FIF00720
C	FIF00730
C WRITE THE LABELS FOR THE OUTPUT.	FIF00740
C	FIF00750
WRITE (56,1108)	FIF00760
WRITE (56,1109)	FIF00770
IF (MOPT .EQ.1) WRITE (6,11) IMONTH, IDAY, IYEAR, LL	FIF00780
IF (MOPT .EQ.1) WRITE (56,11) IMONTH, IDAY, IYEAR, LL	FIF00790
IF (MOPT .EQ.2) WRITE (6,21) IDAY, IYEAR, LL	FIF00800
IF (MOPT .EQ.2) WRITE (56,21) IDAY, IYEAR, LL	FIF00810
WRITE (6,12)	FIF00820
WRITE (56,22)	FIF00830
C	FIF00840
CREAD LABS AND NECKEL DATA FOR SOLAR FLUX	FIF00850
C	FIF00860
DO 121 IJ = 1,4	FIF00870
121 READ (20,1003) LINE	FIF00880
IK=1	FIF00890
DO 122 IJ = 1,20	FIF00900
READ (20,23) WAVE (IK), F0IRR (IK), WAVE (IK+1), F0IRR (IK+1), WAVE (IK+2),	FIF00910
1 F0IRR (IK+2)	FIF00920
IK=IK+3	FIF00930
122 CONTINUE	FIF00940
IK=IK-1	FIF00950
C	FIF00960
C START OF LOOP FOR THE NUMBER OF THE DATA POINTS TO BE PROCESSED	FIF00970
C LFILE IS USED TO SET THE VALUE FOR THE FILE NUMBER NFILE TO READ	FIF00980
C THE LOOK-UP TABLE FOR CHOSEN WAVELENGTH.	FIF00990
C	FIF01000
LFILE=6	FIF01010
2000 DO 999 NUM=1, INUM	FIF01020
IF (NUM .GT.1) REWIND NFILE1	FIF01030
IF (NUM .GT.1) REWIND NFILE2	FIF01040
C *****	FIF01050
C * READ MEASURED PARAMETERS *	FIF01060
C *****	FIF01070
C TIME IN CDT (MTIME IN HOURS AND MINUTES), WAVELENGTH (MWAV IN	FIF01080
C MICROMETERS), OPTICAL THICKNESS (MTAU) FOR MWAV, SOLAR ZENITH ANGLE	FIF01090
C MTHET0 IN DEGREES), OBSERVATION SCAN ANGLE (MTHET IN DEGREES),	FIF01100
C OBSERVATION AZIMUTH ANGLE (MPHI IN DEGREES), OBSERVATION HEIGHT (MHGHT	FIF01110
C IN KILOMETERS), INTENSITY (MINT IN REFLECTANCE OR ABSOLUTE UNITS) IF	FIF01120
C NOPT IS 1; AND SURFACE REFLECTANCE (MRHO) IF NOPT IS 2.	FIF01130
C TAUGHW (ABSORPTION FOR CARBONDIOXIDE AND OZONE), TAUGLW (ABSORPTION	FIF01140
C FOR WATER) FOR MEASURED WAVELENGTH, HEIGHT FROM THE SURFACE ABOVE SEA-	FIF01150
C LEVEL (SHGHT IN KILOMETERS). (LOOK DOCUMENTATION PAGE 19)	FIF01160
C	FIF01170
IF (NOPT.EQ.1)	FIF01180
1 READ (5,13) MTIME, MWAV, MTAU, MTHET0, MTHET, MPHI, MHGHT, MINT, TAUGLW,	FIF01190
1 TAUGHW, SHGHT	FIF01200

IF (NOPT.EQ.2)	FIF01210
1 READ (5,13) MTIME, MWAV, MTAU, MTHET0, MTHET, MPHI, MHGHT, MRHO, TAUGLW,	FIF01220
1 TAUGHW, SHGHT	FIF01230
C	FIF01240
C IF TAUGLW (ABSORPTION FOR WATER) IS 0.0 THE DEFAULT VALUE IS COMPUTED	FIF01250
C BY INTERPOLATING LINEARLY FOR THE MEASURED WAVELENGTH MWAV. IF MWAV IS	FIF01260
C OUT OF RANGE NO EXTRAPOLATION IS ALLOWED, THE PROGRAM SENDS CONTROL TO	FIF01270
C PROCESS NEW DATA POINT.	FIF01280
C	FIF01290
IF (TAUGLW .GT. 0.0) THEN	FIF01300
GO TO 360	FIF01310
ELSE	FIF01320
CALL INTERP (1, 8, MWAV, WAVEN, TAUGL, YY, IJK, NUM, LOPT)	FIF01330
IF (LOPT .EQ. 0) THEN	FIF01340
WRITE (6, 24) MWAV, NUM	FIF01350
GO TO 999	FIF01360
ELSE	FIF01370
TAUGLW = YY (1)	FIF01380
ENDIF	FIF01390
ENDIF	FIF01400
C	FIF01410
C IF TAUGHW (ABSORPTION FOR GASES) IS 0.0 THE DEFAULT VALUE IS COMPUTED	FIF01420
C BY INTERPOLATING LINEARLY FOR THE MEASURED WAVELENGTH MWAV. IF MWAV IS	FIF01430
C OUT OF RANGE NO EXTRAPOLATION IS ALLOWED, THE PROGRAM SENDS CONTROL TO	FIF01440
C PROCESS NEW DATA POINT.	FIF01450
C	FIF01460
360 CONTINUE	FIF01470
IF (TAUGHW .GT. 0.0) THEN	FIF01480
GO TO 350	FIF01490
ELSE	FIF01500
CALL INTERP (1, 8, MWAV, WAVEN, TAUGH, YY, IJK, NUM, LOPT)	FIF01510
IF (LOPT .EQ. 0) THEN	FIF01520
WRITE (6, 25) MWAV, NUM	FIF01530
GO TO 999	FIF01540
ELSE	FIF01550
TAUGHW = YY (1)	FIF01560
ENDIF	FIF01570
ENDIF	FIF01580
350 CONTINUE	FIF01590
C	FIF01600
C*****	FIF01610
C* CALL TO SUBROUTINE FINDW	FIF01620
C*****	FIF01630
C SUBROUTINE FINDW PICKS TWO WAVELENGTHS WAV1 AND WAV2 BETWEEN WHICH	FIF01640
C MEASURED WAVELENGTH MWAV LIES AND SETS FILE NUMBERS NFILE1 AND NFILE2	FIF01650
C TO READ THE REQUIRED DATA SET FOR THE TWO WAVELENGTHS FROM LOOK-UP	FIF01660
C TABLE. THE MWAV SHOULD BE IN RANGE OF 0.486 - 2.189 UM, NO EXTRAPOLAT-	FIF01670
C ION IS ALLOWED.	FIF01680
C	FIF01690
CALL FINDW (MWAV, II, NUM, KOPT, IMM, WAV1, WAV2)	FIF01700
IF (KOPT.EQ.0) GO TO 999	FIF01710
NFILE1 = LFILE+II	FIF01720
NFILE2 = LFILE+IMM	FIF01730
C	FIF01740
C*****	FIF01750
C* CALL TO SUBROUTINE INTSFX	FIF01760
C*****	FIF01770
C SUBROUTINE INTSFX INTERPOLATES TO COMPUTE THE VALUES OF R FOR	FIF01780
C 365 DAYS. THESE VALUES WILL BE USED TO COMPUTE THE CORRECTED VALUES	FIF01790
C OF SOLAR FLUX FOR THE DAY MONTH AND YEAR FOR WHICH MEASURED DATA	FIF01800
C IS GIVEN. R IS SUN-EARTH DISTANCE .	FIF01810

C		FIF01820
	CALL INTSFX(R)	FIF01830
C		FIF01840
C	CHANGE MONTH AND DAY TO THE JULIAN DATE IF MOPT IS 1.	FIF01850
C		FIF01860
	IF (MOPT.EQ.2) THEN	FIF01870
	IQ=IDAY	FIF01880
	ELSE	FIF01890
	IS=IDAY+1	FIF01900
	IM=IMONTH-1	FIF01910
	IQ=0	FIF01920
	DO 20 IJ=1, IM	FIF01930
	IF (MOD (IYEAR, 4) .EQ.0) THEN	FIF01940
	IQ=IQ+LEAP (IJ)	FIF01950
	ELSE	FIF01960
	IQ=IQ+NLEAP (IJ)	FIF01970
	ENDIF	FIF01980
20	CONTINUE	FIF01990
	IQ=IQ+IS	FIF02000
	ENDIF	FIF02010
C		FIF02020
C	COMPUTE SOLAR FLUX FOR THE MEASURED WAVELENGTH MWAV FROM LABS AND	FIF02030
C	NECKEL DATA BY INTERPOLATION	FIF02040
C		FIF02050
	IJK=0	FIF02060
	LNUM=0	FIF02070
	CALL INTERP (1, IK, MWAV, WAVE, F0IRR, YY, IJK, LNUM, LOPT)	FIF02080
		FIF02090
C		FIF02100
C	COMPUTE CORRECTED SOLAR FLUX FOR THE DAY OF YEAR FOR WHICH	FIF02110
C	MEASUREMENT ARE MADE. (SEE DOCUMENTATION EQ.6)	FIF02120
C		FIF02130
C	R(IQ)=1.	FIF02140
	FFLUX=YY(1) / (R(IQ) * R(IQ))	FIF02150
C		FIF02160
C		FIF02170
C	COMPUTE THE OBSERVATION ZENITH ANGLE FOR THE SCAN ANGLE OF	FIF02180
C	THE SATELLITE OR AIRCRAFT (SEE DOCUMENTATION EQ.9)	FIF02190
C	RAD=RADIUS OF EARTH	FIF02200
C		FIF02210
	DEGRAD=ARCOS (-1.) / 180.	FIF02220
	RADDEG=180. / ARCOS (-1.)	FIF02230
	RAD=6370.	FIF02240
	MTHET=ASIN ((1. + (MHGHT/RAD)) * (SIN (MTHET*DEGRAD))) * RADDEG	FIF02250
C		FIF02260
C	IF IOPT EQ 1 CONVERT MEASURED RADIANCE TO ABSOLUTE UNITS.	FIF02270
C	IF IOPT IS 2 CONVERT MEASURED RADIANCE FROM ABSOLUTE UNITS TO	FIF02280
C	REFLECTANCE UNITS.	FIF02290
C		FIF02300
	AMU0=COS (MTHET0*DEGRAD)	FIF02310
	IF (IOPT .EQ.1 .AND. NOPT.EQ.1) AMINT=(MINT*FFLUX*AMU0) / PI	FIF02320
	IF (IOPT .EQ.2 .AND. NOPT.EQ.1) AMINT=MINT	FIF02330
	IF (IOPT .EQ.2 .AND. NOPT.EQ.1) MINT=(MINT*PI) / (FFLUX*AMU0)	FIF02340

```

C ***** FIF02350
C * READ FROM LOOK-UP TABLE. * FIF02360
C ***** FIF02370
C ***** FIF02380
C * WAV=WAVELENGTHS(8) (.486, .587, .639, .663, .837, .845, 1.663, 2.189) * FIF02390
C * MICROMETERS. * FIF02400
C * LTHET0=NUMBER OF THETA0(SOLAR ZENITH ANGLE) * FIF02410
C * THET0=(10,20,30,40,50,60,66,72,78 DEGREES) * FIF02420
C * LTHE =NUMBER OF THE(OBSERVATION ZENITH ANGLE) * FIF02430
C * THE=(0,6,.....72 DEGREES EVERY 6 DEGREES) * FIF02440
C * LPHI =NUMBER OF PHI(OBSERVATION AZIMUTH ANGLE) * FIF02450
C * PHI=(0,5,10,20,30,40,60,80,90,100,110,120,130,140,150,160,170, * FIF02460
C * 175,180 DEGREES) * FIF02470
C * LTAU =NUMBER OF OPTH(OPTICAL THICKNESS) * FIF02480
C * OPTH=(0.0, .25, .50, 1.0) * FIF02490
C * LHGHT = NUMBER OF HGHT(OBSERVATION HEIGHTS) * FIF02500
C * HGHT=(80.0, 4.5, .45 KM) * FIF02510
C ***** FIF02520
C LTHET0=9 FIF02530
C LTHE=13 FIF02540
C LPHI=19 FIF02550
C LTAU=4 FIF02560
C LHGHT=3 FIF02570
C READ OBSERVATION ZENITH ANGLE(THE), AND OBSERVATION AZIMUTH ANGLE FIF02580
C FROM LOOK-UP TABLE.STORE INTEGER ARRAY ANGLE IN REAL ARRAY PHI . FIF02590
C FIF02600
C FIF02610
C READ(NFILE1,1000) (THE(I), I=1, LTHE) FIF02620
C READ(NFILE1,1001) (ANGLE(I), I=1, LPHI) FIF02630
C READ(NFILE2,1000) (THE(I), I=1, LTHE) FIF02640
C READ(NFILE2,1001) (ANGLE(I), I=1, LPHI) FIF02650
C DO 30 IPHI=1, LPHI FIF02660
C 30 PHI(IPHI)=ANGLE(IPHI) FIF02670
C FIF02680
C READ WAVELENGTH(WAV), OPTICAL THICKNESS(OPTH), SOLAR ZENITH ANGLE FIF02690
C (THET0), REFLECTANCE OF ATMOSPHERE(SBARW), FLUX INCIDENT ON FIF02700
C SURFACE(FDOWNW) FROM LOOK-UP TABLE. FIF02710
C FIF02720
C IF WAVELENGTH IS 1.663 OR 2.189, THE LOOK-UP TABLE IS AVAILABLE ONLY FIF02730
C FOR 2 OPTICAL THICKNESSES OF 0.0 AND .25. FIF02740
C FIF02750
C DO 9995 IWAV = 1,2 FIF02760
C IF(IWAV .EQ. 1) NFILE = NFILE1 FIF02770
C IF(IWAV .EQ. 2) NFILE = NFILE2 FIF02780
C IF(NFILE .GT. 12) LTAU=2 FIF02790
C DO 100 ITHET0=1, LTHET0 FIF02800
C DO 101 ITAU=1, LTAU FIF02810
C DO 102 IHGHT=1, LHGHT FIF02820
C READ(NFILE,1002) WAV, OPTH(ITAU), THET0(ITHET0), SBARW(IWAV, ITAU), FIF02830
C 1 FDOWNW(IWAV, ITHET0, ITAU) FIF02840
C READ(NFILE,1003) LINE FIF02850
C FIF02860
C READ ATMOSPHERIC RADIANCE (INTW) AS FUNCTION OF SOLAR ZENITH ANGLE, FIF02870
C OPTICAL THICKNESS, HEIGHT, OBSERVATION ZENITH ANGLE, AND OBSERVATION FIF02880
C AZIMUTH ANGLE FROM LOOK-UP TABLE. FIF02890
C FIF02900
C DO 103 ITHE=1, LTHE FIF02910
C READ(NFILE,1004) (INTW(IWAV, ITHET0, ITAU, IHGHT, ITHE, IPHI), IPHI=1, 10) FIF02920
C READ(NFILE,1004) (INTW(IWAV, ITHET0, ITAU, IHGHT, ITHE, IPHI), FIF02930
C 1 IPHI=11, 19) FIF02940
C 103 CONTINUE FIF02950

```

C		FIF02960
C	READ TRANSMISSION FROM SURFACE(PITW) AS FUNCTION OF OBSERVATION	FIF02970
C	ZENITH ANGLE, OPTICAL THICKNESS, AND HEIGHT.	FIF02980
C		FIF02990
	READ(NFILE,1005)(PITW(IWAV,ITHE,ITAU,IHGHT),ITHE=1,LTHE)	FIF03000
102	CONTINUE	FIF03010
101	CONTINUE	FIF03020
100	CONTINUE	FIF03030
9995	CONTINUE	FIF03040
C		FIF03050
C	*****	FIF03060
C	*CALL TO SUBROUTINE INTHGH	FIF03070
C	*****	FIF03080
C	SUBROUTINE INTHGH INTERPOLATES THE VALUES OF INTW, AND PITW FOR THE	FIF03090
C	MEASURED HEIGHT MHGHT(SEE DOCUMENTATION SECTION 3.6)	FIF03100
C		FIF03110
	CALL INTHGH(LTAU,LTHE,LPHI,LTHET0,INTW,MHGHT,PITW,INTWH,PITWH)	FIF03120
C		FIF03130
C	ADJUST LOOK-UP TABLE FOR FOR SURFACE LEVEL(SEE DOCUMENTATION EQ.	FIF03140
C	18, 19 AND 20)	FIF03150
C		FIF03160
	WAV1 = WAV1 * EXP((SHGHT-.4)/36.)	FIF03170
	WAV2 = WAV2 * EXP((SHGHT-.4)/36.)	FIF03180
C		FIF03190
C	INTERPOLATE INTWH,PITWH,SBARW,FDOWNW FOR THE MEASURED WAVELENGTH	FIF03200
C	MWAV.(SEE DOCUMENTATION 3.1, PAGE 12 - 15)	FIF03210
C		FIF03220
	ALPHA = (ALOG(MWAV) - ALOG(WAV2)) / (ALOG(WAV1) - ALOG(WAV2))	FIF03230
	DO 200 ITAU = 1,LTAU	FIF03240
	SBAR(ITAU) = EXP((ALPHA * ALOG(SBARW(1,ITAU))) +	FIF03250
1	((1.-ALPHA) * ALOG(SBARW(2,ITAU))))	FIF03260
	DO 201 ITHE = 1,LTHE	FIF03270
	PIT(ITHE,ITAU) = EXP((ALPHA * ALOG(PITWH(1,ITHE,ITAU))) +	FIF03280
1	((1.-ALPHA) * ALOG(PITWH(2,ITHE,ITAU))))	FIF03290
	DO 202 IPHI = 1,LPHI	FIF03300
	DO 203 ITHET0 = 1,LTHET0	FIF03310
	FDOWN(ITHET0,ITAU) = EXP((ALPHA * ALOG(FDOWNW(1,ITHET0,ITAU))) +	FIF03320
1	((1.-ALPHA) * ALOG(FDOWNW(2,ITHET0,ITAU))))	FIF03330
	INT(ITHET0,ITAU,ITHE,IPHI) =	FIF03340
	1 EXP((ALPHA * ALOG(INTWH(1,ITHET0,ITAU,ITHE,IPHI)))	FIF03350
	1 + ((1.-ALPHA) * ALOG(INTWH(2,ITHET0,ITAU,ITHE,IPHI))))	FIF03360
203	CONTINUE	FIF03370
202	CONTINUE	FIF03380
201	CONTINUE	FIF03390
200	CONTINUE	FIF03400
C		FIF03410
C	COMPUTE DELTAH AND DELTAL AS EXCESS OR DEFICIT IN UPPER (OZONE,CARBO	FIF03420
C	N-DIOXIDE) AND LOWER(WATER) ATMOSPHERE RESPECTIVELY.	FIF03430
C		FIF03440
	AVTAGH = EXP((ALPHA * ALOG(TAUGH(II))) +	FIF03450
1	((1.-ALPHA) * ALOG(TAUGH(IMM))))	FIF03460
	DELTAH = TAUGHW - AVTAGH	FIF03470
	AVTAGL = EXP((ALPHA * ALOG(TAUGL(II))) +	FIF03480
1	((1.-ALPHA) * ALOG(TAUGL(IMM))))	FIF03490
	DELTAL = TAUGLW - AVTAGL	FIF03500
C		FIF03510
C	COMPUTE FDOWN, SBAR, PIT AND INT AFTER ADJUSTING FOR THE EXCESS AND	FIF03520
C	DEFICIT OF GASEOUS ABSORPTION (SEE EQ. 17A, 17B, 17C, 17D)	FIF03530
C		FIF03540

```

DO 908 ITHET0=1,LTHET0
  AMUTH0 = COS(THET0(ITHET0) * DEGRAD)
  THDOWN=EXP(-DELTAH/AMUTH0)
  TLDOWN=EXP(-DELTAL/AMUTH0)
DO 908 ITAU=1,LTAU
908   FDOWN(ITHET0,ITAU)= FDOWN(ITHET0,ITAU)*THDOWN*TLDOWN
DO 909 ITAU=1,LTAU
909   SBAR(ITAU)= SBAR(ITAU)* EXP(-DELTAL * 2)
DO 910 ITAU=1,LTAU
DO 910 ITHE=1,LTHE
  AMUTH = COS(THET0(ITHE) * DEGRAD)
  THUP=EXP(-DELTAH/AMUTH)
  TLUP=EXP(-DELTAL/AMUTH)
910   PIT(ITHE,ITAU)=PIT(ITHE,ITAU)*THUP*TLUP
DO 912 ITAU=1,LTAU
DO 912 ITHET0=1,LTHET0
  AMUTH0 = COS(THET0(ITHET0) * DEGRAD)
DO 912 ITHE=1,LTHE
  AMUTH = COS(THET0(ITHE) * DEGRAD)
DO 912 IPHI=1,LPHI
912   INT(ITHET0,ITAU,ITHE,IPHI)=INT(ITHET0,ITAU,ITHE,IPHI)*
1   (EXP(-(DELTAL/2.)+DELTAH)*((1./AMUTH)+(1./AMUTH0)))

C *****
C * INTERPOLATION OF ATMOSPHERIC RADIANCE AND FLUX INCIDENT ON GROUND*
C * ON MEASURED SOLAR ZENITH ANGLE. *
C *****
C INT(THET0,OPHT,HGHT,THE,PHI) IS INTERPOLATED FOR
C MEASURED MTHET0 TO GET NEW VARIABLE NEWINT(TAU,THE,PHI).
C FDOWN (THET0,TAU) IS INTERPOLATED FOR MEASURED MTHET0 TO
C GET NEW VARIABLE NFDOWN(TAU).
C
701  CONTINUE
DO 240 I=1,30
  NEW(I)=0.0
240  NEWN(I)=0.0
DO 104 ITAU=1,LTAU
DO 105 ITHE=1,LTHE
DO 106 IPHI=1,LPHI
DO 107 ITHET0=1,LTHET0
  NEW(ITHET0)=INT(ITHET0,ITAU,ITHE,IPHI)
  NEWN(ITHET0)=FDOWN(ITHET0,ITAU)
107  CONTINUE
  IJK=1
C
C CALL SUBROUTINE INTERP TO INTERPOLATE INT.
C IF MTHET0 IS OUT OF RANGE OF VALUES OF THET0 SUBROUTINE INTERP
C RETURNS THE VALUE OF LOPT = 0 AND THE NEW DATA POINT WILL BE READ.
C
  CALL INTERP(1,LTHET0,MTHET0,THET0,NEW,YY,IJK,NUM,LOPT)
  IF(LOPT.EQ.0) GO TO 999
  NEWINT(ITAU,ITHE,IPHI)=YY(1)
  IJK=IJK+1
C
C CALL SUBROUTINE INTERP TO INTERPOLATE FDOWN.
C IF MTHET0 IS OUT OF RANGE OF VALUES OF THET0 SUBROUTINE INTERP
C RETURNS THE VALUE OF LOPT = 0 AND THE NEW DATA POINT WILL BE READ.
C

```

CALL INTERP(1,LTHET0,MTHET0,THET0,NEWN,YY,IJK,NUM,LOPT)	FIF04140
IF(LOPT.EQ.0) GO TO 999	FIF04150
NFDOWN(ITAU)=YY(1)	FIF04160
106 CONTINUE	FIF04170
105 CONTINUE	FIF04180
104 CONTINUE	FIF04190
C *****	FIF04200
C * INTERPOLATION OF THE ATMOSPHERIC RADIANCE ON MEASURED AZIMUTH *	FIF04210
C * ANGLE. *	FIF04220
C *****	FIF04230
C NEWINT(TAU,THETA,PHI) IS INTERPOLATED FOR MEASURED MPHI	FIF04240
C TO GET NEW VARIABLE NEWNEW(TAU,THETA).	FIF04250
C	FIF04260
DO 241 I=1,30	FIF04270
NEW(I)=0.0	FIF04280
241 NEWN(I)=0.0	FIF04290
DO 108 ITAU=1,LTAU	FIF04300
DO 109 ITHE=1,LTHE	FIF04310
DO 110 IPHI=1,LPHI	FIF04320
NEW(IPHI)=NEWINT(ITAU,ITHE,IPHI)	FIF04330
110 CONTINUE	FIF04340
IJK=3	FIF04350
C	FIF04360
C CALL SUBROUTINE INTERP TO INTERPOLATE ON PHI.	FIF04370
C IF MPHI IS OUT OF RANGE OF VALUES OF PHI SUBROUTINE INTERP	FIF04380
C RETURNS THE VALUE OF LOPT = 0 AND THE NEW DATA POINT WILL BE READ.	FIF04390
C	FIF04400
CALL INTERP(1,LPHI,MPHI,PHI,NEW,YY,IJK,NUM,LOPT)	FIF04410
IF(LOPT.EQ.0) GO TO 999	FIF04420
NEWNEW(ITAU,ITHE)=YY(1)	FIF04430
109 CONTINUE	FIF04440
108 CONTINUE	FIF04450
C *****	FIF04460
C* INTERPOLATION OF ATMOSPHERIC RADIANCE AND TRANSMISSION/PI FROM *	FIF04470
C* SURFACE ON MEASURED OBSERVATION ZENITH ANGLE. *	FIF04480
C *****	FIF04490
C NEWNEW(OPTH,THE) IS INTERPOLATED FOR MEASURED THETA(MTHET)	FIF04500
C TO GET NEW VARIABLE FINT(TAU). TRANSMISSION FACTOR PIT IS	FIF04510
C INTERPOLATED TO GET FT(TAU).	FIF04520
C	FIF04530
DO 242 I=1,30	FIF04540
NEW(I)=0.0	FIF04550
242 NEWN(I)=0.0	FIF04560
DO 111 ITAU=1,LTAU	FIF04570
DO 112 ITHE=1,LTHE	FIF04580
NEW(ITHE)=NEWNEW(ITAU,ITHE)	FIF04590
NEWN(ITHE)=PIT(ITHE,ITAU)	FIF04600
112 CONTINUE	FIF04610
IJK=4	FIF04620
C	FIF04630
C CALL SUBROUTINE INTERP TO INTERPOLATE RADIANCE ON MTHET.	FIF04640
C IF MTHET IS OUT OF RANGE OF VALUES OF THE SUBROUTINE INTERP	FIF04650
C RETURNS THE VALUE OF LOPT = 0 AND THE NEW DATA POINT WILL BE READ	FIF04660
C	FIF04670
CALL INTERP(1,LTHE,MTHET,THE,NEW,YY,IJK,NUM,LOPT)	FIF04680
IF(LOPT.EQ.0) GO TO 999	FIF04690
FINT(ITAU)=YY(1)	FIF04700
IJK=5	FIF04710
C	FIF04720

C CALL SUBROUTINE INTERP TO INTERPOLATE PIT ON MTHET.	FIF04730
C IF MTHET IS OUT OF RANGE OF VALUES OF THE SUBROUTINE INTERP	FIF04740
C RETURNS THE VALUE OF LOPT = 0 AND THE NEW DATA POINT WILL BE READ.	FIF04750
C	FIF04760
CALL INTERP (1, LTHE, MTHET, THE, NEWN, YY, IJK, NUM, LOPT)	FIF04770
IF (LOPT.EQ.0) GO TO 999	FIF04780
FT (ITAU) = YY (1)	FIF04790
111 CONTINUE	FIF04800
C*****	FIF04810
C*	FIF04820
C* INTERPOLATE RADIANCE (FINT), FLUXDOWN (NFDOWN), TRANSMISSION (FT) AND*	FIF04830
C* SBAR (SBAR) ON MEASURED OPTICAL THICKNESS (MTAU) .	FIF04840
C*	FIF04850
C*****	FIF04860
C CALL SUBROUTINE INTEXP WHICH PERFORMES EXPONANTIAL INTERPOLATION,	FIF04870
C IF VALUE OF IGNORE RETURNED FROM SUBROUTINE INTEXP IS 1 LINEAR INTER-	FIF04880
C POLATION IS PERFORMED USING SUBROUTINE INTERP.	FIF04890
C	FIF04900
CALL INTEXP (OPTH, FINT, MTAU, YY, LTAU, IGNORE)	FIF04910
C	FIF04920
C IF MTAU IS OUT OF RANGE OF VALUES OF OPTH SUBROUTINE INTERP	FIF04930
C RETURNS THE VALUE OF LOPT = 0 AND THE NEW DATA POINT WILL BE READ	FIF04940
C	FIF04950
IJK=6	FIF04960
IF (IGNORE .EQ.1) THEN	FIF04970
CALL INTERP (1, LTAU, MTAU, OPTH, FINT, YY, IJK, NUM, LOPT)	FIF04980
IF (LOPT.EQ.0) GO TO 999	FIF04990
ENDIF	FIF05000
FINTN=YY (1)	FIF05010
CALL INTEXP (OPTH, NFDOWN, MTAU, YY, LTAU, IGNORE)	FIF05020
IF (IGNORE .EQ.1) THEN	FIF05030
CALL INTERP (1, LTAU, MTAU, OPTH, NFDOWN, YY, IJK, NUM, LOPT)	FIF05040
IF (LOPT.EQ.0) GO TO 999	FIF05050
ENDIF	FIF05060
FDOWNN=YY (1)	FIF05070
CALL INTEXP (OPTH, FT, MTAU, YY, LTAU, IGNORE)	FIF05080
IF (IGNORE .EQ.1) THEN	FIF05090
CALL INTERP (1, LTAU, MTAU, OPTH, FT, YY, IJK, NUM, LOPT)	FIF05100
IF (LOPT.EQ.0) GO TO 999	FIF05110
ENDIF	FIF05120
FTN=YY (1)	FIF05130
CALL INTEXP (OPTH, SBAR, MTAU, YY, LTAU, IGNORE)	FIF05140
IF (IGNORE .EQ.1) THEN	FIF05150
CALL INTERP (1, LTAU, MTAU, OPTH, SBAR, YY, IJK, NUM, LOPT)	FIF05160
IF (LOPT.EQ.0) GO TO 999	FIF05170
ENDIF	FIF05180
SBARN=YY (1)	FIF05190
C*****	FIF05200
C* COMPUTE SURFACE REFLECTANCE RHO (SEE DOCUMENTATION EQ.2,3)	FIF05210
C*****	FIF05220
C COMPUTE F = (MINT-FINTN) / (FDOWNN*FTN)	FIF05230
C SURFACE REFLECTANCE RHO=F / (1+(F*SBARN (TAU)))	FIF05240
C IF NOPT IS 2 REFLECTANCE IS COMPUTED.	FIF05250
C	FIF05260
IF (NOPT.EQ.2) GO TO 56	FIF05270
F=(MINT-FINTN) / (FDOWNN* FTN)	FIF05280
RHOS=F / (1.+(F*SBARN))	FIF05290

```

C ***** FIF05300
C * COMPUTE IRRADIANCE IN WATTS/METER**2/UM, AND ABSOLUTE RADIANCE * FIF05310
C * IN WATTS/METER* *2/UM/SR. * FIF05320
C ***** FIF05330
C COMPUTE IRRADIANCE AIRR=(FDOWNN*FFLUX* MU0)/(1-SBARN.RHOS) FIF05340
C COMPUTE ABSOLUTE RADIANCE=(RHOS*FDOWN*FFLUX*AMU0)/(PI*(1-SBAR*RHOS)) FIF05350
C FIF05360
C      AIRR=(FDOWNN * FFLUX* AMU0)/(1.-SBARN*RHOS) FIF05370
C      ARAD=(RHOS*FDOWNN*FFLUX* AMU0)/(PI*(1.-SBARN*RHOS)) FIF05380
C ***** FIF05390
C *WRITE OUTPUT,ALL MEASURED PARAMETERS WHICH ENTER AS INPUT; AND * FIF05400
C *COMPUTED IRRADIANCE AIRR, ABSOLUTE RADIANCE ARAD,AND SURFACE * FIF05410
C *REFLECTANCE AT GROUND LEVEL. * FIF05420
C ***** FIF05430
C      WRITE(6,1006)MTIME,MWAV,MTAU,MTHET0,MTHET,MPHI,MHGHT,AMINT,MINT, FIF05440
C      1AIRR,ARAD,RHOS FIF05450
C      WRITE(56,1107)MTIME,MWAV,MTAU,MTHET0,MTHET,MPHI,MHGHT,AMINT, FIF05460
C      1MINT,FINTN,FDOWNN,FTN,SBARN FIF05470
C      GO TO 9987 FIF05480
C ***** FIF05490
C* NOPT IS 2 * FIF05500
C* COMPUTE REFLECTANCE MINT (SEE DOCUMENTATION(ABSTRACT)) * FIF05510
C ***** FIF05520
C COMPUTE MINT=FINTN+(FTN*FDOWNN*RHOS)/(1.-(SBARN*RHOS)) FIF05530
C FIF05540
C      56 CONTINUE FIF05550
C      RHOS=MRHO FIF05560
C      MINT=FINTN+(FTN*FDOWNN*RHOS)/ FIF05570
C      1((1.-(SBARN*RHOS))) FIF05580
C ***** FIF05590
C * COMPUTE IRRADIANCE IN WATTS/METER**2/UM, AND ABSOLUTE RADIANCE * FIF05600
C * IN WATTS/METER* *2/UM/SR. * FIF05610
C ***** FIF05620
C COMPUTE IRRADIANCE AIRR=(FDOWNN*FFLUX* MU0)/(1-SBARN.RHOS) FIF05630
C COMPUTE ABSOLUTE RADIANCE=(RHOS*FDOWN*FFLUX*AMU0)/(PI*(1-SBAR*RHOS)) FIF05640
C FIF05650
C      AIRR=(FDOWNN * FFLUX* AMU0)/(1.-SBARN*RHOS) FIF05660
C      ARAD=(RHOS*FDOWNN*FFLUX* AMU0)/(PI*(1.-SBARN*RHOS)) FIF05670
C ***** FIF05680
C *WRITE OUTPUT,ALL MEASURED PARAMETERS WHICH ENTER AS INPUT; AND * FIF05690
C *COMPUTED IRRADIANCE AIRR, ABSOLUTE RADIANCE ARAD,AND SURFACE * FIF05700
C *REFLECTANCE AT GROUND LEVEL. * FIF05710
C ***** FIF05720
C      IF(IOPT .EQ.1 .AND. NOPT.EQ.2 )AMINT=(MINT*FFLUX*AMU0)/PI FIF05730
C      IF(IOPT .EQ.2 .AND. NOPT.EQ.2) AMINT=MINT FIF05740
C      IF(IOPT .EQ.2 .AND. NOPT.EQ.2) MINT=(MINT*PI)/(FFLUX*AMU0) FIF05750
C      WRITE(6,1006)MTIME,MWAV,MTAU,MTHET0,MTHET,MPHI,MHGHT,AMINT,MINT, FIF05760
C      1AIRR,ARAD,RHOS FIF05770
C      WRITE(56,1107)MTIME,MWAV,MTAU,MTHET0,MTHET,MPHI,MHGHT,AMINT, FIF05780
C      1MINT,FINTN,FDOWNN,FTN,SBARN FIF05790
9987 CONTINUE FIF05800
999 CONTINUE FIF05810
      WRITE(6,1007) FIF05820
      STOP FIF05830
      9 FORMAT(3I5) FIF05840
      10 FORMAT(4I5,30A1) FIF05850
      11 FORMAT(/,' DATE ',I3,'/',I3,'/',I5,' TIME ZONE',30A1) FIF05860

```



```

12  FORMAT(25X,'|',27X,'FLIGHT LEVEL',28X,'|',13X,'GROUND LEVEL',/,25XFIF05870
1,'|',67X,'|',/,25X,'|',67X,'|',/, FIF05880
1' TIME',2X,'WAVELENGTH',2X,'OPTICAL',2X,'SOLAR',2X, FIF05890
1'OBSERVATION',2X,'OBSERVATION',2X,'OBSERVATION',12X,'RELATIVE',1X,FIF05900
1'|',2X,'DOWNWARD',5X,'UPWARD',/,18X,'THICKNESS',1X, FIF05910
1'ZENITH',3X,'ZENITH',7X,'AZIMUTH', FIF05920
1 6X,'HEIGHT',5X,'RADIANCE',2X,'RADIANCE',1X,'|',3X, FIF05930
1 'IRRADIANCE',3X,'RADIANCE',2X,'REFLECTANCE',/,25X,'|',3X,'ANGLE',FIF05940
14X,'ANGLE',8X,'ANGLE',23X,'RADIANCE*PI/F0/U0',10X,'W/M**2/UM/SR' FIF05950
1,/,6X,'MICROMETERS',8X,'|',3X,'DEG',6X,'DEG',10X,'DEG',11X,'KM', FIF05960
14X,'W/M**2/UM/SR',10X,'|',5X,'W/M**2/UM',/,25X,'|',67X,'|',/25X, FIF05970
1'|',67X,'|') FIF05980
13  FORMAT(I5,1X,F6.3,F6.3,4F7.2,F10.5,3F8.4) FIF05990
21  FORMAT(/,' JULIAN DATE ',I3, '/',I5,' TIME ZONE', 30A1) FIF06000
22  FORMAT(' TIME',2X,'WAVELENGTH',2X,'OPTICAL',2X,'SOLAR',2X, FIF06010
1'OBSERVATION',2X,'OBSERVATION',2X,'OBSERVATION',12X,'RELATIVE',5X,FIF06020
1'LSUB0 ',2X,'FSUBD ',/,18X,'THICKNESS',1X, FIF06030
1'ZENITH',3X,'ZENITH',7X,'AZIMUTH', FIF06040
1 6X,'HEIGHT',5X,'RADIANCE',2X,'RADIANCE',2X, FIF06050
1 'SUPERPRIME',1X,'SUPERPRIME',2X,'T ',2X,'S',/,29X,'ANGLE', FIF06060
14X,'ANGLE',8X,'ANGLE',28X,'RADIANCE*PI/F0/U0',/, FIF06070
16X,'MICROMETERS',13X,'DEG',6X,'DEG',10X,'DEG',11X,'KM',2X, FIF06080
1 'W/M* *2/UM/SR') FIF06090
23  FORMAT(3(8X,F6.4,F11.4,2X)) FIF06100
24  FORMAT(' MEASURED WAVELENGTH(MWAV) ',F6.3,' IS OUT OF RANGE.THE FIF06110
1DATA POINT #',I4,' IS NOT PROCESSED. RANGE IS 0.486-2.189') FIF06120
25  FORMAT(' MEASURED WAVELENGTH(MWAV) ',F6.3,' IS OUT OF RANGE.THE FIF06130
1DATA POINT #',I4,' IS NOT PROCESSED. RANGE IS 0.486-2.189') FIF06140
1000 FORMAT(6X,13F6.0) FIF06150
1001 FORMAT(4X,19I6) FIF06160
1002 FORMAT(11X,F7.3,19X,F5.2,22X,F5.0,/,5X,F7.4,11X,F6.4) FIF06170
1003 FORMAT(132A1) FIF06180
1004 FORMAT(10E12.4) FIF06190
1005 FORMAT(3X,13F6.5) FIF06200
1006 FORMAT(I5,F9.3,5X,F5.2,1X,'|',2X,F5.2,3X,F6.2,7X,F6.2,7X, FIF06210
1 F7.2,3X,F8.2,4X,F8.4,1X,'|',3X,F8.0,3X,F7.1,5X,F7.3) FIF06220
1007 FORMAT(25X,'|',67X,'|',/25X,'|',67X,'|') FIF06230
1008 FORMAT(2F6.3) FIF06240
1107 FORMAT(I5,F9.3,5X,F5.2,6X,F5.2,3X,F6.2,7X,F6.2,7X, FIF06250
1 F6.2,3X,F8.4,6X,F6.4,4X,F6.4,3X,F6.4,3X,F6.4,3X,F6.4,3X,F6.4) FIF06260
1108 FORMAT(45X,'INTERPOLATED RADIATION PARAMETERS') FIF06270
1109 FORMAT(43X,'-----') FIF06280
END FIF06290

```

```

C ***** FIF06300
C * SUBROUTINE READIN * FIF06310
C ***** FIF06320
C THIS SUBROUTINE READS THE DATA FROM UNIT NUMBER 5 TO WRITE ON UNIT FIF06330
C NUMBER 6. FIF06340
C FIF06350
C SUBROUTINE READIN FIF06360
  CHARACTER * 1 LINE(132) FIF06370
  WRITE(6,200) FIF06380
  DO 10 I=1,3 FIF06390
  READ(5,100)LINE FIF06400
  WRITE(6,100)LINE FIF06410
10 CONTINUE FIF06420
  READ(5,101) INUM, (LINE(I), I=6,132) FIF06430
  WRITE(6,101) INUM, (LINE(I), I=6,132) FIF06440
  READ(5,100)LINE FIF06450
  WRITE(6,100)LINE FIF06460
  DO 20 I=1, INUM FIF06470
  READ(5,100)LINE FIF06480
  WRITE(6,100)LINE FIF06490
20 CONTINUE FIF06500
  WRITE(6,201) FIF06510
  REWIND 5 FIF06520
100 FORMAT(132A1) FIF06530
101 FORMAT(I5,127A1) FIF06540
200 FORMAT(/,1X,'START OF INPUT DATA AS READ FROM UNIT NUMBER 5',/) FIF06550
201 FORMAT(/,1X,'END OF INPUT DATA SET AS READ FROM UNIT NUMBER 5',/) FIF06560
  RETURN FIF06570
  END FIF06580
C ***** FIF06590
C * SUBROUTINE FINDW * FIF06600
C ***** FIF06610
C SUBROUTINE FINDW(MWAV,II,INUM,KOPT,IMM,W1,W2) FIF06620
  REAL* 4 MWAV,WAV(8)/.486,.587,.639,.663,.837,.845,1.663,2.189/ FIF06630
C THIS SUBROUTINE PICKS TWO WAVELENGTHS W1 AND W2 BETWEEN WHICH FIF06640
C MEASURED WAVELENGTH MWAV LIES. THE SUBROUTINE PRINTS A ERROR MESSAGE FIF06650
C IF THE MWAV DOES NOT FALL IN THE RANGE OF .486 - 2.189 UM.THE FIF06660
C CONTROL IS RETURNED TO MAIN PROGRAM WITH VALUE OF LOPT. FIF06670
C FIF06680
C FIF06690
  IK = 7 FIF06700
  DO 10 IJ=1,IK FIF06710
  IF(MWAV.LT.WAV(1) .OR. MWAV .GT. WAV(IK+1)) GO TO 20 FIF06720
  IF(MWAV.GE.WAV(IJ) .AND. MWAV .LE. WAV(IJ+1)) GO TO 30 FIF06730
10 CONTINUE FIF06740
  GO TO 20 FIF06750
30 II=IJ FIF06760
  IMM = IJ+1 FIF06770
  W1 = WAV(IJ) FIF06780
  W2 = WAV(IJ+1) FIF06790
  KOPT=1 FIF06800
  RETURN FIF06810
20 WRITE(6,2)MWAV, INUM FIF06820
  KOPT=0 FIF06830
  2 FORMAT(' MEASURED WAVELENGTH(MWAV) ',F6.3,' IS OUT OF RANGE.THE FIF06840
  1DATA POINT #',I4,' IS NOT PROCESSED. ACTUAL RANGE .486-2.189 UM') FIF06850
  RETURN FIF06860
  END

```

```

C ***** FIF06870
C * SUBROUTINE INTSFX * FIF06880
C ***** FIF06890
      SUBROUTINE INTSFX(RR) FIF06900
C FIF06910
C THIS SUBROUTINE INTERPOLATES VALUES OF RR FOR 365 DAYS OF YEAR. FIF06920
C RR IS SUN EARTH DISTANCE. FIF06930
C FIF06940
      REAL * 4 RR(365),DAY(365) FIF06950
      REAL * 4 AMON(25)/1.,15.,32.,46.,60.,74.,91.,106., FIF06960
      1121.,135.,152.,166.,182.,196.,213.,227., FIF06970
      1 224.,258.,274.,288.,305.,319.,325.,349.,365./ FIF06980
      REAL * 4 R(25)/.9832,.9836,.9853,.9878, FIF06990
      1.9909,.9945,.9993,1.0033,1.0076, FIF07000
      1 1.0109,1.0140,1.0158,1.0167,1.0165,1.0149,1.0128,1.0092,1.0057, FIF07010
      1 1.0011,.9972,.9925,.9892,.9860,.9843,.9843/ FIF07020
      DO 100 I=1,365 FIF07030
      DAY(I)=I FIF07040
100 CONTINUE FIF07050
      IJK=0 FIF07060
      NUM=0 FIF07070
      CALL INTERP(365,25,DAY,AMON,R,RR,IJK,NUM,LOPT) FIF07080
      RETURN FIF07090
      END FIF07100
C ***** FIF07110
C * SUBROUTINE INTHGH * FIF07120
C ***** FIF07130
      SUBROUTINE INTHGH(LTAU,LTHE,LPHI,LTHETO,INTW,MHGHT,PITW,INTWH, FIF07140
      1 PITWH) FIF07150
C FIF07160
C THIS SUBROUTINE INTERPOLATES THE VALUES OF INTW AND PITW FOR THE FIF07170
C MEASURED HEIGHT MHGHT FIF07180
C FIF07190
      REAL * 4 INTW(2,9,4,3,13,19),INTWH(2,9,4,13,19),PITW(2,13,4,3), FIF07200
      1 PITWH(2,13,4),HGHT(3)/80.,4.5,.45/,MHGHT FIF07210
      REAL * 4 INTWH1(2,9,4,13,19),PITWH1(2,13,4) FIF07220
      REAL * 4 INTWH2(2,9,4,13,19),PITWH2(2,13,4) FIF07230
C FIF07240
C INTERPOLATES IF MEASURED HEIGHT IS LESS THAN OR EQUAL TO .45KM FIF07250
C (SEE DOCUMENTATION EQU. 21A, 21B) FIF07260
C FIF07270
      IF (MHGHT.LE.HGHT(3)) THEN FIF07280
      DO 100 IWAV = 1,2 FIF07290
      DO 101 ITAU = 1,LTAU FIF07300
      DO 102 ITHE = 1,LTHE FIF07310
      PITWH(IWAV,ITHE,ITAU) = ((PITW(IWAV,ITHE,ITAU,3) * MHGHT) + FIF07320
      1 (HGHT(3)-MHGHT))/HGHT(3) FIF07330
      DO 103 IPHI = 1,LPHI FIF07340
      DO 104 ITHETO = 1,LTHETO FIF07350
      INTWH(IWAV,ITHETO,ITAU,ITHE,IPHI) = FIF07360
      1 (INTW(IWAV,ITHETO,ITAU,3,ITHE,IPHI) * MHGHT) / HGHT(3) FIF07370
      IF (INTWH(IWAV,ITHETO,ITAU,ITHE,IPHI) .LE. 0.0) FIF07380
      1 INTWH(IWAV,ITHETO,ITAU,ITHE,IPHI)=1.E-6 FIF07390
104 CONTINUE FIF07400
103 CONTINUE FIF07410
102 CONTINUE FIF07420
101 CONTINUE FIF07430
100 CONTINUE FIF07440
C FIF07450

```

C INTERPOLATES IF MEASURED HEIGHT LIES BETWEEN .45 AND 4.5 KM	FIF07460
C (SEE DOCUMENTATION 3.6)	FIF07470
C	FIF07480
ELSE	FIF07490
IF(MHGHT .GT. HGHT(3) .AND. MHGHT .LT. HGHT(2)) THEN	FIF07500
C	FIF07510
C EXTRAPOLATES FOR THE HEIGHT LE. TO .45 KM.	FIF07520
C	FIF07530
DO 200 IWAV = 1,2	FIF07540
DO 201 ITAU = 1,LTAU	FIF07550
DO 202 ITHE = 1,LTHE	FIF07560
PITWH1(IWAV,ITHE,ITAU) = ((PITW(IWAV,ITHE,ITAU,3) * MHGHT) +	FIF07570
1 (HGHT(3)-MHGHT))/HGHT(3)	FIF07580
DO 203 IPHI = 1,LPHI	FIF07590
DO 204 ITHET0 = 1,LTHET0	FIF07600
INTWH1(IWAV,ITHET0,ITAU,ITHE,IPHI) =	FIF07610
1 (INTW(IWAV,ITHET0,ITAU,3,ITHE,IPHI) * MHGHT) / HGHT(3)	FIF07620
IF (INTWH1(IWAV,ITHET0,ITAU,ITHE,IPHI) .LE. 0.0)	FIF07630
1 INTWH1(IWAV,ITHET0,ITAU,ITHE,IPHI)=1.E-6	FIF07640
204 CONTINUE	FIF07650
203 CONTINUE	FIF07660
202 CONTINUE	FIF07670
201 CONTINUE	FIF07680
200 CONTINUE	FIF07690
C	FIF07700
C EXTRAPOLATES BETWEEN THE HEIGHTS 4.5 KM AND 80.0 KM.	FIF07710
C	FIF07720
Z = (1. - (EXP(-MHGHT/9.)))	FIF07730
Z1= (1. - (EXP(-HGHT(2)/9.)))	FIF07740
Z2= (1. - (EXP(-HGHT(1)/9.)))	FIF07750
DO 300 IWAV = 1,2	FIF07760
DO 301 ITAU = 1,LTAU	FIF07770
DO 302 ITHE = 1,LTHE	FIF07780
PITWH2(IWAV,ITHE,ITAU) =	FIF07790
1PITW(IWAV,ITHE,ITAU,2) +	FIF07800
1 (((PITW(IWAV,ITHE,ITAU,1) -	FIF07810
1 PITW(IWAV,ITHE,ITAU,2)) / (Z2 - Z1)) * (Z - Z1))	FIF07820
DO 303 IPHI = 1,LPHI	FIF07830
DO 304 ITHET0 = 1,LTHET0	FIF07840
INTWH2(IWAV,ITHET0,ITAU,ITHE,IPHI) =	FIF07850
1 INTW(IWAV,ITHET0,ITAU,2,ITHE,IPHI) +	FIF07860
1 (((INTW(IWAV,ITHET0,ITAU,1,ITHE,IPHI) -	FIF07870
1 INTW(IWAV,ITHET0,ITAU,2,ITHE,IPHI)) / (Z2 - Z1)) * (Z - Z1))	FIF07880
304 CONTINUE	FIF07890
303 CONTINUE	FIF07900
302 CONTINUE	FIF07910
301 CONTINUE	FIF07920
300 CONTINUE	FIF07930
C	FIF07940
C CHOSSES THE VALUES THAT SHOW NOMINAL ATMOSPHERIC EFFECT. LOWER VALUES	FIF07950
C OF INTENSITY AND HIGHER VALUES OF PIT ARE PICKED.	FIF07960
C	FIF07970

DO 400 IWAV = 1,2	FIF07980
DO 401 ITAU = 1,LTAU	FIF07990
DO 402 ITHE = 1,LTHE	FIF08000
IF (PITWH1(IWAV,ITHE,ITAU) .LE. PITWH2(IWAV,ITHE,ITAU))GO TO 405	FIF08010
PITWH(IWAV,ITHE,ITAU) = PITWH1(IWAV,ITHE,ITAU)	FIF08020
DO 403 IPHI = 1,LPHI	FIF08030
DO 404 ITHETO = 1,LTHETO	FIF08040
INTWH(IWAV,ITHETO,ITAU,ITHE,IPHI) =	FIF08050
1INTWH1(IWAV,ITHETO,ITAU,ITHE,IPHI)	FIF08060
404 CONTINUE	FIF08070
403 CONTINUE	FIF08080
GO TO 402	FIF08090
405 CONTINUE	FIF08100
PITWH(IWAV,ITHE,ITAU) = PITWH2(IWAV,ITHE,ITAU)	FIF08110
DO 407 IPHI = 1,LPHI	FIF08120
DO 406 ITHETO = 1,LTHETO	FIF08130
INTWH(IWAV,ITHETO,ITAU,ITHE,IPHI) =	FIF08140
1INTWH2(IWAV,ITHETO,ITAU,ITHE,IPHI)	FIF08150
406 CONTINUE	FIF08160
407 CONTINUE	FIF08170
402 CONTINUE	FIF08180
401 CONTINUE	FIF08190
400 CONTINUE	FIF08200
C	FIF08210
C INTERPOLATE FOR THE HEIGHT BETWEEN 4.5 KM. AND 80.0 KM.	FIF08220
C	FIF08230
ELSE	FIF08240
IF(MHGHT .GE. HGHT(2)) THEN	FIF08250
Z = (1. - (EXP(-MHGHT/9.)))	FIF08260
Z1= (1. - (EXP(-HGHT(2)/9.)))	FIF08270
Z2= (1. - (EXP(-HGHT(1)/9.)))	FIF08280
C WRITE(6,10001)Z,Z1,Z2	FIF08290
DO 600 IWAV = 1,2	FIF08300
DO 601 ITAU = 1,LTAU	FIF08310
DO 602 ITHE = 1,LTHE	FIF08320
PITWH(IWAV,ITHE,ITAU) =	FIF08330
1PITW(IWAV,ITHE,ITAU,2) +	FIF08340
1 ((PITW(IWAV,ITHE,ITAU,1) -	FIF08350
1 PITW(IWAV,ITHE,ITAU,2)) / (Z2 - Z1)) * (Z -Z1))	FIF08360
DO 603 IPHI = 1,LPHI	FIF08370
DO 604 ITHETO = 1,LTHETO	FIF08380
INTWH(IWAV,ITHETO,ITAU,ITHE,IPHI) =	FIF08390
1 INTW(IWAV,ITHETO,ITAU,2,ITHE,IPHI) +	FIF08400
1 (((INTW(IWAV,ITHETO,ITAU,1,ITHE,IPHI) -	FIF08410
1 INTW(IWAV,ITHETO,ITAU,2,ITHE,IPHI)) / (Z2 - Z1)) * (Z -Z1))	FIF08420
604 CONTINUE	FIF08430
603 CONTINUE	FIF08440
602 CONTINUE	FIF08450
601 CONTINUE	FIF08460
600 CONTINUE	FIF08470
ELSE	FIF08480
ENDIF	FIF08490
ENDIF	FIF08500
ENDIF	FIF08510
RETURN	FIF08520
END	FIF08530

```

C ***** FIF08540
C * SUBROUTINE INTERP * FIF08550
C ***** FIF08560
C SUBROUTINE INTERP (I,M,X1,X,Y,Y1,IJK,INUM,LOPT) FIF08570
C FIF08580
C THIS SUBROUTINE IS A GENERAL PURPOSE ROUTINE AND INTERPOLATES FIF08590
C LINEARLY.VALUE OF Y1 IS INTERPOLATED FOR X1.NO EXTRAPOLATION IS FIF08600
C ALLOWED. FIF08610
C REAL*4 X1(I),X(M),Y(M),Y1(I) FIF08620
C DO 290 LK = 1,I FIF08630
C XBAR=X1(LK) FIF08640
C LL=M-1 FIF08650
C DO 230 IL=1,LL FIF08660
C IF(XBAR .LT.X(1))GO TO 300 FIF08670
C IF(XBAR .GT.X(LL+1)) GO TO 300 FIF08680
C IF(XBAR .GE.X(IL) .AND.XBAR.LE. X(IL+1)) GO TO 250 FIF08690
C GO TO 230 FIF08700
250 PPHI=X(IL) FIF08710
C SPHI=X(IL+1) FIF08720
C PINTEN=Y(IL) FIF08730
C SINTEN=Y(IL+1) FIF08740
30 Y1(LK)=PINTEN+((SINTEN-PINTEN)*((XBAR-PPHI)/(SPHI-PPHI))) FIF08750
C GO TO 290 FIF08760
230 CONTINUE FIF08770
290 CONTINUE FIF08780
C LOPT=1 FIF08790
C RETURN FIF08800
C THE PROGRAM DOES NOT ALLOW ANY EXTRAPOLATION .IT WILL PRINT AN ERROR FIF08810
C MESSAGE .IJK IDENTIFIES THE ARRAY BEING SENT FOR INTERPOLATION. FIF08820
300 LOPT=0 FIF08830
C IF(IJK .EQ.1) WRITE(6,1)XBAR,INUM FIF08840
C IF(IJK .EQ.2) WRITE(6,1)XBAR,INUM FIF08850
C IF(IJK .EQ.3) WRITE(6,2)XBAR,INUM FIF08860
C IF(IJK .EQ.4) WRITE(6,3)XBAR,INUM FIF08870
C IF(IJK .EQ.5) WRITE(6,3)XBAR,INUM FIF08880
C IF(IJK .EQ.6) WRITE(6,4)XBAR,INUM FIF08890
1 FORMAT(1X,' MEASURED SOLAR ZENITH ANGLE(MTHET0)',F5.1,' IS OUT OFFIF08900
1 RANGE.ACTUAL RANGE 10 -78 DEGREES. THE DATA POINT #',I4,' IS NOT FIF08910
1 PROCESSED.') FIF08920
2 FORMAT(1X,' MEASURED OBSERVATION AZIMUTH ANGLE(MPHI)',F6.1,' IS OUFIF08930
1T OF RANGE.ACTUAL RANGE 0 -180 DEGREES.THE DATA POINT #',I4,' IS NFIF08940
1OT PROCESSED.') FIF08950
3 FORMAT(1X,' MEASURED OBSERVATION ZENITH ANGLE(MTHETA)',F5.1,' IS OFIF08960
1UT OF RANGE.ACTUAL RANGE 0 -72 DEGREES.THE DATA POINT #',I4,' IS NFIF08970
1OT PROCESSED.') FIF08980
4 FORMAT(1X,' MEASURED OPTICAL THICKNESS(MTAU) ',F5.3,' IS OUT OF RFIF08990
1ANGE . ACTUAL RANGE 0.0-1.0 . THE DATA POINT #',I4,' IS NOT PROCESFIF09000
1SED.') FIF09010
C RETURN FIF09020
C END FIF09030
C SUBROUTINE INTEXP (X,Y,MTAU,YY,LTAU,IGNORE) FIF09040
C FIF09050
C THIS SUBROUTINE IS A GENERAL PURPOSE ROUTINE AND INTERPOLATES FIF09060
C EXPONANTIALY.IGNORE SENDS VALUE OF 0 IF SUBROUTINE INTEXP IS FIF09070
C USED AND 1 IF IT FINDS THE FUNCTION TO BE LINEAR. FIF09080
C FIF09090
C REAL * 4 X(LTAU),Y(LTAU),MTAU,YY(1),TOL,C FIF09100
C COMMON/FF/XS(3),YS(3) FIF09110
C EXTERNAL FMIN FIF09120
C FIF09130

```

```

C VALUE OF IGNORE IS SET TO 0 AND IF MEASURED OPTICAL THICKNESS IS LESS FIF09140
C THEN OR EQUAL TO 0.25 THEN THE FUNCTIONS OF OPTICAL THICKNESSES OF FIF09150
C 0.0 ,0.25, 0.50 ARE USED. FIF09160
C FIF09170
      IGNORE=0 FIF09180
      IF (MTAU.LE. 0.25) THEN FIF09190
      MM=1 FIF09200
      MN=3 FIF09210
C FIF09220
C IF MEASURED OPTICAL THICKNESS IS GREATER THAN 0.25 THEN FUNCTIONS FIF09230
C OF OPTICAL THICKNESSES OF 0.25, 0.50 AND 1.00 ARE USED. FIF09240
C FIF09250
      ELSE FIF09260
      MM=2 FIF09270
      MN=4 FIF09280
      ENDIF FIF09290
      IS=0 FIF09300
      DO 10 IJ = MM,MN FIF09310
      IS=IS+1 FIF09320
      XS(IS)=X(IJ) FIF09330
      YS(IS)=Y(IJ) FIF09340
10 CONTINUE FIF09350
C FIF09360
C SYSTEMS SUBROUTINE IMSL (ZXGSN) IS CALLED TO GET THE MINIMAL OF FIF09370
C FUNCTION FMIN. FIF09380
C FIF09390
C A IS LOWER END-POINT OF THE INTERVAL IN WHICH MINIMUM OF FMIN IS TO BE FIF09400
C LOCATED. FIF09410
C B IS THE UPPER END-POINT OF THE INTERVAL. FIF09420
C TOL IS LENGTH OF THE FINAL SUBINTERVAL CONTAINING THE MINIMUM. FIF09430
C C IS OUTPUT , THE APPROXIMATE MINIMUM OF THE FUNCTION FMIN ON THE FIF09440
C ORIGINAL INTERVAL(A,B) FIF09450
C IER RETURNS THE VALUE OF 0 IF NO ERROR IS FOUND . FIF09460
C FIF09470
      A = 0.01 FIF09480
      AA = 0.01 FIF09490
      B = 10 FIF09500
      TOL=1.E-4 FIF09510
      CALL ZXGSN(FMIN,A,B,TOL,C,IER) FIF09520
C FIF09530
C THE IF STATEMENT BELOW DECIDES IF THE FUNCTION IS LINEAR OR NOT. FIF09540
C IF THE FUNCTION IS LINEAR THE VALUE OF IGNORE IS SET TO 1 AND FIF09550
C CONTROL IS SEND BACK TO MAIN PROGRAM. FIF09560
C FIF09570
      IF ((C-AA) .LT. .001) THEN FIF09580
      IGNORE=1 FIF09590
      RETURN FIF09600
      ELSE FIF09610
C FIF09620
C IF FUNCTION IS NOT LINEAR ,EXPONANTIAL INTERPOLATION IS USED, AND INTE FIF09630
C INTERPOLATED VALUE FOR MTAU IS YY(1) IS COMPUTED FOR THE FUNCTION. FIF09640
C FIF09650
      BB=(YS(1)-YS(2))/((EXP(-C*XS(1)))-(EXP(-C*XS(2)))) FIF09660
      AA=YS(1)-(BB *(EXP(-C*XS(1)))) FIF09670
      YY(1)=AA+(BB *(EXP(-C*MTAU))) FIF09680
      ENDIF FIF09690
      RETURN FIF09700
      END FIF09710

```

	FUNCTION FMIN(C)	FIF09720
C		FIF09730
C	FUNCTION FMIN IS FUNCTION TO BE MINIMIZED.	FIF09740
C		FIF09750
	REAL C	FIF09760
	COMMON/FF/XS(3),YS(3)	FIF09770
	P = (YS(1) - YS(2)) / (YS(3) - YS(2))	FIF09780
	PF = EXP(-C * XS(1)) - EXP(-C*XS(2))	FIF09790
	PG = EXP(-C * XS(3)) - EXP(-C*XS(2))	FIF09800
	PP=PF/PG	FIF09810
	FMIN=(P-PP)**2	FIF09820
	RETURN	FIF09830
	END	FIF09840

Report Documentation Page

1. Report No. NASA TM-100751		2. Government Accession No.		3. Recipient's Catalog No.	
4. Title and Subtitle Algorithm for Atmospheric Corrections of Aircraft and Satellite Imagery				5. Report Date December 1989	
				6. Performing Organization Code 613	
7. Author(s) Robert S. Fraser, Richard A. Ferrare, Yoram J. Kaufman, and Shana Mattoo				8. Performing Organization Report No. 90B00032	
				10. Work Unit No. RTOP No. 677-22-29-01	
9. Performing Organization Name and Address Goddard Space Flight Center Greenbelt, Maryland 20771				11. Contract or Grant No. NAS5-30430 NAG5-203	
				13. Type of Report and Period Covered Technical Memorandum	
12. Sponsoring Agency Name and Address National Aeronautics and Space Administration Washington, DC 20546-0001				14. Sponsoring Agency Code	
15. Supplementary Notes R.S. Fraser: Goddard Space Flight Center, Greenbelt, Maryland 20771; R.A. Ferrare: University Space Research Association, Greenbelt, Maryland 20771; Y.J. Kaufman: University of Maryland, College Park, Maryland 20742; S. Mattoo: Applied Research Corporation, Landover, Maryland 20785.					
16. Abstract This report describes a simple and fast atmospheric correction algorithm used to correct radiances of scattered sunlight measured by aircraft and/or satellite above a uniform surface. The atmospheric effect, the basic equations, a description of the computational procedure, and a sensitivity study are discussed. The program is designed to take the measured radiances, view and illumination directions, and the aerosol and gaseous absorption optical thicknesses to compute the radiance just above the surface, the irradiance on the surface, and surface reflectance. Alternatively, the program will compute the upward radiance at a specific altitude for a given surface reflectance, view and illumination directions, and aerosol and gaseous absorption optical thicknesses. The algorithm can be applied for any view and illumination directions and any wavelength in the range 0.48 um to 2.2 um. The relation between the measured radiance and surface reflectance, which is expressed as a function of atmospheric properties and measurement geometry, is computed using a radiative transfer routine. The results of the computations are tabulated in a look-up table, which forms the basis of the correction algorithm. The algorithm can be used for atmospheric corrections in the presence of a rural aerosol. The sensitivity of the derived surface reflectance to uncertainties in the model and input data is discussed.					
17. Key Words (Suggested by Author(s)) Earth Sciences Atmospheric Correction Remote Sensing Satellite Imagery				18. Distribution Statement Unclassified - Unlimited Subject Category 43	
19. Security Classif. (of this report) Unclassified		20. Security Classif. (of this page) Unclassified		21. No. of pages 106	
				22. Price	